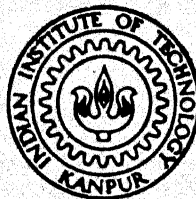# INVESTIGATIONS INTO MICROHARDNESS OF CHIPS DURING ACCELERATED CUTTING

by

SANJAY KUMAR

DEPARTMENT OF MECHANICAL ENGINEERING

INDIAN INSTITUTE OF TECHNOLOGY, KANPUR

JANUARY, 1987

Manufacturing Scien Lab.

INVESTIGATIONS INTO MICROHARDNESS OF CHIPS DURING ACCELERATED CUTTING

A Thesis Submitted
In Partial Fulfilment of the Requirements
for the Degree of

MASTER OF TECHNOLOGY

by

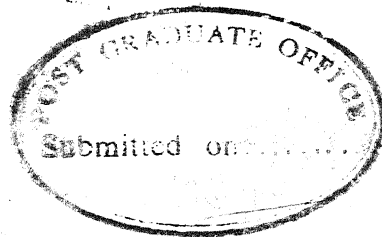### SANJAY KUMAR

to the

DEPARTMENT OF MECHANICAL ENGINEERING

INDIAN INSTITUTE OF TECHNOLOGY, KANPUR

JANUARY, 1987

ME-1987-M-KUM-INV

CERTIFICATE

Certified that this work entitled 'Investigations Into Microhardness **of Chips** During Accelerated Cutting' has been carried out under our supervision and that it has not been submitted elsewhere for a degree.

(Dr. G.K. Lal)
Professor
Dept. of Mech. Engg.
I.I.T. Kanpur.

Date:

(Dr. V.K. Jain)
Asst. Professor
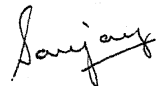Dept. of Mech. Engg.
I.I.T. Kanpur.

Date : 26 Jan. 1987

CONTENTS

ABSTRACT

It has been found that shear strain acceleration governs the machining parameters like tool-chip interface temperature, shear angle, tool **wear** etc. It has been speculated that microhardness of the chips for the same machining conditions but for different shear strain acceleration would be different.

To test this hypothesis, experiments have been conducted using mild steel as work material and cemented carbide bits as tools . Experiments were performed in two ways i.e., longitudina turning and accelerated cutting. Chips were collected at the same machining conditions but at different shear strain accelera tion. Microhardness of the chips has been measured using Leitz- microhardness tester and the results have been analysed using a computer program CADEAG-1.

Using the responses (i.e., microhardnesses), mathematic models have been evolved. Effects of different parameters (cutti speed, feed etc.) on the microhardness of the chips in all the three cases have been studied. It has been concluded that micro- hardness of the chips is governed by shear strain rate and shear strain acceleration and their governing parameters.

NOMENCLATURE

$\delta,$ = Cutting ratio

γ = Shear strain

$\dot{\gamma}$ = Shear strain rate $\sec^{-1}$

$\ddot{\gamma}$ = Shear strain acceleration $\sec^{-2}$

$\gamma_{act},$
α_{act} = Actual rake angle

α = rake angle

ϕ = Shear angle

V_c = Cutting speed in m/s

V_f = Cutting speed in facing in m/s

V_t = Cutting speed in taper turning in m/s

θ = Semi taper angle

D = Diameter of work piece in m.

VPN = Vicker's Point Number

σ = Shear stress N/mm^2

= Dislocation density

G = Shear Modulus N/mm^2

f = Feed rate mm/rev

t_1 = Undeformed chip thickness mm

t_2 = Deformed chip thickness mm

N = Spindle speed rpm.

BUE = Built up edge

PSDZ = Primary shear deformation zone

μH = Microhardness VPN

LIST OF FIGURES

CHAPTER - I

INTRODUCTION AND LITERATURE SURVEY

1.1 INTRODUCTION

The developments in nuclear and space technology have posed production problems in machining of hard, high strength and heat resistant metals and alloys. But, simultaneous developments in tools and their coating materials have provided the solutions to these problems. Therefore, the need for testing the machinability of these newly developed, diffult to machine materials is being increasingly felt.

The machinability of materials is normally evaluated by expensive and time consuming lougitudinal turning tests. Alternatives to these tests are accelerated cutting tests like facing test [1] and taper turning test [2]. In accelerated cutting, the cutting speed varies continuously, where as in longitudinal turning, it is constant. These accelerated cutting tests provide quick estimates of machinability and are also economically viable. However, contrary to conventional longitudinal turning tests, the stress field in these tests is varying continuously. Hence, care has to be exercised while using machinability data obtained from these tests. Also, extrapolations may lead to inaccurate results.

In industry, facing and taper turning operations are quite often used during machining. Therefore, an in -depth study of the accelerated cutting tests and their effects on

machining parameters is of immense importance.

Longitudinal turning tests have been studied
deeply by a large number of research workers all over the
world. Effects of independant parameters like cutting speed,
feed rate, depth of cut, tool angles etc. an dependant machi-
ning parameters like shear angle [3,4], cutting forces [5],
shear flow stress [6], tool chip interface temperature etc.
have been studied. But no work has been reported about the
effects of these independant parameters on variation of
microhardness of chips during longitudinal turning as well as
accelerated cutting tests. This study would help in a better
understanding of the metallurgical changes taking place in the
chip material, while passing through primary and secondary
shear deformation zone.

1.1.2. Objective of Present Work

It was envisaged that the microhardness of the
chips under the same machining conditions (feed rate, cutting
speed, rake angle, depth of cut etc.), but at different shear
strain acceleration would be different. Also, the microhardness
of the chips would have a significant influence on tool wear.
Thus, the measurement of microhardness variation could provide
sufficient insight into the cutting process so as to become
a response (like shear angle, shear flow stress etc.) for
evaluating machinability.

To test the above hypothesis, a set of experiments
were performed using cemented carbide tips as tools and Mild ste

as work material. Experiments were designed such that
longitudinal turning and accelerated cutting were carried
out under almost similar machining conditions. The shear
angle and microhardness of about 300 specimens, so collected
was measured and the various results analysed using a software
package known as CADEAG - 1.

To predict the independant, interactive and higher
order éffects of different independant parameters (or factors)
experiments were planned using central composite rotatable
design with half replicate [7].

1.2 LITERATURE SURVEY :

1.2.1 Microhardness distribution in PSDZ.

No previous work has been reported, in the author's
knowledge, on microhardness variation of chips. Clack and
Brewer [8] have attempted to study the microhardness variation
within and around the cutting zone by freezing the chip using
quick stop device (QSD). Their primary concern, however, had
been to determine the thickness of the primary shear deforma-
tion zone. It is achieved by locating the boundary where
sudden change in microhardness, in the grid pattern marked
on workpiece before conducting the experiments, takes place.

Mills and Akhatar [9] have also conducted some
experiments about the measurement of microhardness of ferrite,
in the work material before machining and not that of chips.

4
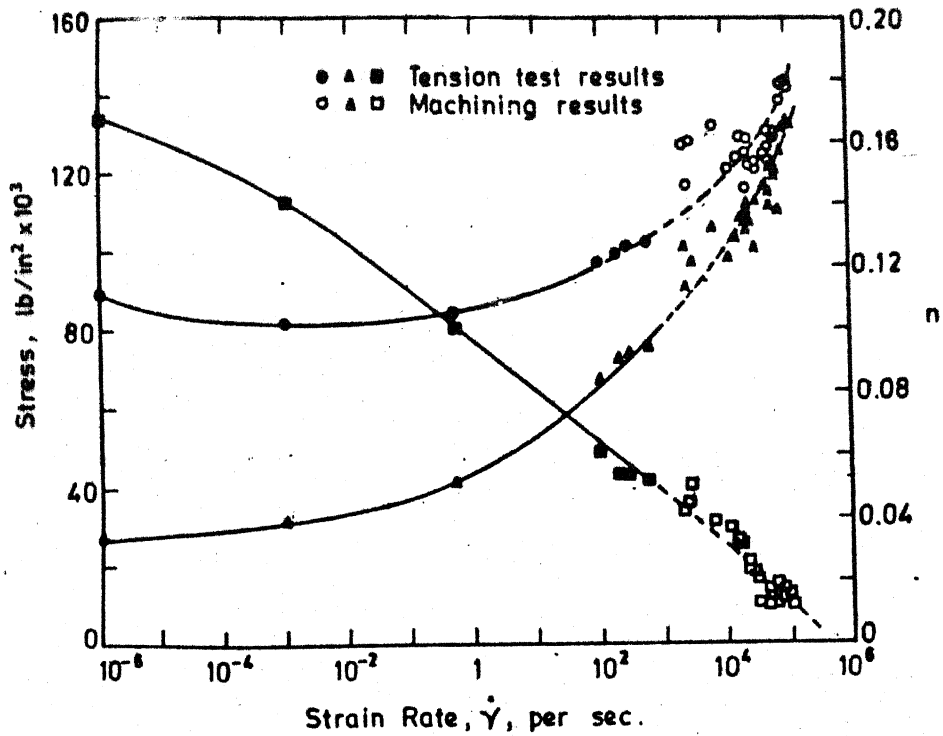
Fig. 1.1 Values of n, σ_1 and σ_0 calculated from machining and tension test results. for mild steel.
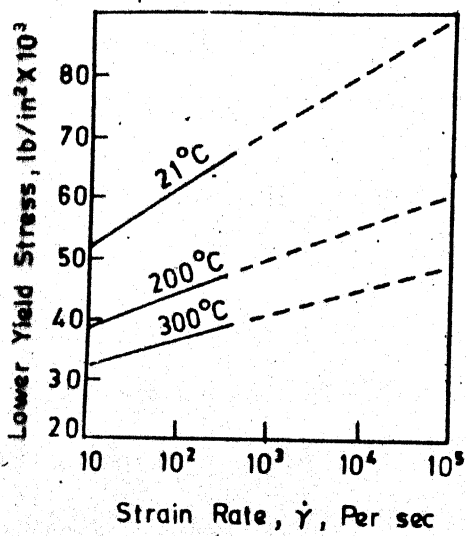
Fig. 1.2 Lower yield vs strain rate plots.
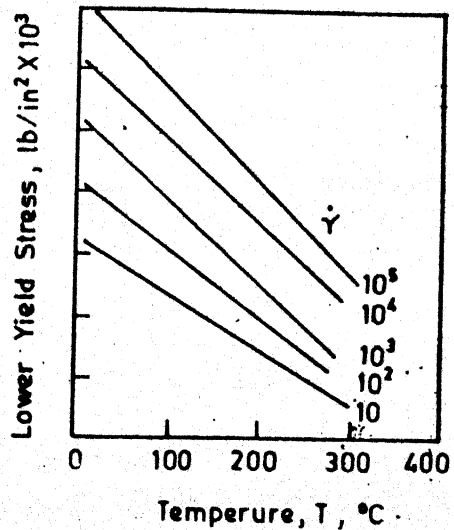
Fig. 1.3 Lower yield vs temp. plots.

Thus no literature is available as to show the effects of independant machining parameters on microhardness of chips during machining (longitudinal as well as accelerated cutting).

1.2.2 Shear flow stress dependance on strain rate and temperature:

The shear flow stress variation with shear strain rates has been investigated by many researchers. [6,10,11,12]. Manjoine [11] has proved that the yield point stress, taken as the stress at lower yield point, increases continuously with the rate of strain Fig. (1.1). Ohmeri and Oshimaya [12] showed that for strain rate varying from 10 to 10^5 second^{-1}, the yield stress increases linearly with log of strain rate (log $\dot{\gamma}$) and decreases with increase in temperature Figrs [1.2, 1.3].

1.2.3 Effect of independant machining parameters on specific cutting work and cutting ratio:

Based on a wide spectrum of experiments, Zorev [13] obtained the following results for cutting ratio (δ) variation Figs (1.4) and (1.5). Cutting ratio is defined as the ratio of deformed chip thickness and the undeformed chip thickness. Zorev [13] explained these results on the basis of the effects of various factors (cutting speed, feed, depth of cut, rake angle etc.) on angle of action, actual rake angle (α_{act}), mean coefficient of friction, strain hardening effect and direct effect of cutting speed.
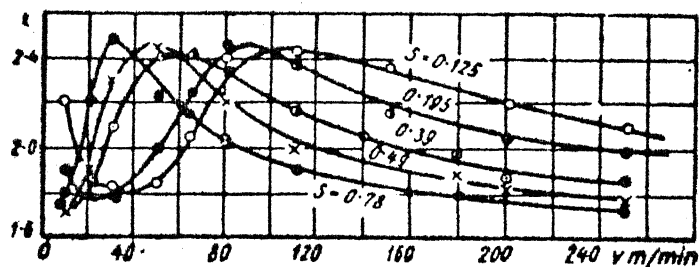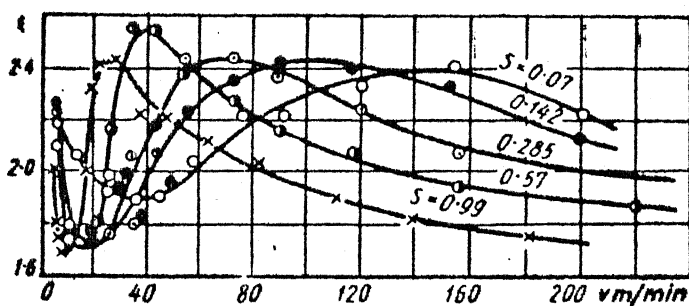
FIG. 1.4 Influence of cutting speed on cutting ratio during longitudinal turning of 40 steel at different feeds (tool 20A-0, $t = 4$ mm).
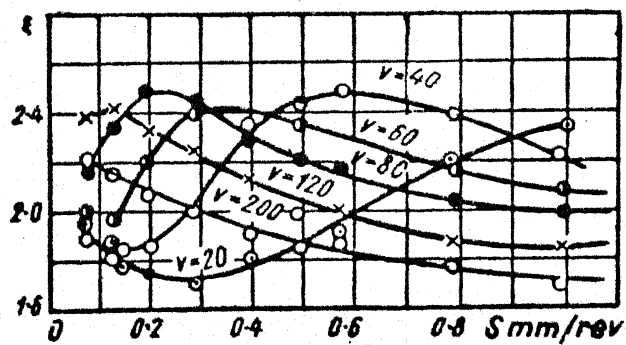
FIG. 1.5 Influence of feed on cutting ratio during longitudinal turning of 40 steel at different cutting speeds (tool 20A-0, $t = 4$ mm).
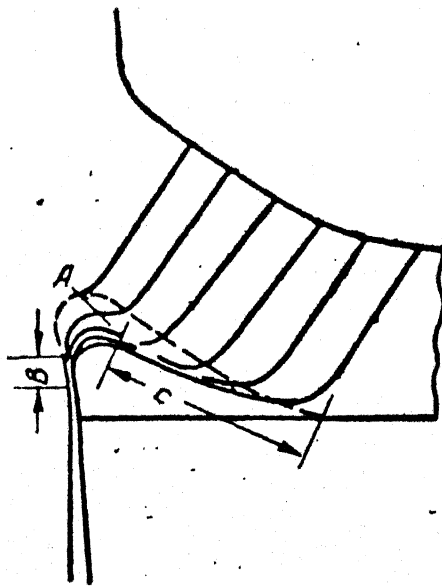
Fig. 1.6 Diagram showing region of continuous plastic deformation
(sector (A)) and sectors where plastic deformation may be accompanied
by rupture (B and C).
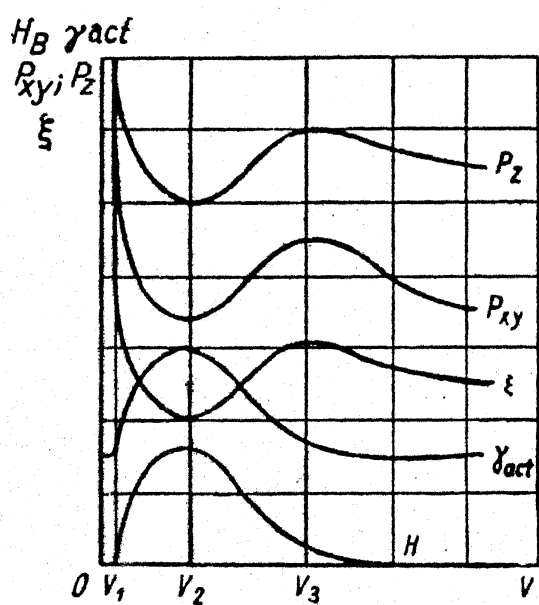
FIG. 1.7. Diagram of typical influence of cutting speed on the cutting ratio and the projections of the cutting force when cutting steel with a small rake angle.
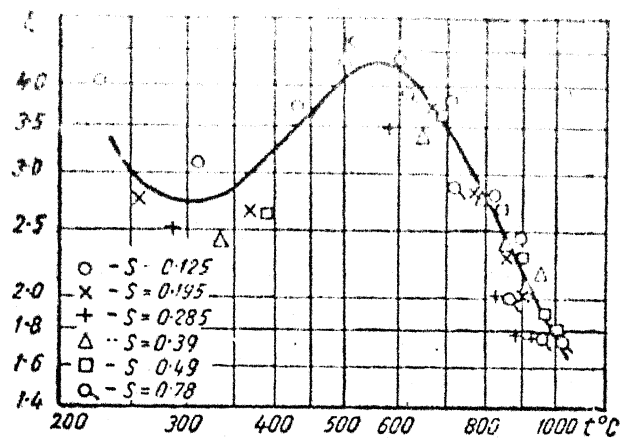
FIG. 1.8. Relationship of the cutting ratio to mean chip-tool contact temperature during longitudinal turning of 35Kh3MN steel (tool 20A-0, $t = 4$ mm, $s = 0.125$–0.78 mm/rev, $v = 10$–250 m/min).
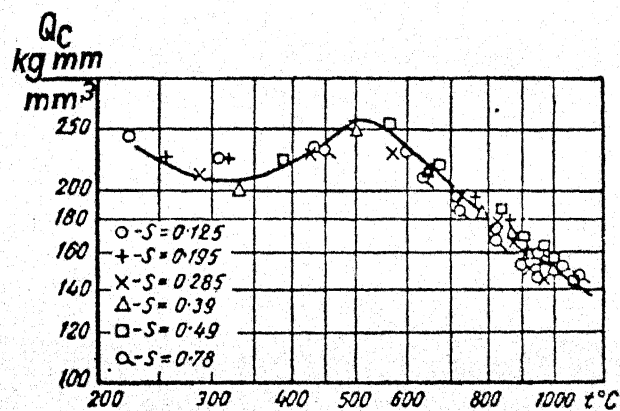
FIG. 1.8. Relationship of specific work of chip formation to mean chip-tool contact temperature during longitudinal turning of 35Kh3MN steel (tool 20A-0, $t = 4$ mm, $s = 0.125$–0.78 mm/rev, $v = 10$–250 m/min).
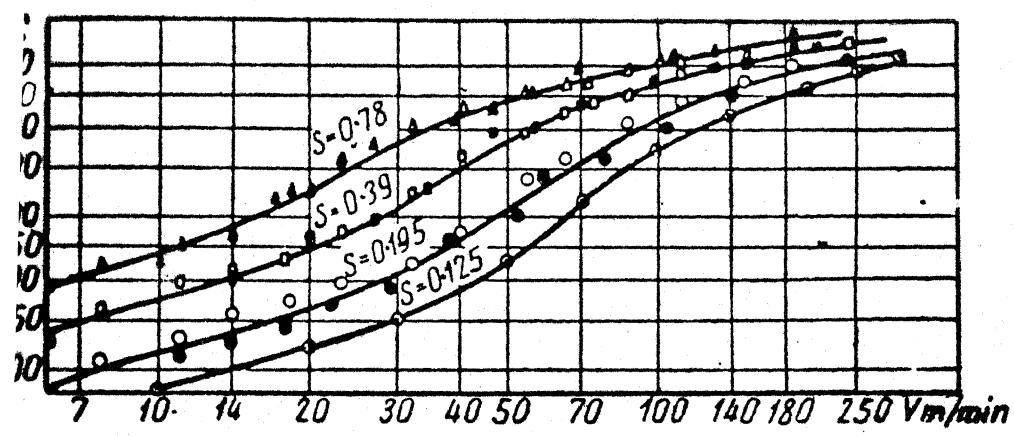
FIG. Influence of cutting speed on mean chip-tool contact temperature during longitudinal turning of 40 steel (tool 20A-0, $t = 4$ mm). The white and black points correspond to two series of experiments.
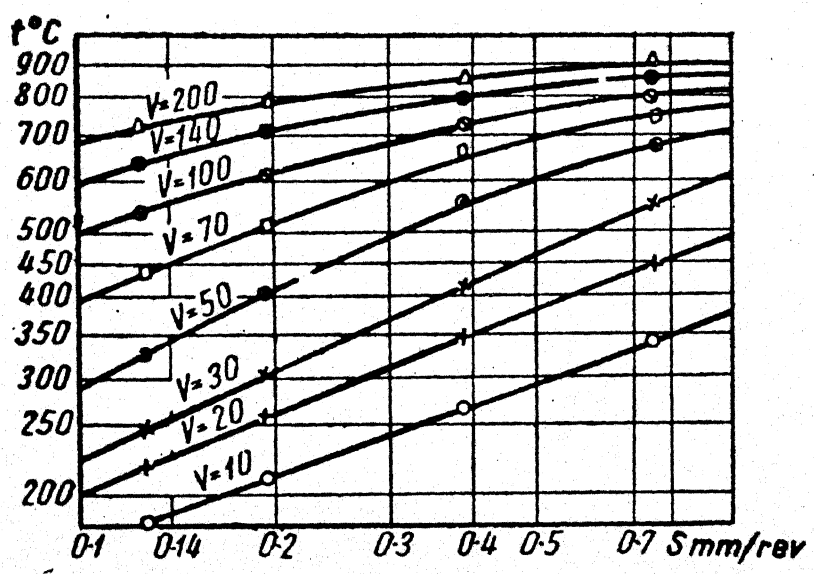
FIG. Influence of feed on mean chip-tool contact temperature. (tool 20A-0, 40 steel, $t = 4$ mm).
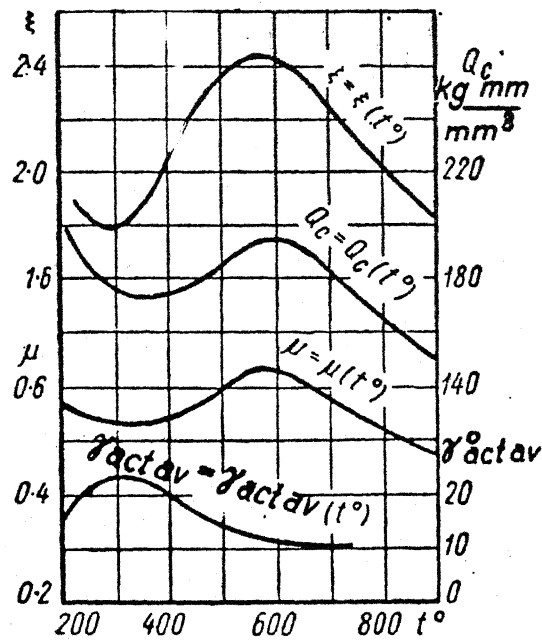
FIG. 1.11 Combination of mean probable relationships of cutting ratio, specific work of chip formation, mean coefficient of friction and average actual cutting angle with the mean tool-chip temperature (40 steel, $\gamma = 10°$, $t = 4$ mm, $s = 0.125$–0.78 mm/rev, $v = 10$–170 m/min).
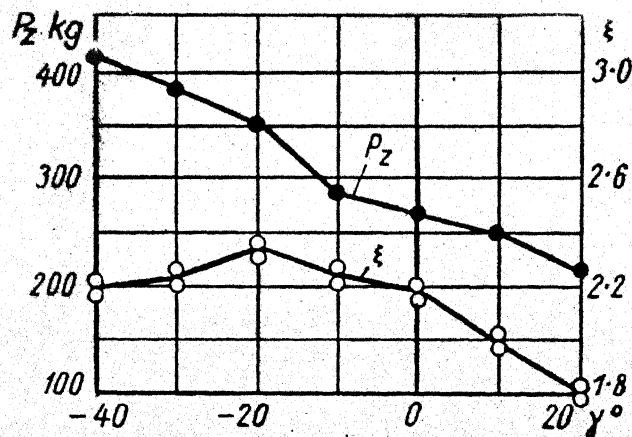
FIG. 1.12 Influence of rake angle on cutting ratio and vertical projection of force when cutting 40 steel ($t = 2$ mm, $s = 0.55$ mm/rev, $v = 149$ m/min).

For low rake angle, as cutting speed increases from near zero, the mean coefficient of friction at the tool-chip interface increases. Strain hardening of material also occurs. In the secondary shear zone, a stressed state is created where plasticity condition is not fulfilled. (Difference of principal normal stresses is less than shear flow stress).

Mean coefficient of friction and strain hafdening increase upto about $300^{o}C$. Thus have the possibility of a built up edge [BUE] is maximum. However, after $300^{o}C$, shear flow stress decreases due to thermal softening which dominates strain hardening. Shear flow of material in the upper zone (zone A Fig. 1.6) of the BUE starts and the BUE starts becoming smaller. (Though BUE is formed intermittently, this can be assumed to be a fixed zone for short periods of times). At about $600^{o}C$ the entire BUE disintegrates due to thermal softening and the actual rake angle becomes equal to the initial rake angle. The effect of BUE on actual rake angle and cutting ratio is shown in Fig. (1.7).

The effect of temperature on cutting ratio (∂) and specific cutting work [6] is shown in Fig. (1.8). The effect of strain hardening can be observed in the variation of specific cutting work (Q_c) with temperature (and so with cutting speed also as temperature rises with cutting speed Figs (1.9) and (1.10)). Specific chip formation work (Q_c) is the sum of specific friction work (Q_f) depending on mean coefficient of friction (on took rake face) and the plastic deformation

$$Q_c = Q_f + Q_d \qquad\qquad (1.1)$$

However, cutting ratio should increase at low feed and low cutting speed, but it shows a decrease. Zorev explained these results by suggesting that the effect of BUE (and hence α_{act}) dominates the effect of strain hardening and mean coefficient of friction. Thus even though both strain hardening and friction coefficient are increasing , the specific cutting work and cutting ratio decrease in region I due to a sharp decrease in actual rake angle value. Fig. (1.11)

Fig. (1.12) shows that there is a sharp fall in cutting force and cutting ratio with rise in actual rake angle.

In region II, thermal softening dominates strain hardening. But the effect of reducing actual rake angle due to disintegrating BUE dominates, leading to an increase in specific cutting work Fig. (1.11).

In region III, the effect of BUE is negligible as at high temperatures the BUE disappears. Here, the effect of thermal softening dominates and the cutting ratio and specific cutting work decrease significantly.

Elaborate studies have been made in the field of mechanics of orthogonal cutting. However, almost all the analysis pertains to the situation when cutting speed is constant throughout the cut (i.e. longitudinal turning). In accelerated cutting, cutting speed varies continuously.

2.1 Shear angle:

Kececioglu obtained photomicrographs of the plastic zone of machining using QSD. Based on his model, where he assumed that the plastic zone could be represented by a parallel sided shear zone, shear plane can be taken as AB. Fig. (2.1).

The shear angle can be expressed in terms of tool rake angle (α) and the chip thickness ratio (r).

$$\tan \phi = \frac{r \cos \alpha}{1 - r \sin \alpha} \tag{2.1}$$

where

$$r = \frac{t_1}{t_2} = \frac{\text{undeformed chip thickness}}{\text{deformed chip thickness}} \tag{2.2}$$

The shear strain (γ) is given by the expression

$$\gamma = \frac{\cos \alpha}{\sin \phi \cos (\phi - \alpha)} \tag{2.3}$$

and the rate of strain $\dot{\gamma}$ ($\frac{d\gamma}{dt}$) is obtained by differentiating the above expression.
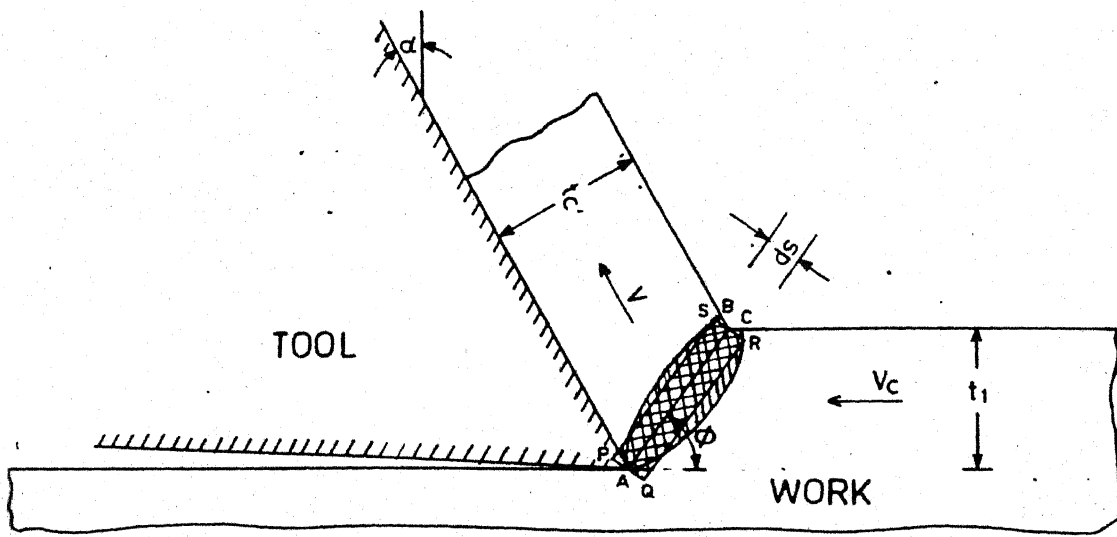
AREA ABC ▨ Plastic deformation zone obtained from photomicrographs.
AREA PQRS ▨ Approximation of ABC in to a parallel sided zone.
Fig. 2.1 Chip formation and deformation during orthogonal cutting.
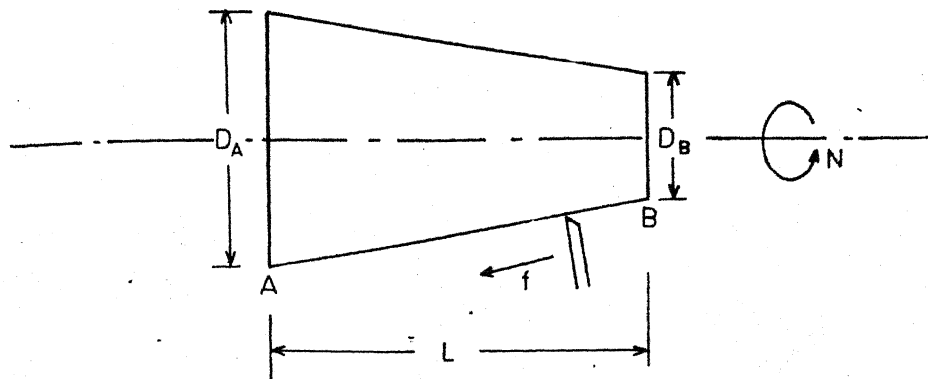
Fig. 2.2   Taper turning
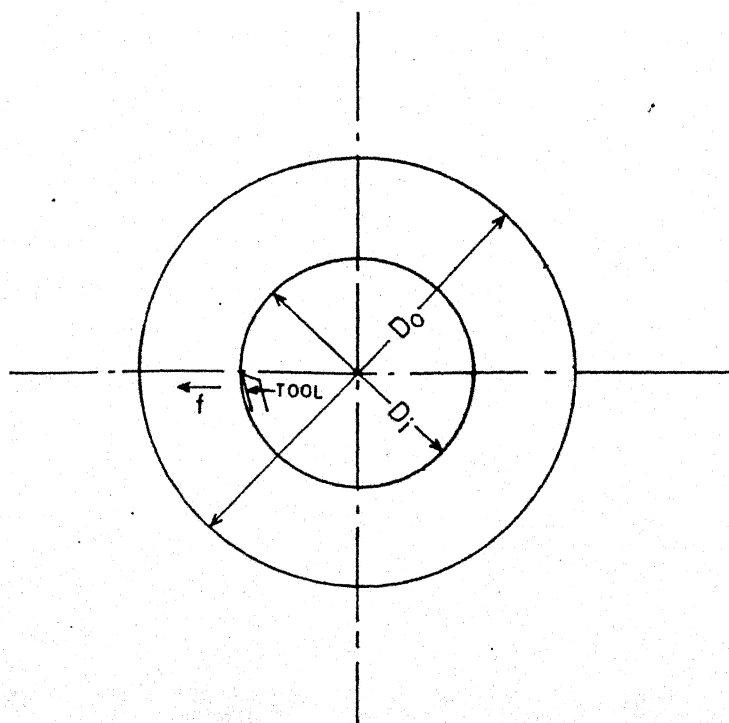
Fig. 2.3   Facing

$$\dot{\gamma} = \frac{V_c \; \text{Cos} \; \alpha}{ds \; \text{Cos}(\phi-\alpha)} \quad \text{sec}^{-1} \tag{2.4}$$

where 'ds' is the thickness of the primary shear deformation zone.

2.2 Strain Acceleration:

2.2.1 Strain acceleration during taper turning

Fig. (2.2) shows that cutting speed increases when machining from smaller end towards larger end.

$$V_t = \frac{\pi \, N}{60} \left[D_B + \frac{D_A - D_B}{L} \cdot \frac{N.f.t}{1000. \; 60} \right] \tag{2.5}$$

from equations (2.4) and (2.5)

$$\dot{\gamma} = \frac{\pi \, N}{60} \left[D_B + \frac{D_A - D_B}{L} \cdot \frac{N.f.t}{1000.60} \right] \frac{\text{Cos} \; \alpha. \; 1000}{ds.\text{Cos} \; (\phi-\alpha)} \tag{2.6}$$

ifferentiating with respect to time and simplifying

$$\ddot{\gamma}_t = \frac{2\pi f N^2}{3600} \cdot \frac{\text{Cos} \; \alpha. \; \text{tan} \; \theta_t}{ds \; \text{Cos} \; (\phi-\alpha)} \quad \text{sec}^{-2} \tag{2.7}$$

θ_t = semi-taper angle

$\ddot{\gamma}_t$ = strain acceleration in taper turning

2.2 Strain acceleration during facing :

In case of facing, the cutting speed (V_f) is given Fig. (2.3)

$$V_f = \frac{\pi N}{60} \left(D_i + \frac{2N.f.t}{1000} \right) \quad \text{m/s} \tag{2.8}$$

here D_i is the initial diameter in meters from which facing tarts outwards. Substituting equation (2.8) in equation (2.4)

$$\dot{\gamma}_f = \frac{\pi N}{60} \left[D_i + \frac{2N.f.t}{60.1000} \right] \frac{Cos\ \alpha.1000}{ds\ Cos(\phi-\alpha)}\ sec^{-1} \qquad (2.9)$$

where $\dot{\gamma}_f$ is the strain rate in facing.

Differentiating equation (2.9)

$$\ddot{\gamma}_f = \frac{2\pi N^2 f}{3600} \cdot \frac{Cos\ \alpha}{ds\ Cos(\phi-\alpha)}\ sec^{-2} \qquad (2.10)$$

where γ_f is the strain acceleration in facing.

2.3.1 Dislocation and material property effects:

Seegar [14] represented the flow stress (σ) of a metal as the sum of a thermal (σ^t) and an athermal (σ_i) component.

$$\sigma = \sigma^t + \sigma_i \qquad (2.11)$$

σ_i is also termed as the internal stress, and depends on temperature only through elastic constants and lattice parameters. This athermal stress thus represents the long range obstacles to dislocation movement, a typical example being other dislocations on parallel slip planes.

The thermal stress term (σ^t) represents the short range barriers to dislocations movement and is of greater immediate significance as it explains the thermal softening effect. Obstacles having a stress field of less than a few atomic diameters are considered short range. These can however be overcome by thermal activation. A few common examples being Peierls - Nabarro stress, forest dislocations, cross-slip

of screw dislocations etc. At high temperatures (above 300°C) these short range barriers are overcome. Thus the thermal part of the flow stress reduces, leading to what is termed as thermal softening.

Strain hardening on the other hand is caused by increase in dislocation density and their interaction. This causes formation of forest dislocations, jogs etc., which impede dislocation movement leading to higher flow stress [15].

2.3.2 Interrelationship of dislocation interactions with
strain acceleration and effect on shear flow stress:

Shear strain rate $(\dot{\gamma})$ can be related to dislocation velocity and density [15] as

$$\dot{\gamma} = a\ \rho\ b\ v \qquad\qquad (2.12)$$

where   is the mobile dislocation density, 'b' the 'Burger Vector' 'v' the dislocation velocity and 'a' is a geometric constant less than one. Li (16) has shown that there exists a power law between average dislocation velocity (v) and the shear stress (σ)

$$v = B\ (\sigma^*)^{m^*} \qquad\qquad (2.13)$$

where σ^* is the reduced stress and is approximately equal to σ. B and m^* are essentially characteristic material constants. m^* bears an inverse relationship with strain rate sensitivity m; m^* varying between 1.6 to 40 [15]. Also Seegar [14] has proposed that shear flow stress (σ) varies with dislocation density as
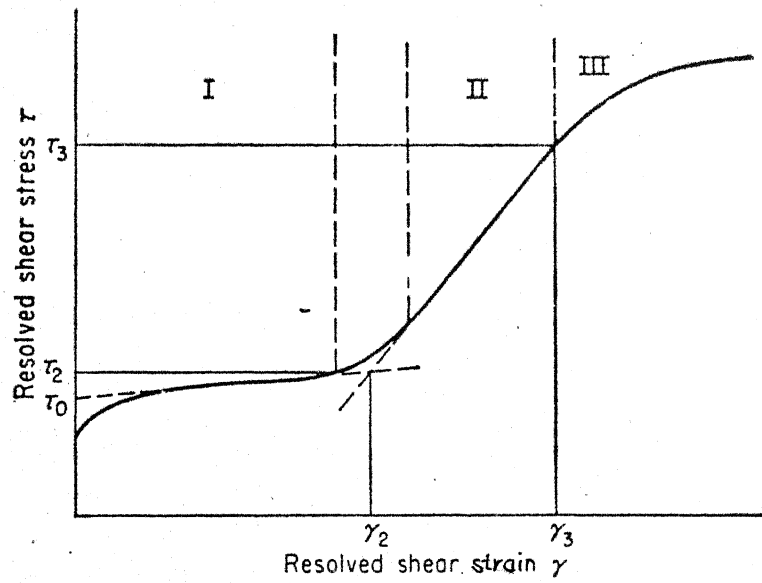
Fig. 2.4 Generalized flow curve for fcc single crystals.

in stage II of the generalized flow curve for single crystals Fig. (2.4). 'G' is the shear modulus of elasticity, 'b' the burger vector and 'α' a constant.

The microhardness of ferrite the specimen will vary somewhat proportionally to the shear flow stress of the material. Now, differentiating equation (2.12) to get an expression for shear strain acceleration

$$\dot{\gamma} = \frac{d\dot{\gamma}}{dt} = a\,\rho\,b\,\frac{dv}{dt} + a\,v\,b\,\frac{d\rho}{dt} \tag{2.15}$$

'a' is a constant and 'b' is the burgervector which does not vary with time. Again, taking the logarithm of equation (2.13) and differentiating

$$\ln v = \ln B + m^* \ln (\sigma^*)$$

$$\frac{1}{v}\frac{dv}{dt} = \frac{m^*}{\sigma} \cdot \frac{d\sigma}{dt} \tag{2.16}$$

(σ^* being approximately equal to σ)

Again differentiating equation (2.14) we have

$$\frac{d\sigma}{dt} = \alpha' \frac{Gb}{\rho^{1/2}} \cdot \frac{d\rho}{dt} \tag{2.17}$$

α' is the new constant.

Using equations (2.15, 2.16 and 2.17)

$$\ddot{\gamma} = a\,\rho\,b\,v\,\frac{m^*}{\sigma} \cdot \frac{d\sigma}{dt} + \frac{a\,v\,b\,\rho^{1/2}}{\alpha'\,Gb} \cdot \frac{d\sigma}{dt}$$

$$\ddot{\gamma} = \rho^{1/2}\,a\,v\,\frac{d\sigma}{dt}\left(\frac{m^*}{\sigma}\,b\,\rho^{1/2} + \frac{1}{\alpha'G}\right) \tag{2.18}$$

The variation of shear flow stress with time was found by using the results of shear flow stress in accelerated cutting

80 rpm. were converted to shear flow stress versus time. This was then fitted to the power law equation ($\sigma = at^b$) using the software CURVE.FOR. The coefficients 'b' and 'a' were found to be 0.126 and 37.2 respectively. The correlation coefficient was 0.62. This gave values of $\frac{d\sigma}{dt}$ between 0.101 and 0.032 for cutting speeds between 0.34 m/s and 0.58 m/s. This showed that the variation of $\frac{d\sigma}{dt}$ was small and that the shear flow stress could be taken to vary as the reciprocal of strain acceleration.

By reasoning, at a certain strain rate achieved through a high strain acceleration, the dislocation interaction may not occur (due to lack of time), to the extent it would have been at that strain rate attained in the normal way. (say longitudinal turning i.e. without strain acceleration). Also phenomenon like jog formation may be inhibited or at least reduced. This would lead to lower deformation forces and hence a lower shear flow stress.

In the cutting zone in accelerated cutting, the strain rate is continuously changing. The friction at the tool-chip interface is also changing with normal force. Temperature is increasing with cutting speed and thus with time. Strain acceleration could also be causing a temperature lag effect. The analysis of such a complex situations is not theoretically possible, specially as the instantaneous values of temperature at tool-chip interface, the diffusion rate and the friction state are not known.

A set of experiments was designed using shear strain
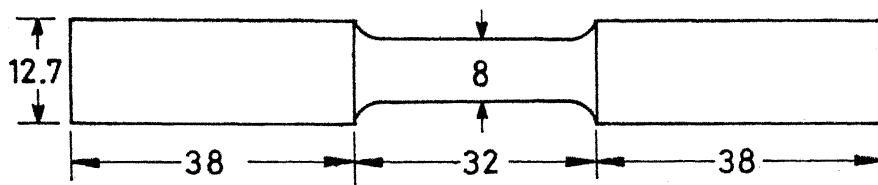
(Dimensions are in mm)

Fig. 2.5 Dimensions of sample used for torsion test.

I	$0.100 \ sec^{-2}$
II	$0.112 \ sec^{-2}$
III	$0.124 \ sec^{-2}$
IV	$0.170 \ sec^{-2}$

Shear Strain Rate (sec^{-1})

Shear Stress (kg/mm^2)
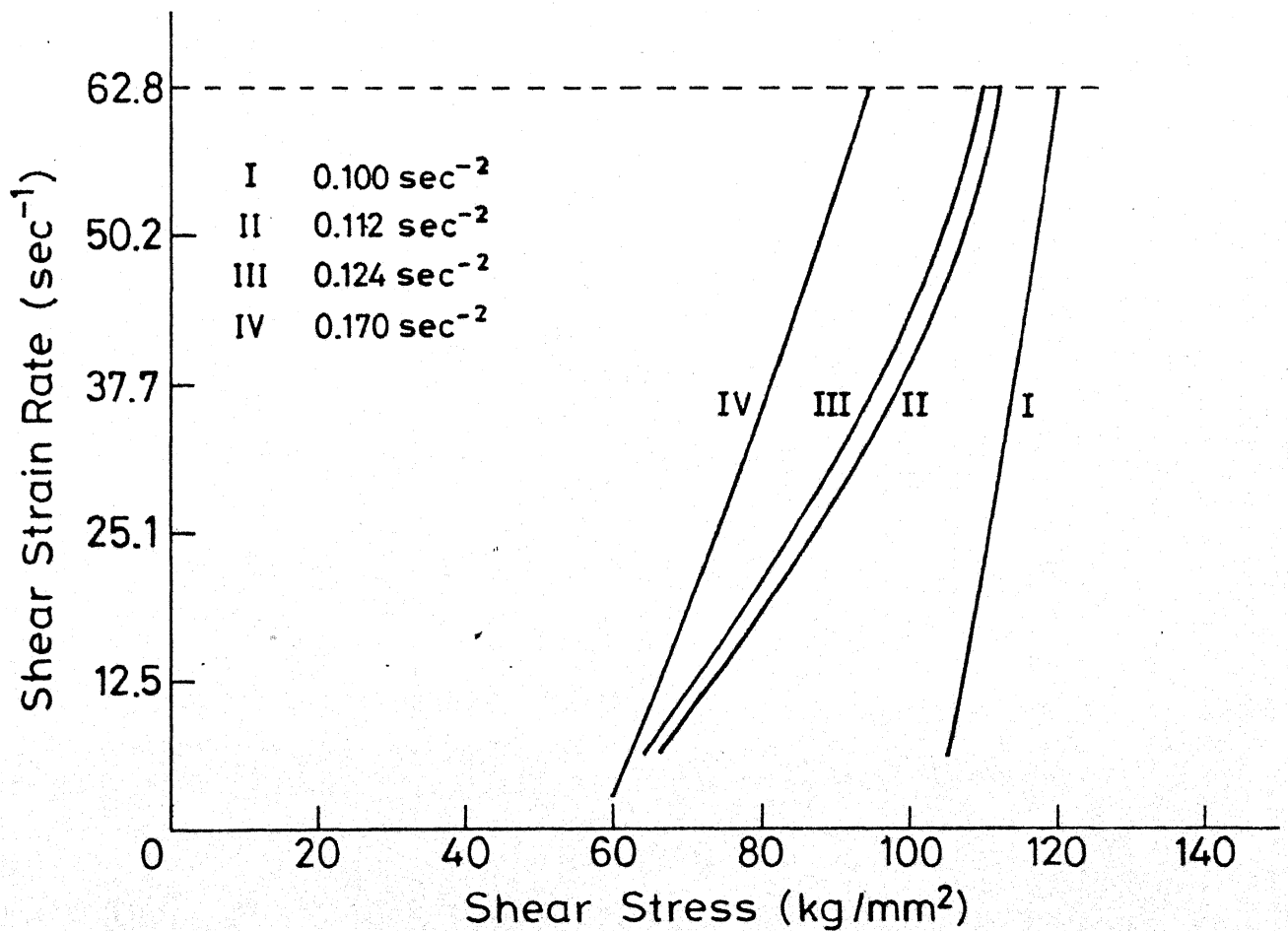
were used as shown in Fig. (2.5). The tests were done
on INSTRON UNIVERSAL TESTING MACHINE Model No. 1195.
About 20 specimens were tested at four values of strain
acceleration. This was achieved by varying strain rates in
steps of 5 seconds initially. To change the strain accele-
ration, steps of 3 seconds or less (as required) were taken
for a given strain rate and then the next strain rate step
was taken. It was found that the material yielded at lower
shear flow stress, at a certain shear strain rate level, if
higher strain acceleration was used. This observation proved
our hypothesis(as discussed above) that the shear flow stress
should reduce at higher strain acceleration.

CHAPTER 3

EXPERIMENTATION

The present work is carried out to determine the
effect of shear strain acceleration and its governing parameters
on microhardness of chips. This microhardness is then compared
with that obtained during longitudinal turning under the same
machining conditions (feed rate, rake angle, cutting speed, etc)
It is expected that shear strain acceleration and its governing
parameters will substantially affect the microhardness of the
chips.

A number of important factors like feed rate, cutting
speed, taper angle and spindle speed were considered to
formulate a set of cutting conditions in accordance with central
composite rotatable design with half replicate [7]. Depth of
cut and tool angles (tool bit type) were kept the same throu-
ghout the experimentation.

Four variables (spindle speed , taper angle, feed rate,
and cutting speed) for taper turning; three variables (spindle
speed, feed rate and cutting speed) for facing ; and two varia-
bles (cutting speed and feed rate) for longitudinal turning
were chosen to correlate the effects of shear strain acceleration and
its governing parameters on microhardness of the chips and
other responses (viz. shear angle).

In H.S.S tools [6], fast wear of tools is a major
handicap. This causes a reduction in depth of cut as the cut

proceeds. So, in the work reported in this thesis, cemented carbide tips were used as tools. Also higher cutting speeds (30 m/min to 60 m/min) were used since wear of tool was no longer a constraint. The wear of the carbide tips was checked under a tool makers microscope and found negligible.

3.1. Specifications:

1. Lathe : LB17; Machine no. 8285 HMT. India.
2. Triangular carbide tips: Indian Tool Manufacturers Ltd. TPUN 110304 Batch ST3/P30.
3. Tool rake angle = 0°.
4. Work Material :- Mild steel.
5. Leitz Microhardness tester:- Miniload-2.
6. Shadow Graph: MP 320 Carl Zeiss Jena.
7. Zeiss Universal Microscope.

3.2 Design of experiments:

The design of experiments is the procedure of selecting a number of trials and conditions for running them, essential and sufficient for solving the problem that has been set with the required precision. The following features are of great importan

1. Striving to minimize the total number of trials.
2. Simultaneous variation of all variables, determini a process according to rules of algorithm.
3. The selection of a clear-cut strategy, permitting the investigator to make substantial decisions after each series of trials.

In the present investigation, the central composite
rotatable design with half replicate for 2 factors (longi-
tudinal turning) as shown in table (1a); 3 factors (facing)
as shown in table (1b); 4 factors (taper turning) as in
table (1c); provided in Appendix 1, were used. The trials
for the experiments were generated with these factors and
their level-values, given in tables(2a,2b,2c) respectively
in the same Appendix. These also give the responses measured.

The values given are the average values. The values
of the standard deviation are also given for each experiment.
The values of the parameters were chosen in accordance with the
limitations of the work piece and the machine tool available.
The work piece was carefully designed so that all the experiments
could be carried out from the same materials.

The measured (and calculated) responses (shear angle
and microhardness) were fitted into a second order model with
the help of the software CADEAG-1.

$$Y_r = B_o + \sum_{i=1}^{n} B_i X_i + \sum_{i=1}^{n} B_{ii} X_{ii}^{2} + \sum_{i<j}^{n} B_{ij} X_i X_j \quad (3.1)$$

The values of the constants (B_i, B_{ii}, B_{ij}) are given
in table (3) in Appendix 1.

3.3 Proceedure:

A M.S. bar of 100mm diameter and suitable length was
rigidly fixed in a 4 jaw chuck. Depth of cut (1 mm) was kept
constant throughout the experimentation . To maiatain approxi-
mately orthogonal cutting conditions, the depth of cut should be

ratio of 8 or more is desirable).However, machine load
(at 500 rpm.) and other considerations (like work piece
size) did not allow a depth of cut larger than 1 mm. This
gave a depth of cut to feed ratio variation between 3.4 and
10. Also, to maintain the cutting edge perpendicular to the
machined surface, triangular tool bits were used, (square
edge tended to rub on the work-piece surface). Special care
was taken, so that all the three types of machining (longitu-
dinal,and taper turning and facing) were done from the same
work piece.

3.3.1 Longitudinal turning:

In logitudinal turning, the spindle speed was kept
low so as to keep the diameter large, for the same cutting
speed Fig. (3.1) and thus effect the minimum reduction in
work piece.

Different diameters corresponding to the different
cutting speeds were turned on the work piece. Chips were
collected after chip formation had stabilized.

3.3.2 Taper turning:

A taper turning attachment was used to provide the
taper, and a cross slide to provide the depth of cut. Tool edge
was kept perpendicular to work piece and a mark was put at the
diameter corresponding to the required cutting speed. Cutting
was started from a reference cutting speed of 0.45 m/s and
continued to the desired cutting speed. Chips were collected
at the instant the tool was at this mark of desired cutting

29
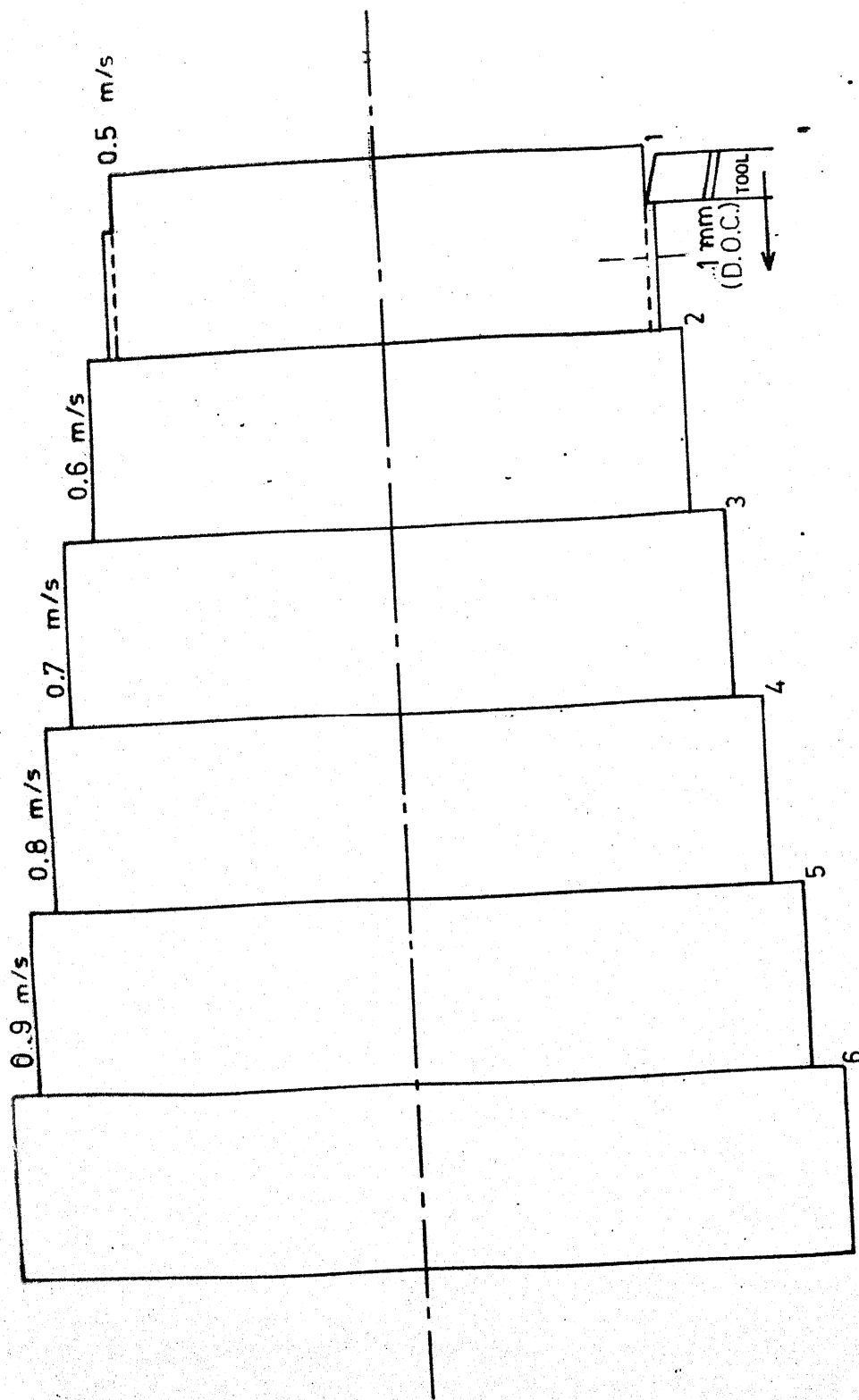
Fig. 3.1 Specialy designed work piece for chips collection during conventional turning at certain cutting speeds denoted by steps 1, 2 ,......6 with constant depth of cut for a treatment combination (Design in Table 2.)
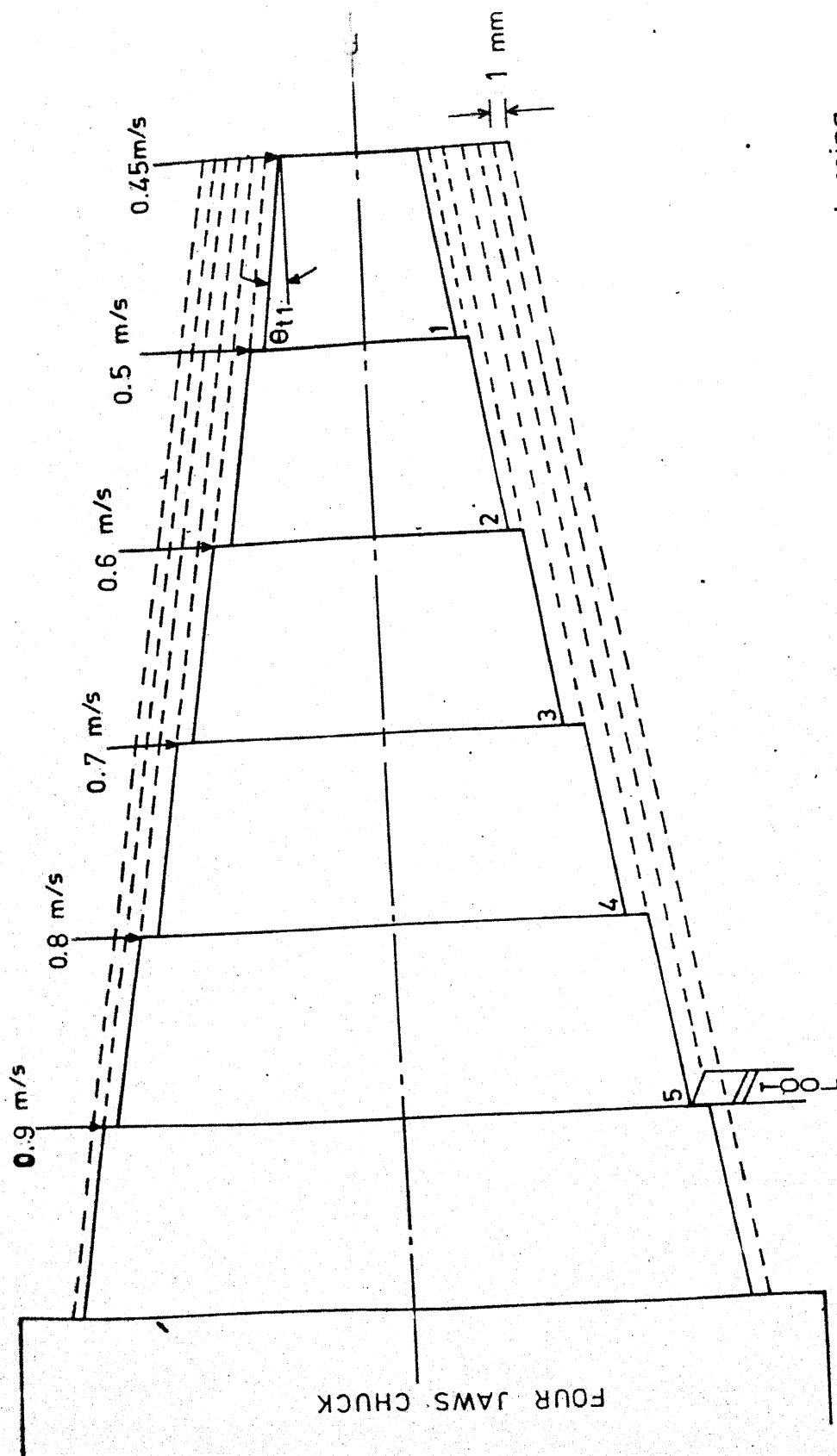
Fig.3.2 Specially designed work piece for chips collection during taper turning at certain cutting speeds denoted by steps 1, 2,....5 with a constant depth of cut for a particular treatment combination.
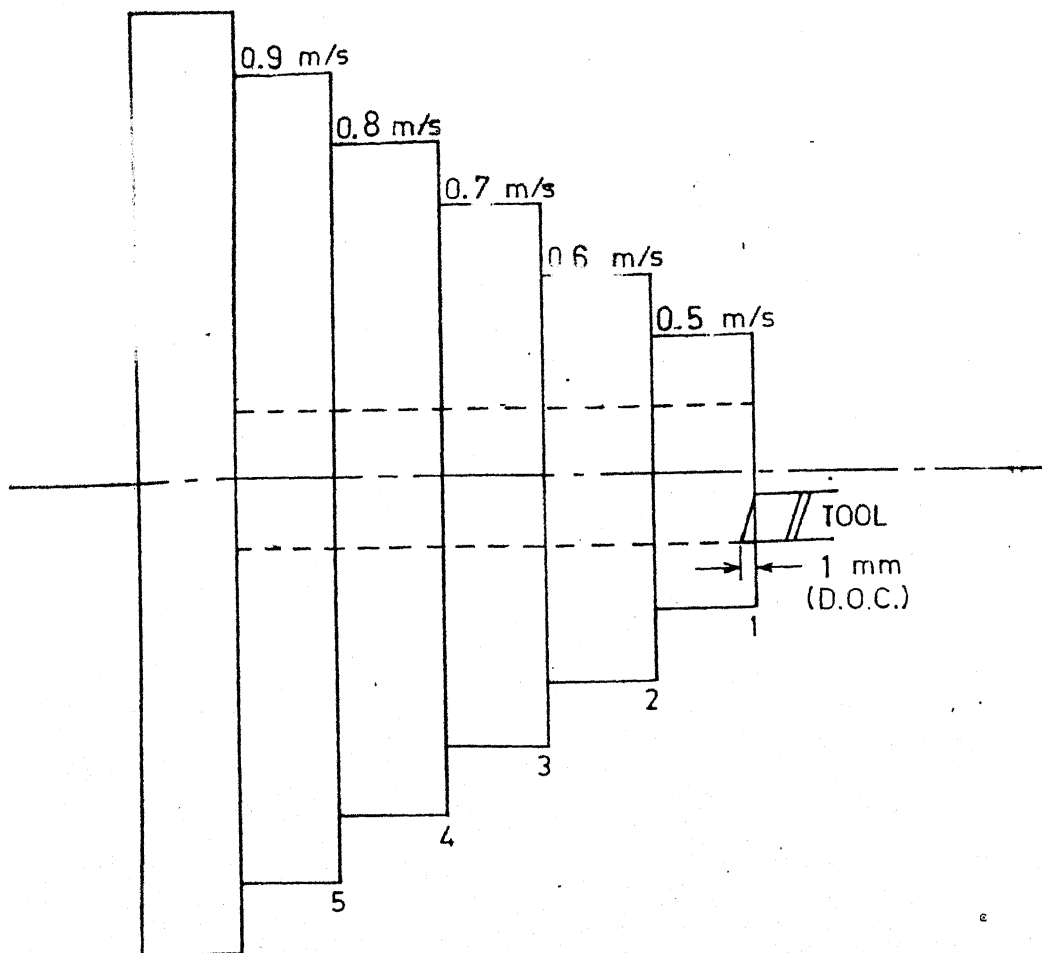
Fig. 3.3 Specially designed work piece for chips collection during facing at certain cutting speeds denoted by steps 1, 2,.... 5 with a constant depth of cut for a treatment combination.

speed. Grooving could not be done as the work piece size was critical and also the cutting characteristics could change. The order of the experiments had to be carefully adjusted. (Table 2c) Fig. (3.2).

3.3.3 Facing:

In facing, a hole of the required diameter (corresponding to reference cutting speed) was bored in the job. (Fig. 3.3). Cross slide was used to provide depth of cut and cross feed to provide the feed. Before starting any trial, the job was turned to the required diameter (corresponding to the required cutting speed). The cutting was started from the inner diameter and the chip was collected at the outer diameter.

3.3.4 Chip preparation:

Chips collected under different machining conditions were ground on a sand stone and then put upright in plasticene. A mould of Aluminium was put around each chip and freshly prepared 'Araldite' adhesive paste was poured into the mould.

This was left for 24 hours to solidify. Then the mould (which had been greased before use) was removed, leaving the chip mounted in the 'Araldite' base.

This mount was ground on a rough abrasive paper belt. Then these were polished using fine emery polishing paper with successively finer grades starting from 1/0 down to 4/0, to bring out the microstructure. Then these mounts were

vehicle. Polishing was done using a thick 'Sylvet' cloth.

3.3.4 Shear angle measurement:

The thickness of the deformed chips was measured
using the shadowgraph. For this purpose three chips were
picked up randomly from each trial. Using these values of
deformed chip thickness in each trial, the values of the
shear angle (see equation 2.1) were calculated. The standard
deviation of these shear angle values has been tabulated
along with the average shear angle values. (Tables 2a,2b,2c).
The scatter was observed since the chip shape was not rectangu-
lar and the appropriate thickness was measured by judgement.

3.3.5 Microhardness measurement:

The mounted chips were then repolished and etched
with nytal solution, in small batches, so that the micro-
hardness of freshly polished chips could be taken.

This was done to using a leitz microhardness tester.
This had a small square pyramidical indentor. A 15 gram load wa
found suitable for a specimen of hardness of the range of mild
steel. The size of the indentation diagonal was measured and
the microhardness was read in VPN, from a conversion chart [18].

Care was taken to take the measurements on ferrite
portions [18] only since the hardness of pearlite varies with
structure (fine or large grained) and composition (cementite
percentage etc.).   The measurement results showed some scatter
[19], hence about 12-16 measurements had been taken for each

CHAPTER 4

RESULTS AND DISCUSSIONS

The experimental observations of shear angle and microhardness of chips were obtained under different cutting conditions, (spindle speed, cutting speed, feed rate etc.) for longitudinal turning, taper turning and facing. Depth of cut was kept constant in all the experiments. The response surface equations (3.1) for both shear angle and microhardness have been established. The details of constants of response surface equations have been given in table (3). The results are discussed in the subsequent sections. While discussing the results, the variation of microhardness in the workpiece along the radius has not been considered. Also the effect of secondary shear zone has not been taken into consideration.

4.1 Shear angle:

4.1.1 Longitudinal turning:

Fig. (4.1a) shows the relationship between cutting speed and shear angle during longitudinal turning. In the begining, shear angle decreases and then it increases with increase in cutting speed. Fig. (4.1b) shows the variation of shear angle with feed rate. Initially, shear angle decreases and then it increases with increase in feed rate. The above results show a variation similar to the results of Zorev [13].

These results can be explained as follows:
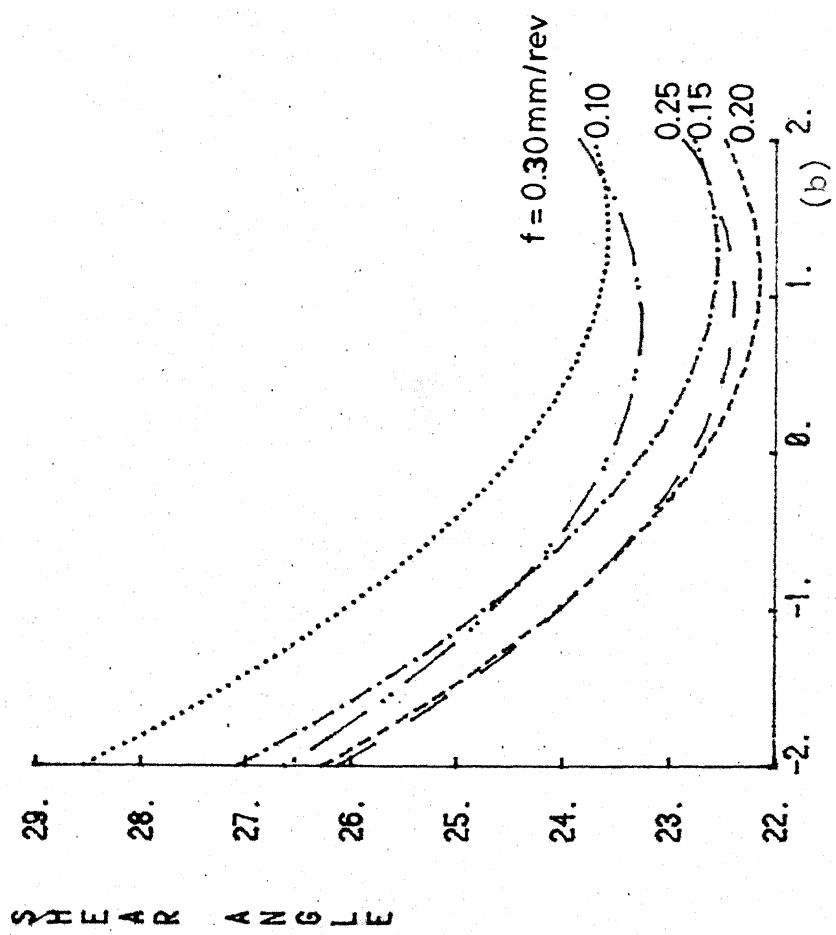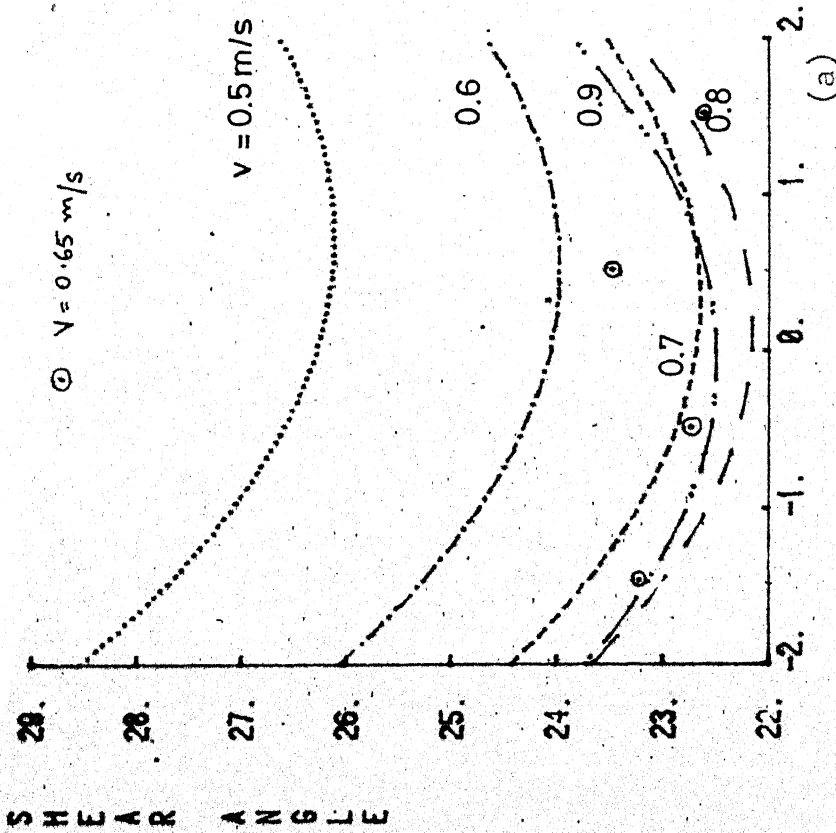
Fig. 4.1 Effect of feed rate and cutting speed on shear angle during longitudinal turning.
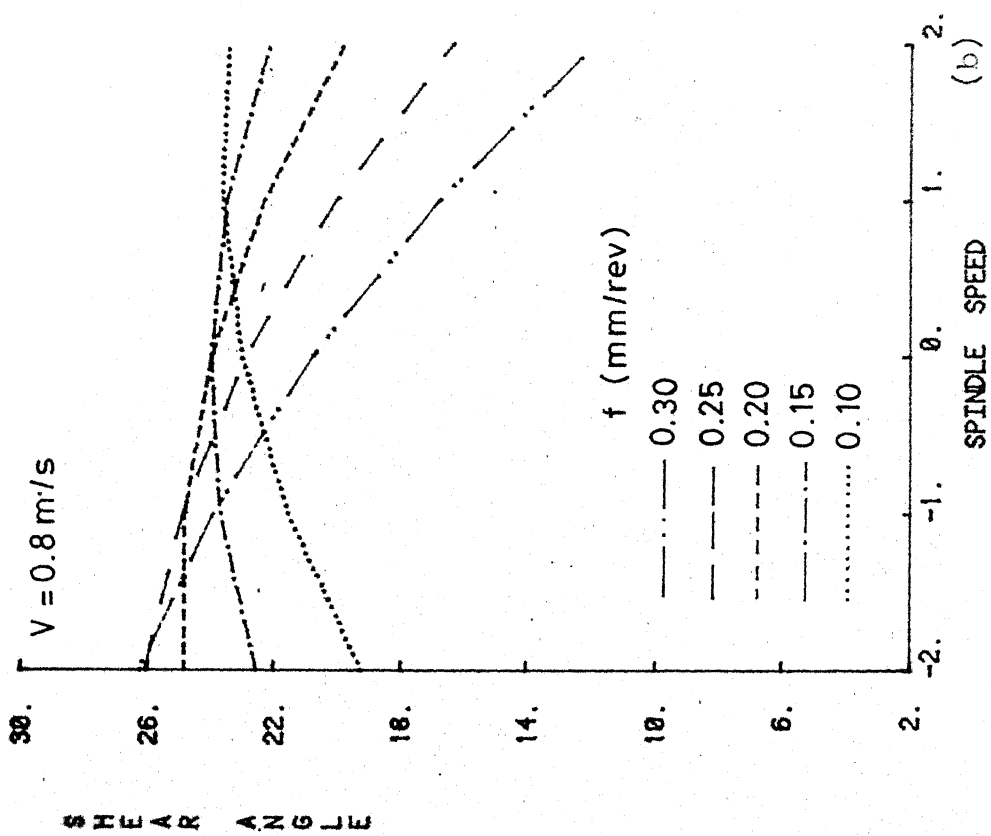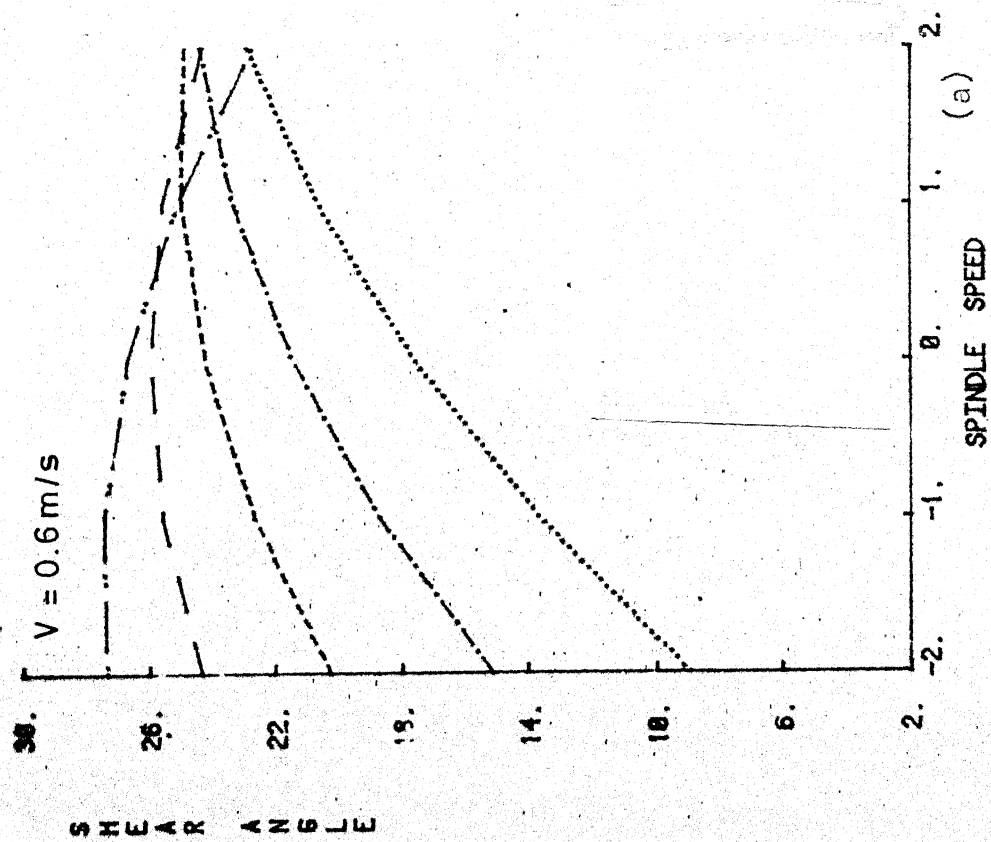
Fig. 4.2 Effect of spindle speed on shear angle during facing.

approximately. [13,19]. As cutting speed increases, mean temperature at tool-chip interface increases, leading to thermal softening. But at about 30 m/min, the size of the bult up edge is maximum. (see Figs (1.4) and (1.7)). As the speed increases, the BUE and hence the actual rake angle starts decreasing. This leads to a rise in specific work done during chip formation (Fig.1.11). It has the dominat effect on specific cutting work as compared to thermal soft-ening. Thus, as the specific cutting work increases the shear angle decreases. However, at cutting speeds near 60 m/min, the thermal softening effect begins to dominate and specific cutting work decreases leading to an increase in shear angle.

Fig. (4.1b) can be explained as follows. Increase in feed rate leads to a rise in temperature, which affects the shape and size of the BUE. The decrease in shear angle with increase in feed is due to the decreasing actual rake angle (due to destruction of BUE) and the subsequent increase is due to thermal softening.

4.1.2 Facing:

Figs (4.2a,b) show the variation of shear angle with spindle speed for constant but different feed rates and cutting speeds. From these figures, it is evident that the trend of relationship between spindle speed and shear angle changes with the change in cutting speed as well as feed rate. For low cutting speed and low feed rate values, the relationship has an increasing trend. But at slightly higher cutting speed and feed rate, shear angle starts decreasing with increase in
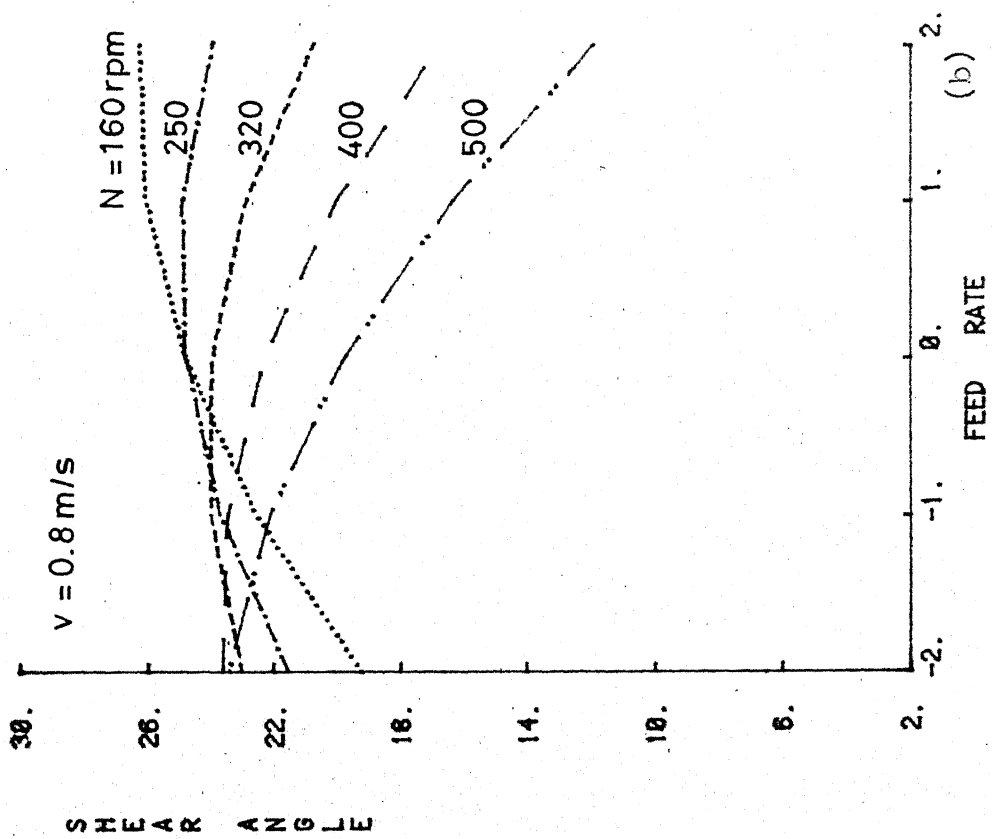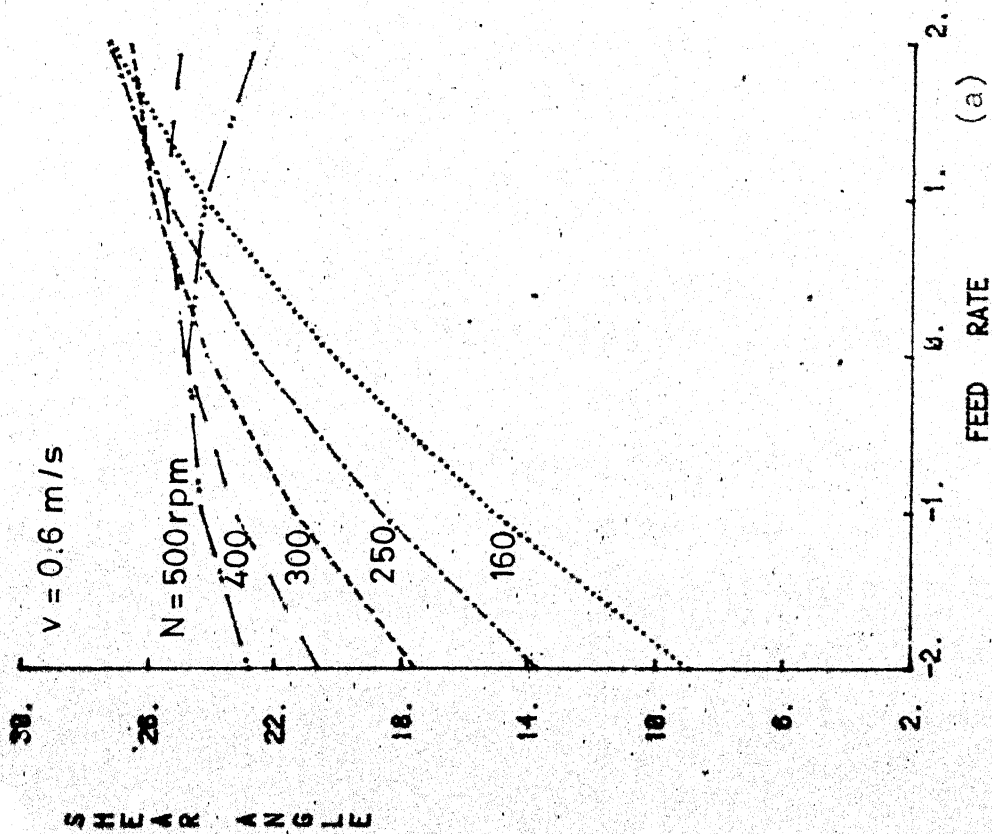
Fig.4.3 Effect of feed rate on shear angle during facing.

spindle speed. Shear angle value reaches a peak earlier
for higher feed rate values than for a lower feed rate value.

Fig. (4.2a) has a relatively low cutting speed of
30 m/s. Here, strain hardening effect is dominated by the
effect of increasing actual rake angle due to BUE formation.
With the increase in actual rake angle, specific cutting
work falls and shear angle increases. (Fig. 1.11, 1.12).

In Fig. (4.2b), shear angle starts to decrease at high
spindle speed and at high feeds. The thermal softening effect
starts from this cutting speed value, but this effect is
dominated by a decrease in actual rake angle value dueto
reduction of BUE. As spindle speed increases, the shear
strain acceleration also increases (a square dependance
exists. (equation 2.7, 2.10)). The specific cutting work
should decrease, but the effect of reducing actual rake angle
appears to dominate and specific cutting work increases at
higher spindle speeds, leading to a decrease in shear angle
value.

Figs (4.3 a,b) show the variation of shear angle
with feed rate for different spindle speeds and cutting speeds.
In Fig. (4.3a), shear angle increases if feed rate is increased,
cutting speed and spindle speed being constant. At higher
spindle speeds and cutting speeds, the shear angle increases,
reaches a peak, and then starts decreasing at low velocities
(Fig. 4.3a), the increase may be due to the dominant effect of
increasing actual rake angle (due to BUE); the effect of
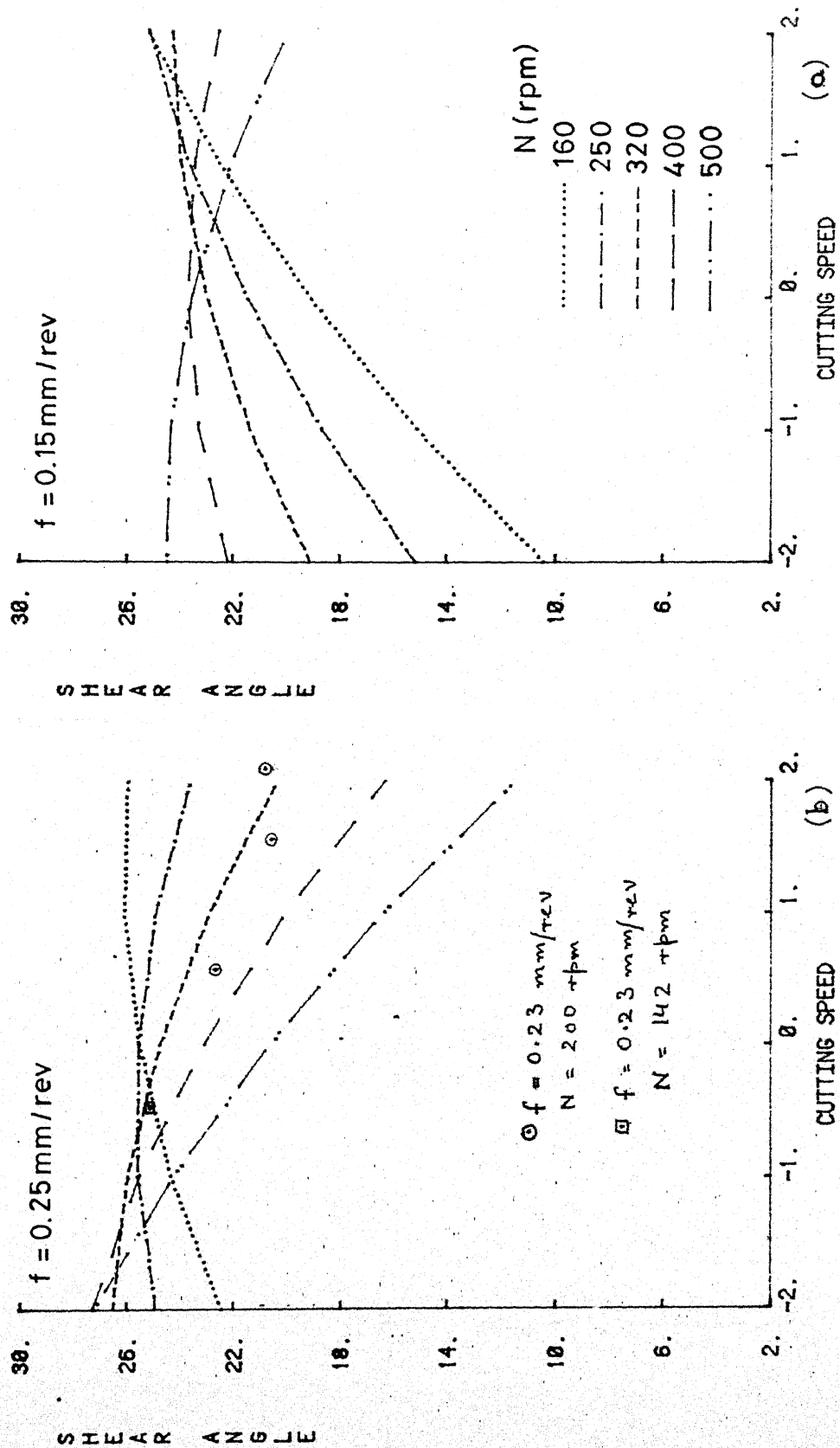
Fig. 4.4 Effect of cutting speed on shear angle during facing.
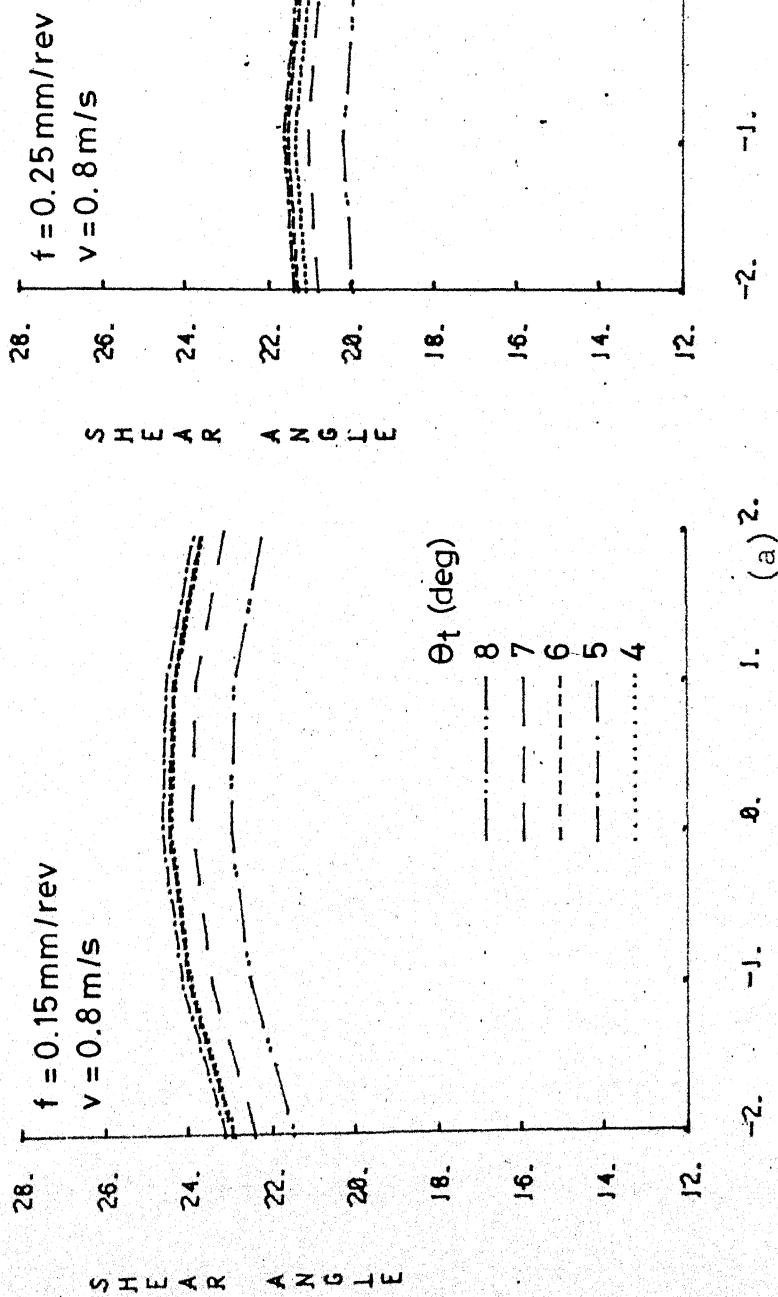
Fig.4.5 Effect of spindle speed on shear angle during taper turning.

41

strain hardening being less dominant. As cutting speed increases, so does the temperature (Fig. 1.9, 1.10) at the tool-chip interface.

Thus, in Fig. (4.3b) the effect of thermal softening causes reduction of BUE and thus leads to reduction in actual rake angle. The reduction in specific cutting work due to thermal softening is dominated by the increase in cutting work due to the decreasing actual rake angle. So shear angle now decreases as feed rate increases (Fig. 1.12).

Figs (4.4 a,b) show the variation of shear angle with cutting speed. For low feed rate and low spindle speed (Fig.4.4a the shear angle increases with cutting speed. For higher feed rate values, the shear angle attains a maxima and then starts decreasing with increase in cutting speed.

The effect of increase in cutting speed is due to increase in the chip-tool interface temperature. This causes an effect similar to that of feed rate. So at low feeds, shear angle increases with cutting speed. For large feeds, shear angle decreases with increase in cutting speed. The decrease is due to the effect of decreasing effective rake angle and the increase is due to the formation of BUE and the resulting increase in effective rake angle.

4.1.3 Taper turning:

Figs. (4.5 a,b) show the variation of shear angle with spindle speed. The value of shear angle decreases with

v = 0.8 m/s
f = 0.25 mm/rev

28.
26.
24.
22.
20.
18.
16.
14.
12.

S
H
E
A
R

A
N
G
L
E

-2.   -1.   0.   1.   2.

TAPER ANGLE

(b)

v = 0.8 m/s
f = 0.15 mm/rev

28.
26.
24.
22.
20.
18.
16.
14.
12.

S
H
E
A
R

A
N
G
L
E

N (rpm)
———— 500
— — 400
– – – 320
–·–· 250
········ 160

-2.   -1.   0.   1.   2.

TAPER ANGLE

(a)
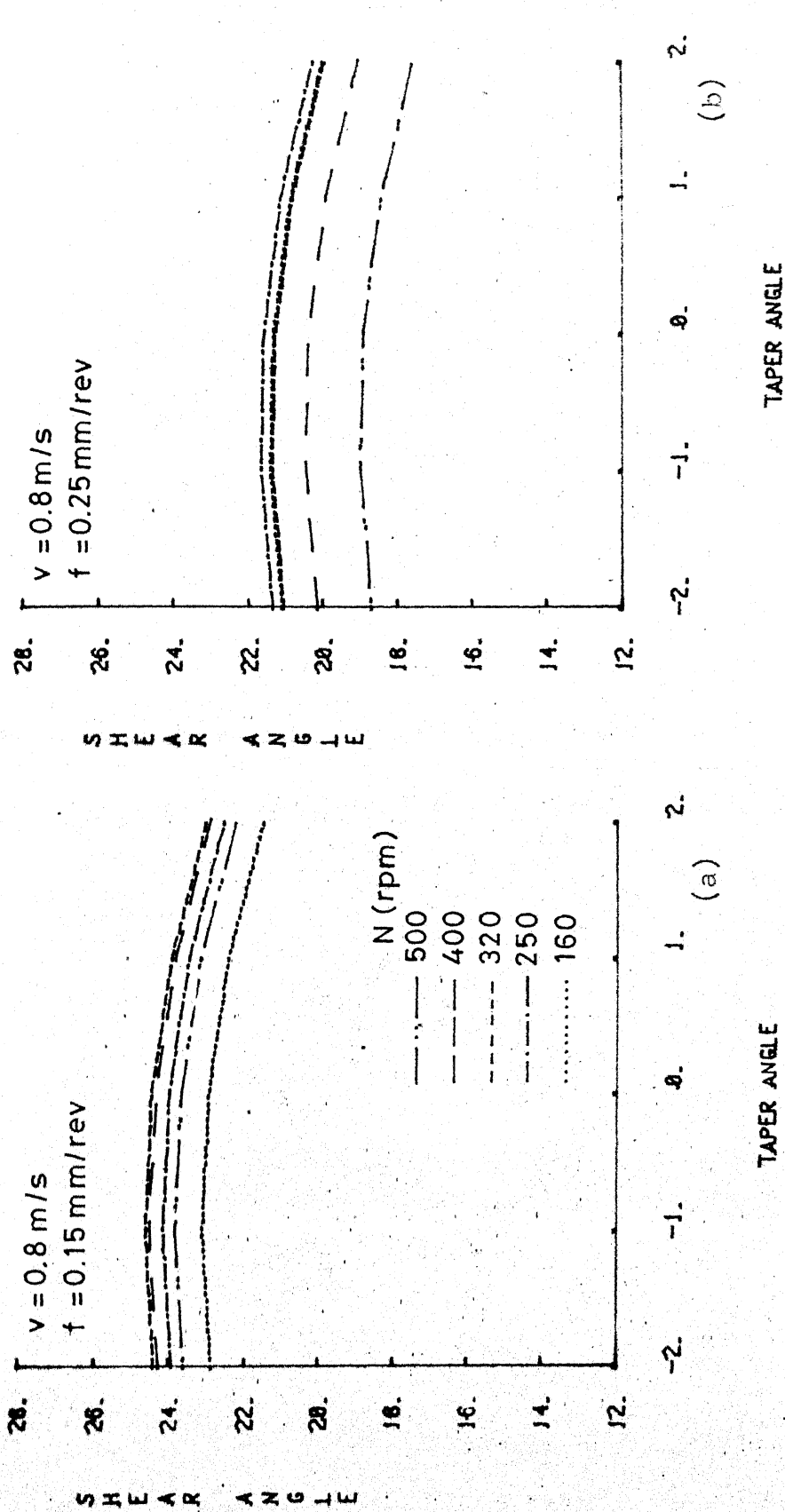
Fig.4.6   Effect of taper angle on shear angle during taper turning.
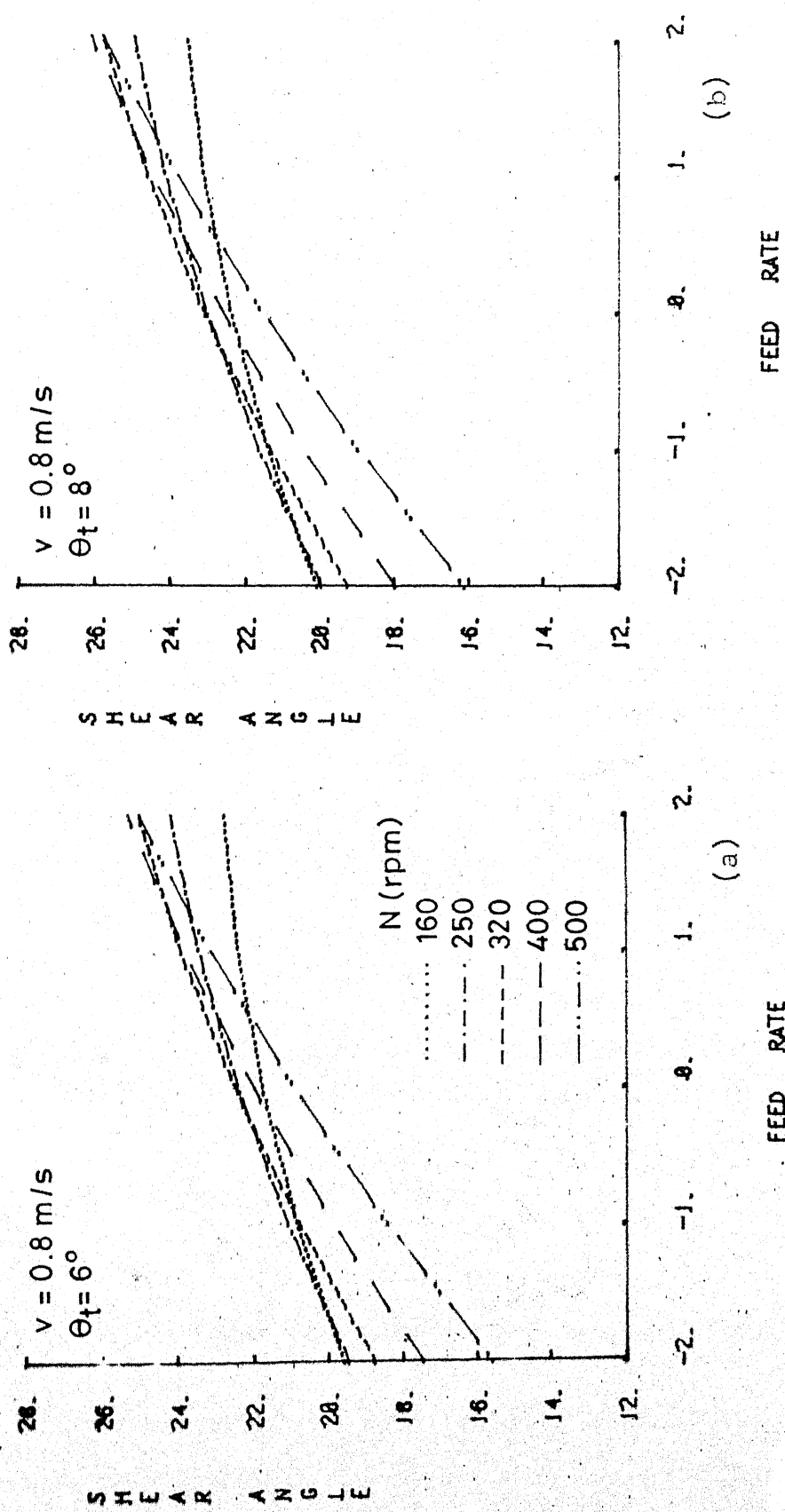
Fig.4.7 Effect of feed rate on shear angle during taper turning.

increasing spindle speed at low feed values. However, it
increases slightly for high feed values.

In Fig. (4.5a), the feed is low but the cutting speed
is high (V=0.8 m/s). The fall in shear angle is due to the
effect of decreasing actual rake angle (and BUE), dominating
the effect of thermal softening. At higher feeds, the effect
of thermal softening dominates and a small rise in shear angle
value results.

Figs.(4.6 a,b) show that the effect of taper angle on
shear angle is negligible. This is as the variation in taper
angle taken is small. A four degree change in taper causes
only a change of .069 in strain rate and strain acceleration.

Figs. (4.7a,b) show the variation of shear angle with
increase in feed rate. Shear angle increases with increase
in feed rate. The cutting speed is relatively high (v=0.8 m/s).
At St this speed, probably the thermal softening effect dominates
the effect of reducing BUE. Due to the effect of strain acce-
leration increase in shear angle is faster for higher spindle
speeds than for lower spindle speeds.

4.2 Microhardness:

4.2.1 Longitudinal turning:

Fig. (4.8 a) shows the variation of microhardness
with feed rate. For low cutting speed values, microhardness
increases with increase in feed rate, while for high cutting
speed values, it decreases.
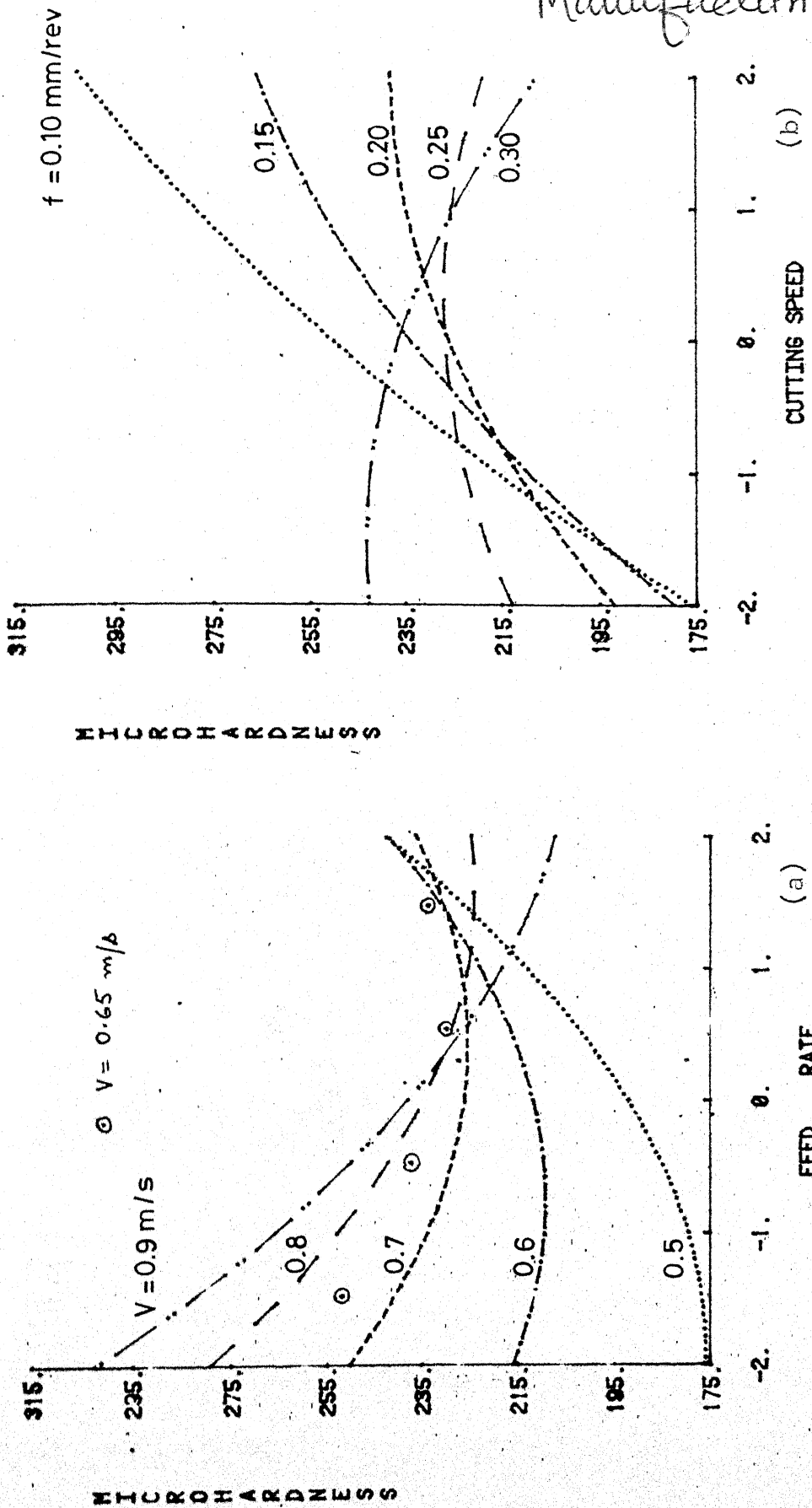
Fig.4.8 Effect of feed rate and cutting speed on microhardness during longitudinal turning.
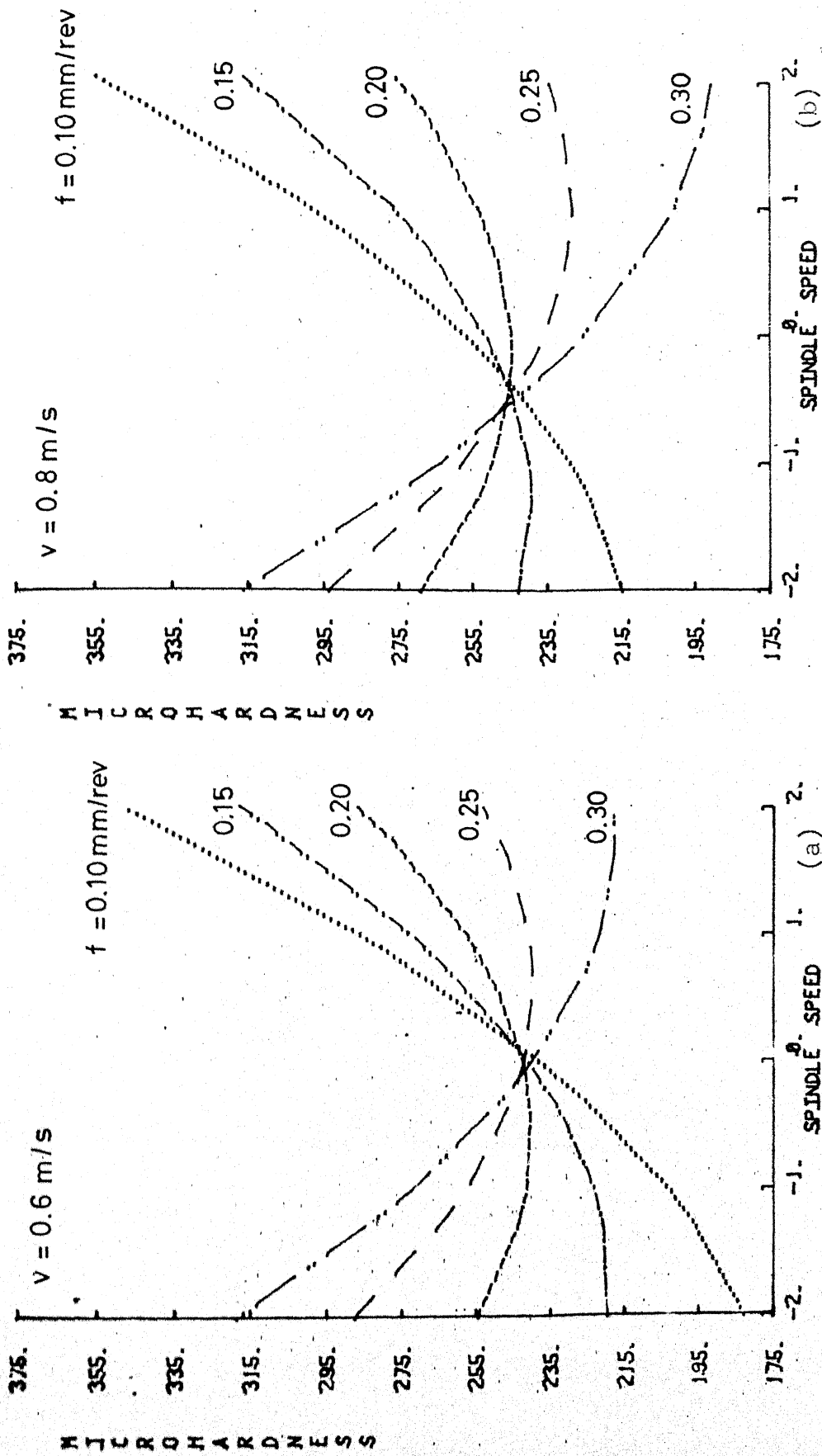
Fig. 4.9 Effect of spindle speed on microhardness during facing.

47
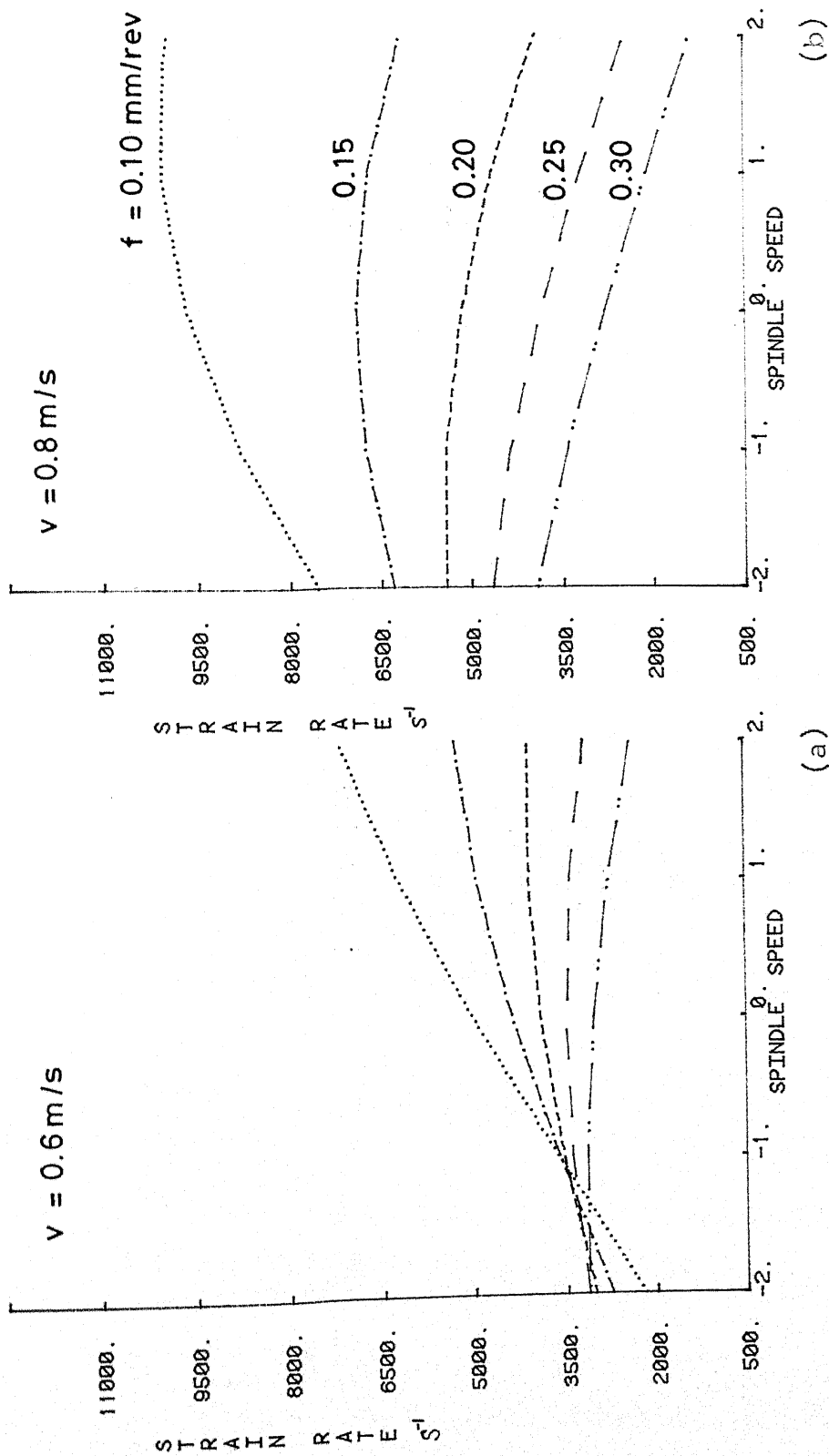
Fig. 4.10 Strain rate variation for Fig. 4.9
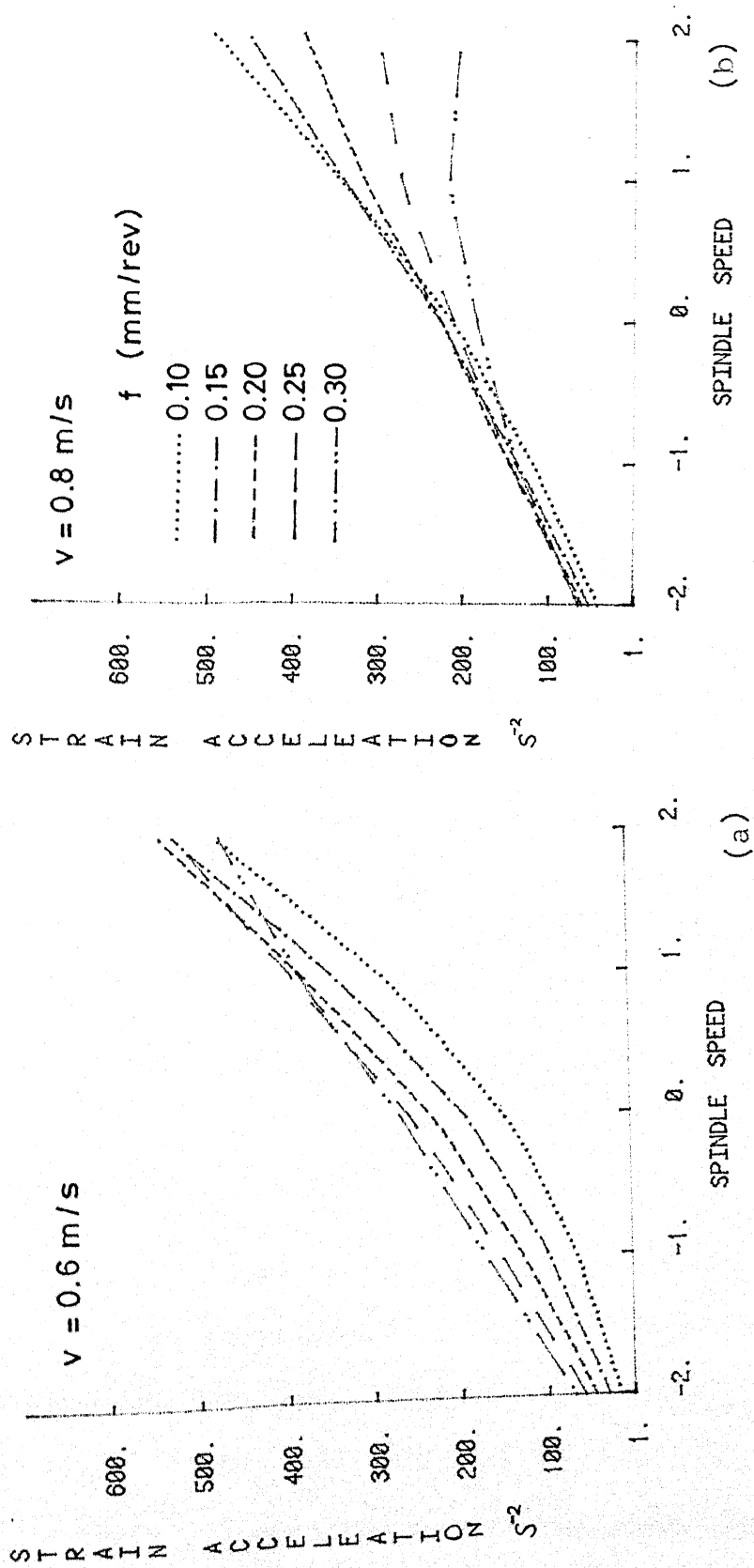
Fig. 4.11 Strain acceleration variation Fig. 4.9.

This variation can be explained as follows: μAt low cutting speeds the increase in strain rate causes strain hardening (equation 2.4), leading to increase in microhardness. At higher cutting speeds, the effect of thermal softening dominates, leading to a decrease in microhardness.

Fig.(4.8b) shows the variation of microhardness with cutting speed. At low feed rates, the microhardness increases with increase in cutting speed. At high feed rates, the micro-hardness decreases with increase in cutting speed.

This can be explained as follows: At low feed rates, the strain rate increases with increase in cutting speed and the strain hardening caused has the dominat effect. So the microhardness increases. At higher feed rates, the thermal softening starts to dominate since heat generation is move. Thus, the microhardness decreases with increase in cutting speed.

4.2.2 Facing:

These results can be explained considering the effects of three factors, namely strain hardening, thermal softening; and strain acceleration.

Fig. (4.9a) shows that at low cutting speeds, microhard-ness of chips increases with spindle speed, for low feed, but it decreases for high feed values. At high cutting speeds Fig. (4.9b) also, this trend is maintained.

This can be explained if we take into account the strain
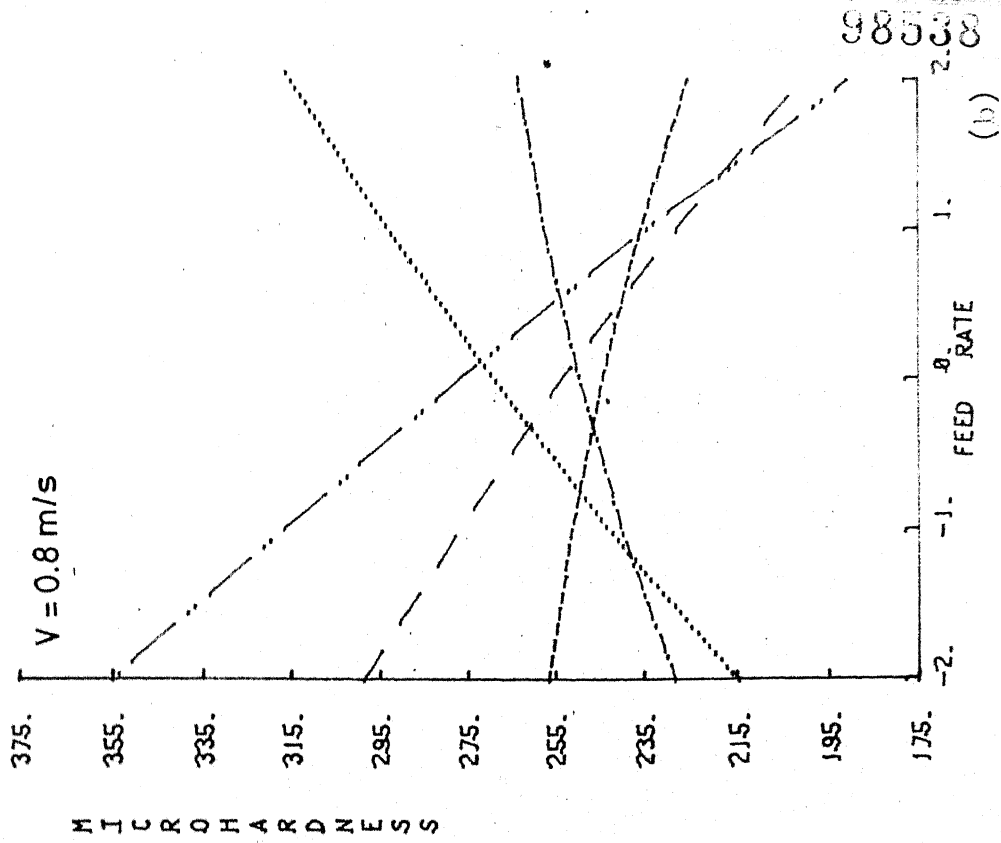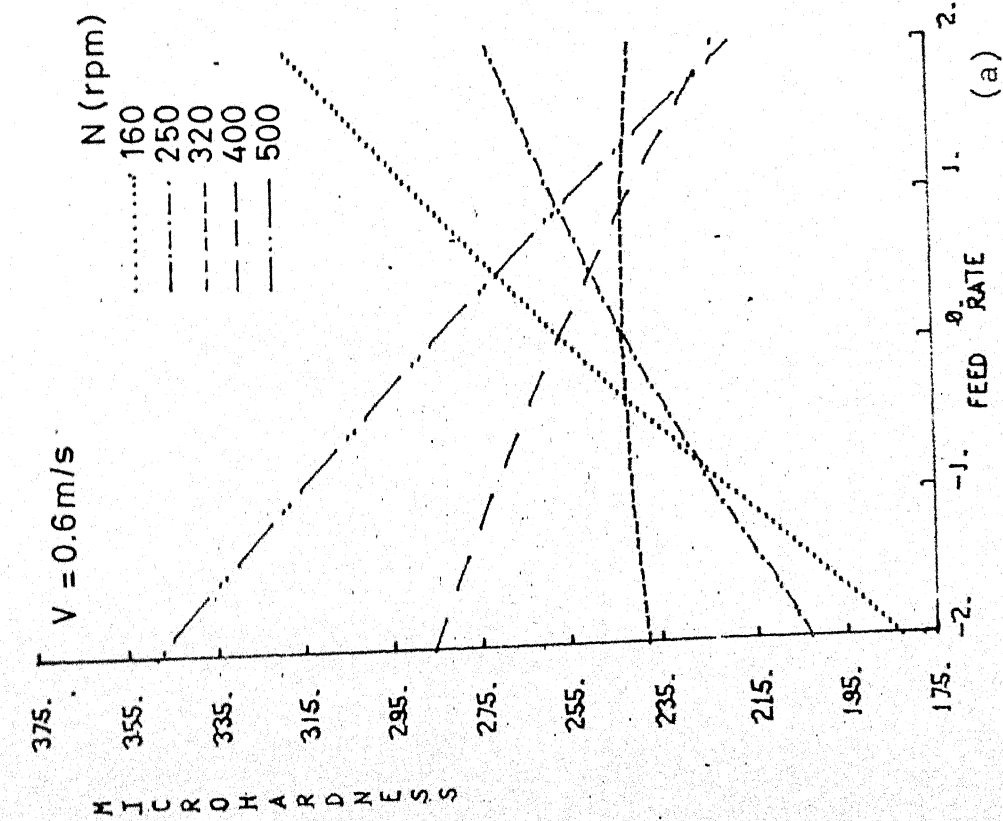
Fig.4.12 Effect of feed rate on microhardness during facing.
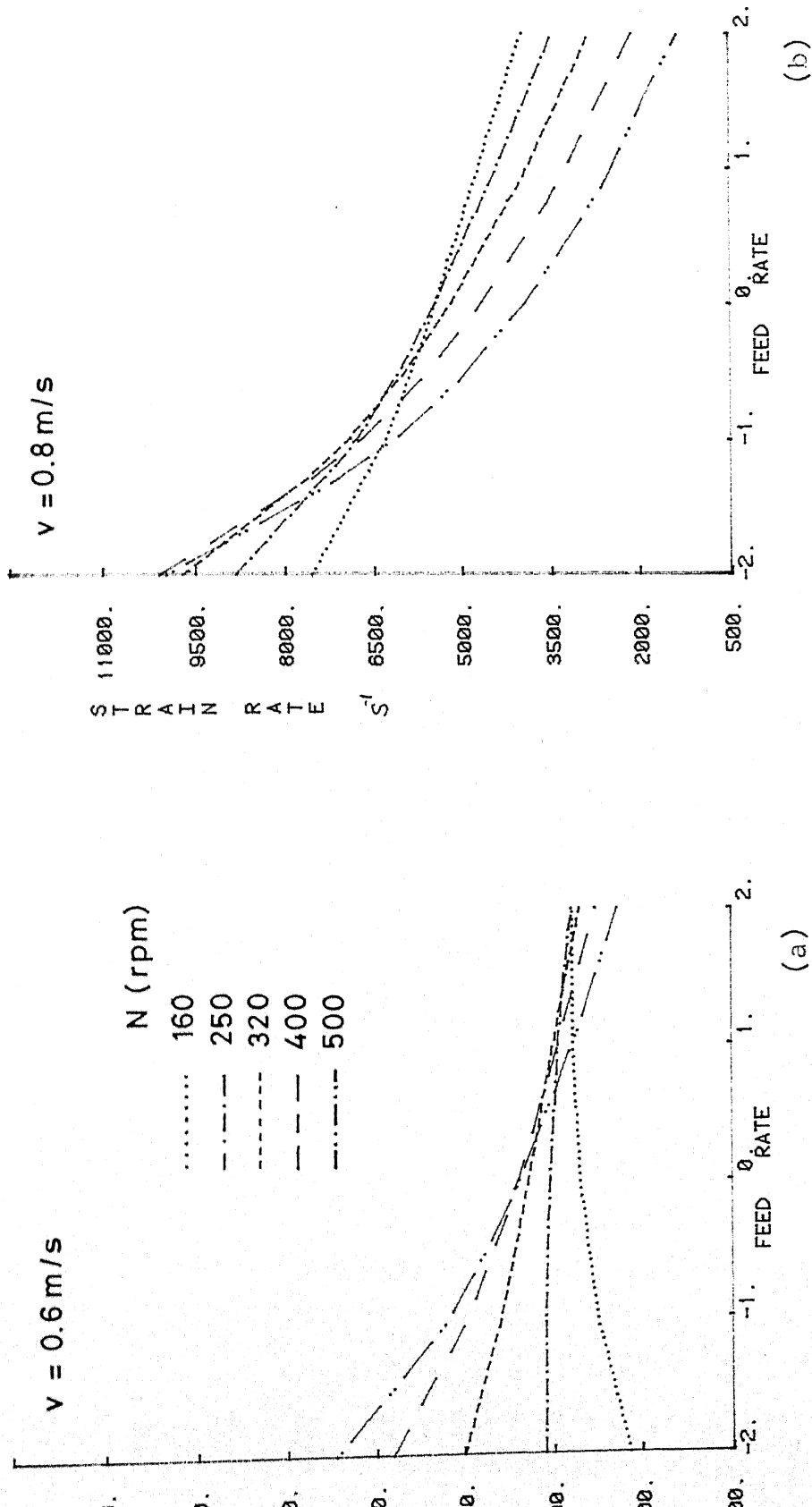
Fig. 4.13 Strain rate variation for Fig. 4.12.
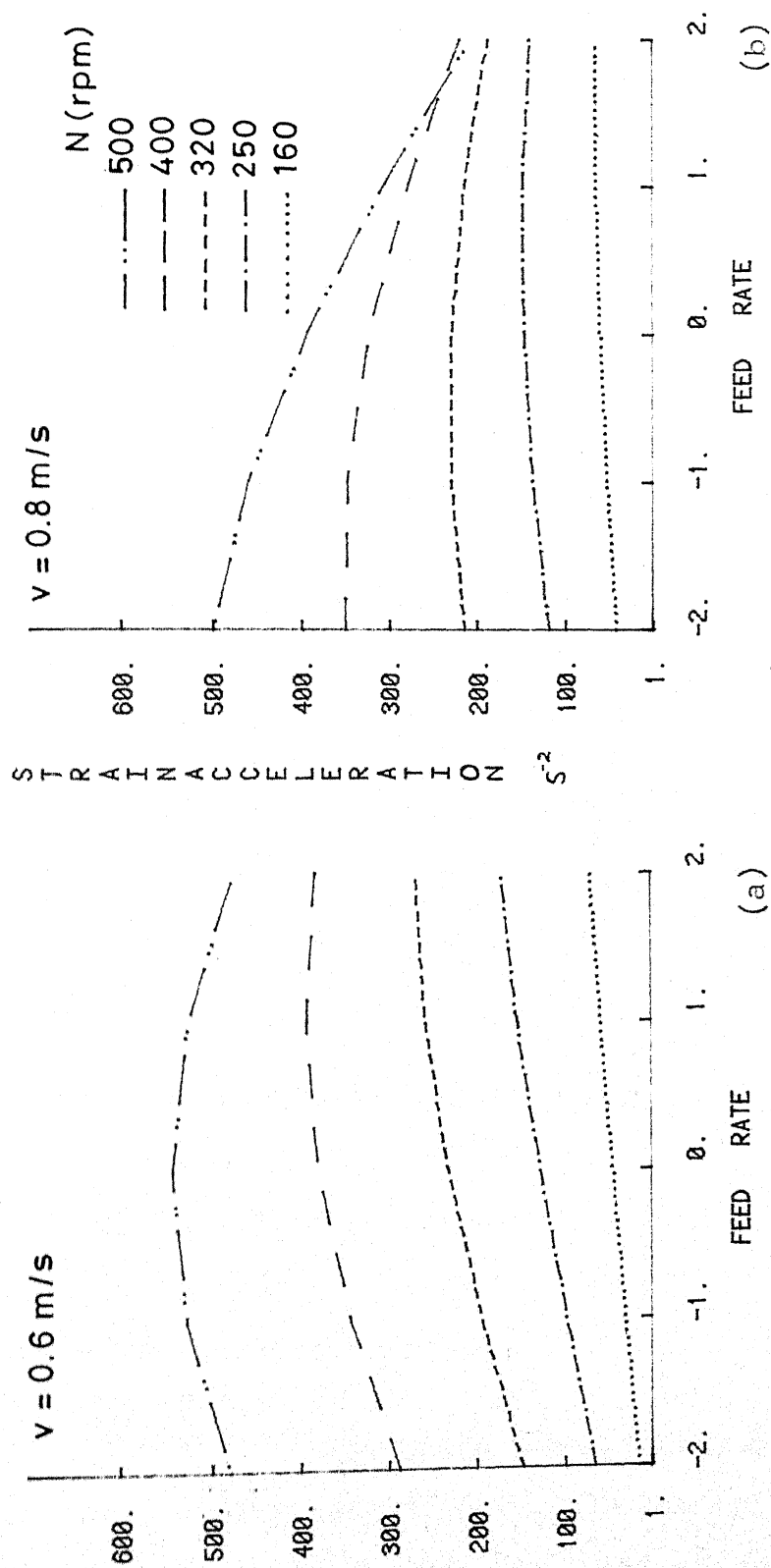
Fig. 4.14 Strain acceleration variation for Fig. 4.12.

Fig. 4.14 Strain acceleration variation for Fig. 4.12.

cutting speed,varies (see ref. 6) as

$$\dot{\gamma} = k. \frac{\text{Sin } \phi \text{ Sin } (45+\phi)}{f \text{ Cos}^2 \phi} \qquad (4.1)$$

where k is a constant. So the effect of variation of shear
angle is reflected in strain rate. For low cutting speed
and feed, the shear angle (and thus strain rate) value
increases sharply with spindle speed. For low cutting speed
and high feed rate, the strain rate value (Fig. 4.10b) incre-
ases slightely and then decreases. Thus the effect of strain
hardening dominates for lower feed values, leading to a rise
in microhardness. For high feed values, the effect of strain
hardening is less. The combined effects of thermal softening
and strain acceleration demonate, leading to a decrease in
microhardness.

At high cutting speed (Fig. 4.11a,b), there is still a
rise in strain rate at low feed and a drop in strain rate at
high feed value, so the same trend as in Fig. (4.9a) is
maintained.

Figs. (4.12a,b) show the variation of microhardness
with feed rate. At low cutting speed, the microhardness incre-
ases for low spindle speeds and decreases for high spindle
speeds. This trend is maintained at higher cutting speeds
(Fig. 4.12b) as well.

The strain rate plots Figs.(4.13a,b) show that the
strain rate at low cutting speed and low spindle speed increases
with increase in feed rate. For high spindle speeds, this

f = 0.30 mm/rev

⊙ f = 0.23 mm/rev
N = 200 rpm

⊡ f = 0.23 mm/rev
N = 142 rpm

CUTTING SPEED

(b)

MICROHARDNESS

375.
355.
335.
315.
295.
275.
255.
235.
215.
195.
175.

f = 0.15 mm/rev

N = 500 rpm

400

320

250

160

CUTTING SPEED

(a)

MICROHARDNESS

375.
355.
335.
315.
295.
275.
255.
235.
215.
195.
175.

Fig. 4.15 Effect of cutting speed on microhardness during facing.

f = 0.30 mm / rev

N (rpm)

.... 160
—·—·— 250
— — — 320
— — — 400
—··—··— 500

S T R A I N — R A T E s^{-1}

11000.

9500.

8000.

6500.

5000.

3500.

2000.

500.

CUTTING SPEED

-2.   -1.   0.   1.   2.

(b)

f = 0.15 mm / rev

CUTTING SPEED

-2.   -1.   0.   1.   2.

(a)
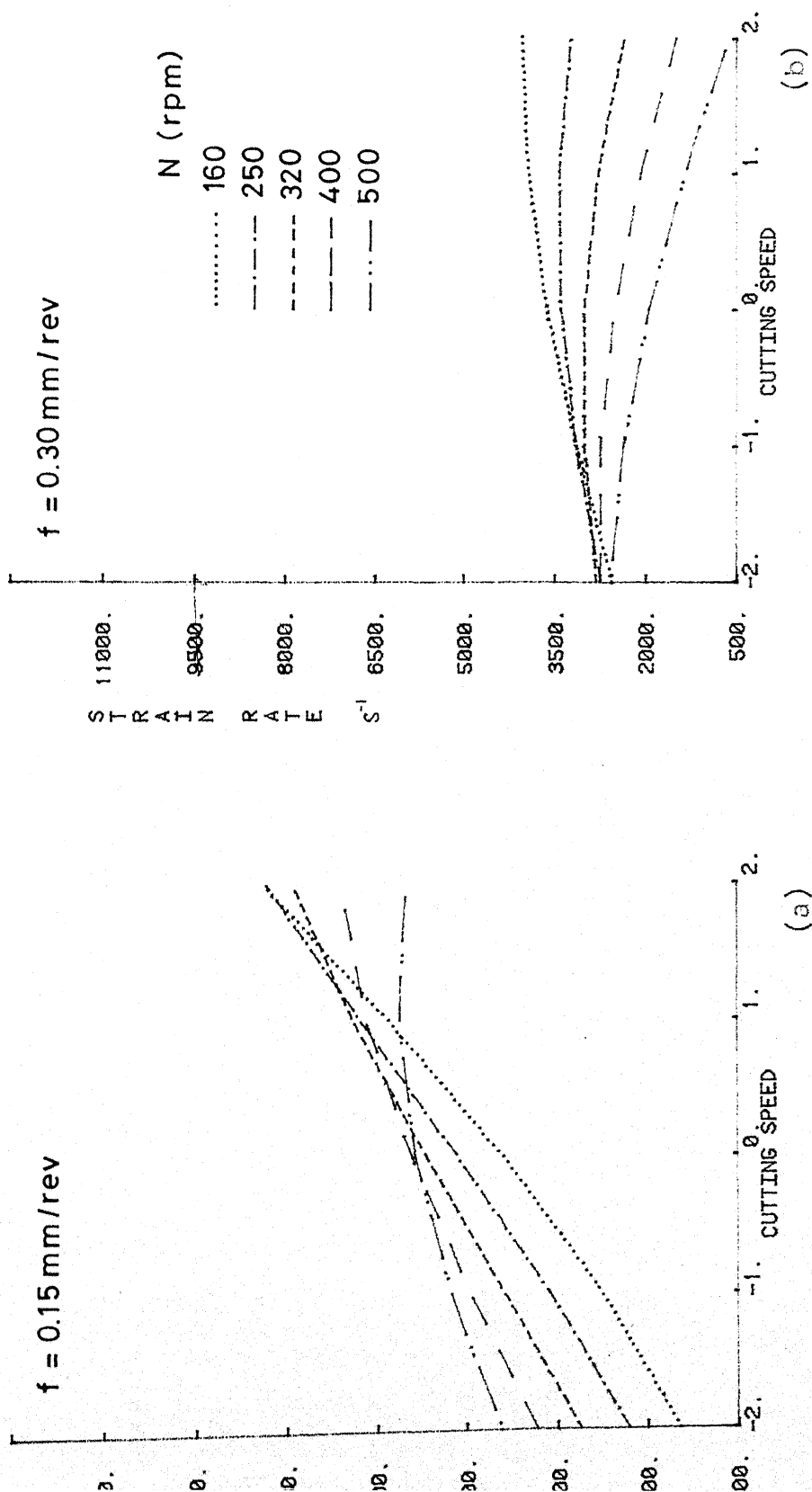
Fig. 4.16 Strain rate variation for Fig. 4.15.
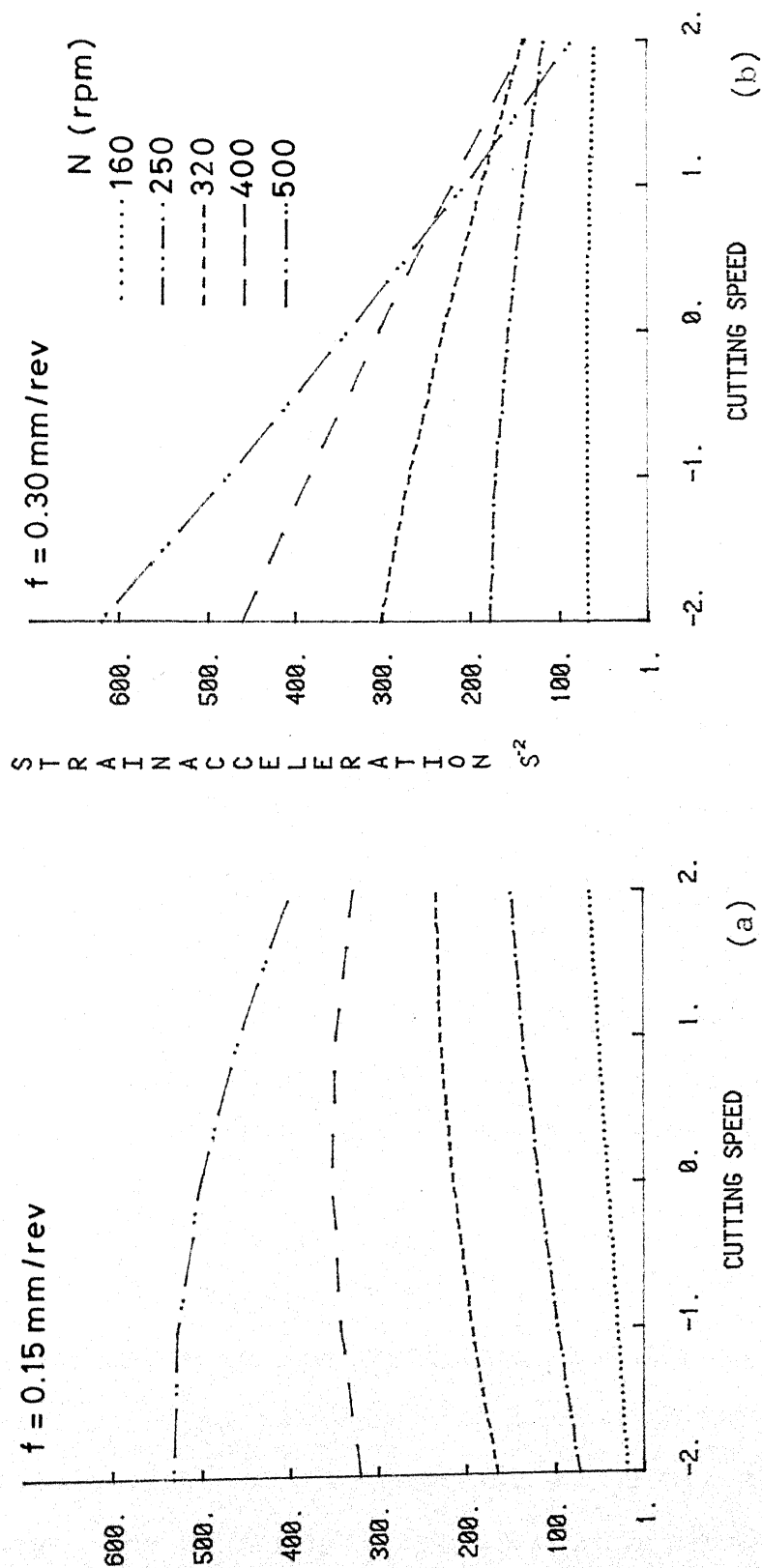
Fig. 4.17 Strain acceleration variation for Fig. 4.15.

decreases with increase in feed rate. At higher cutting
speed, however, strain rate decreases with increase in feed
at all spindle speeds (Fig.4.14a,b).

So at low cutting speed and low spindle speed, the
effect of increasing strain rate dominates, leading to strain
hardening and a rise in microhardness value. At higher spindle
speeds, and low cutting speed, the strain rate decreases slightely
causing lesses strain hardening. Thus the thermal softening
effect dominates leading to a reduction in microhardness value.

At high cutting speed and low spindle speed, strain
rate decreases with increase in feed rate and the microhardness
should decrease but it does not. At high cutting speed and
high spindle speed, microhardness decreases with increase in
feed rate as expected, due to thermal softening.

Fig. (4.15a,b) shows the variation of microhardness
with increase in cutting speed. At low feed rates the micro-
hardness decreases slightely then tends to increase. However,
at high spindle speed,,high feed rate and high cutting speed
(Fig. 4.15b) microhardness starts increasing with increase in
cutting speed.

The decrease in microhardness at low feed and low
spindle speed is due to thermal softening. Strain rate
Fig. (4.17 a,b) is higher for higher spindle speed, so the
absolute value of microhardness is higher at higher spindle
speed. The decrease in microhardness being due to thermal
softening.

Fig.4.18 Effect of spindle speed on microhardness during taper turning.
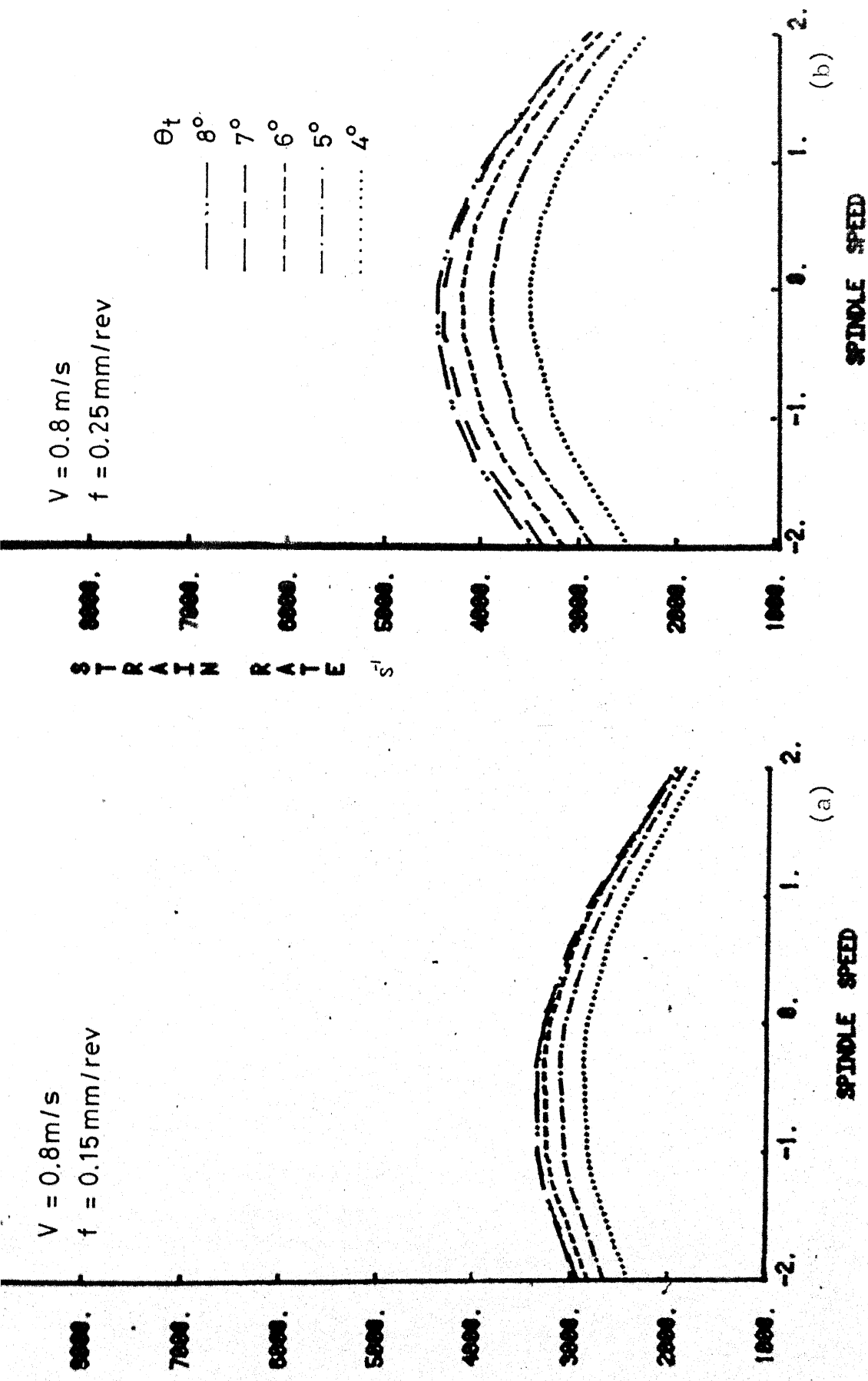
Fig. 4.19 Strain rate variation for Fig. 4.18.
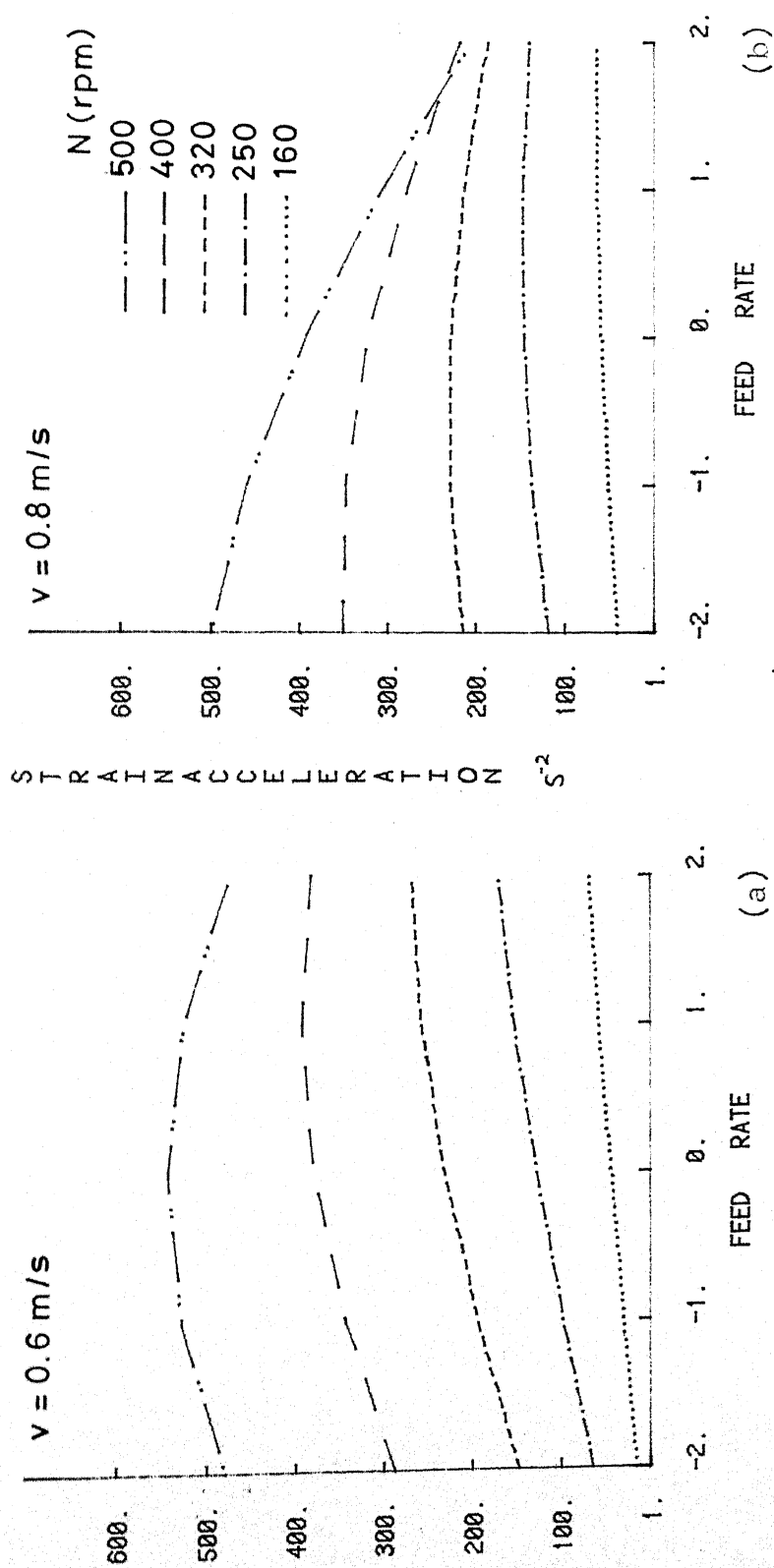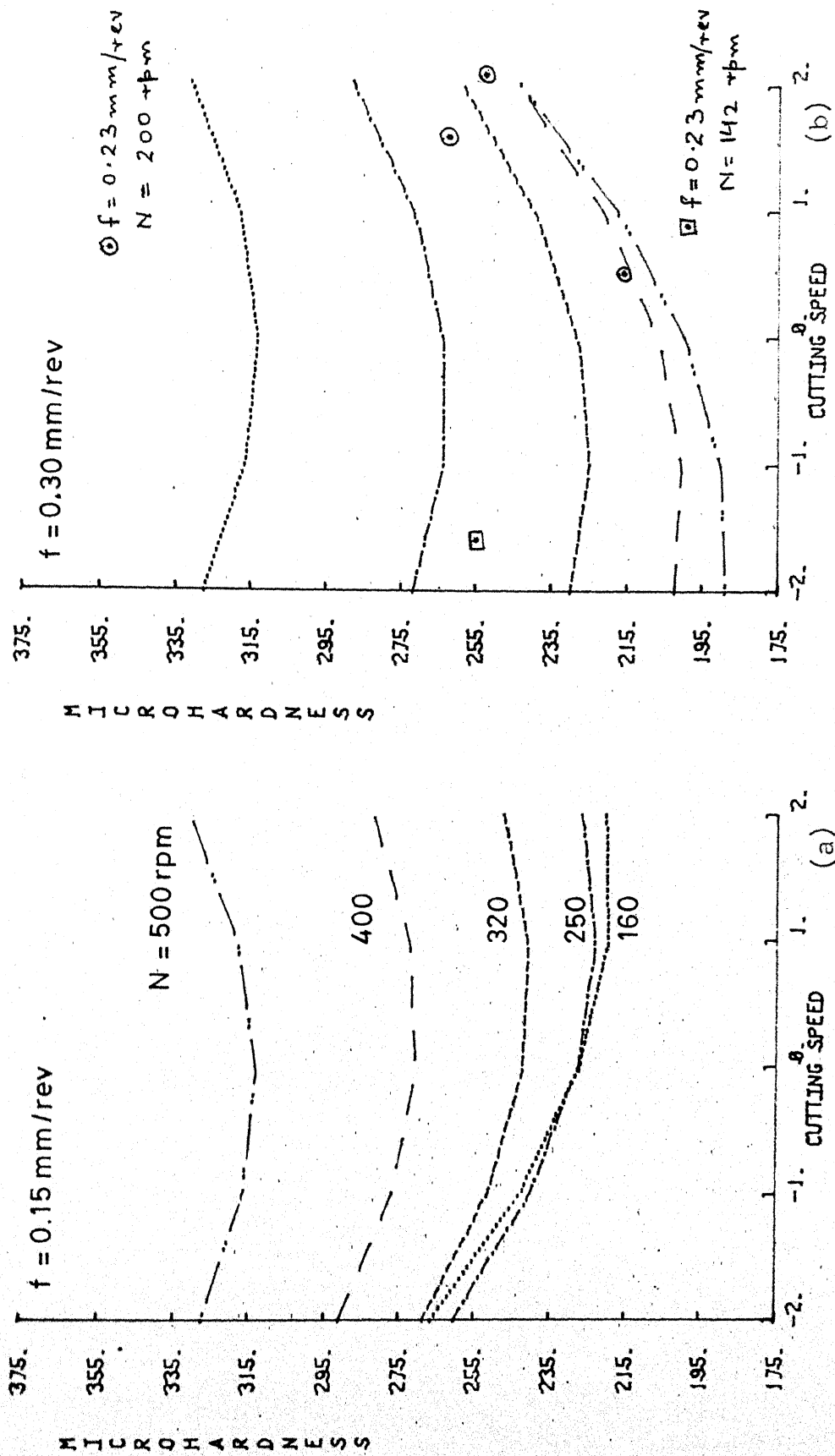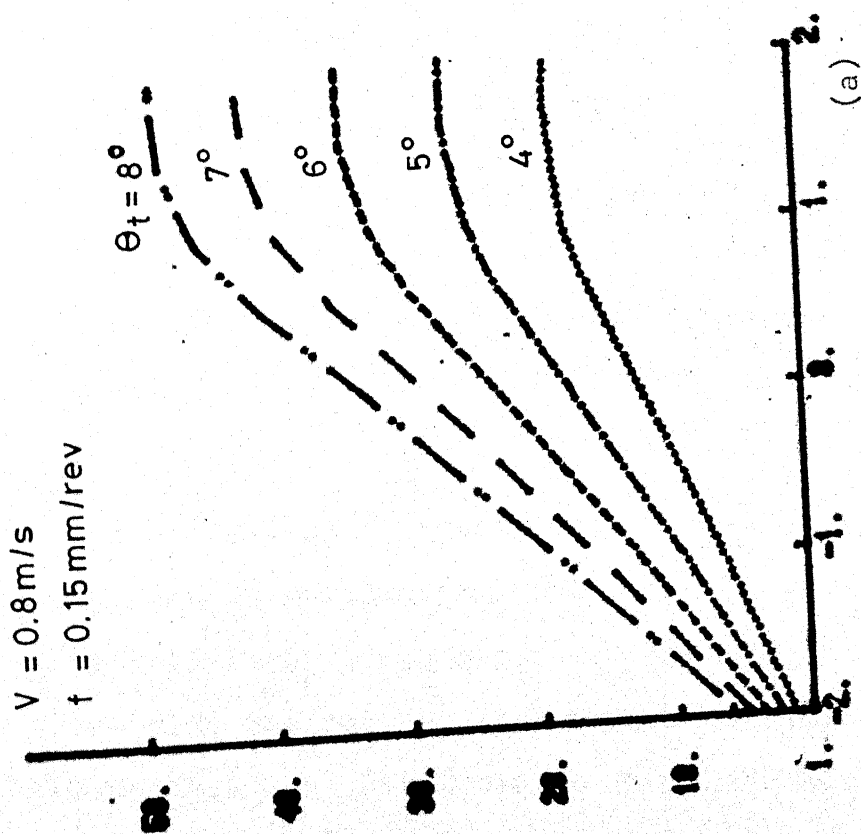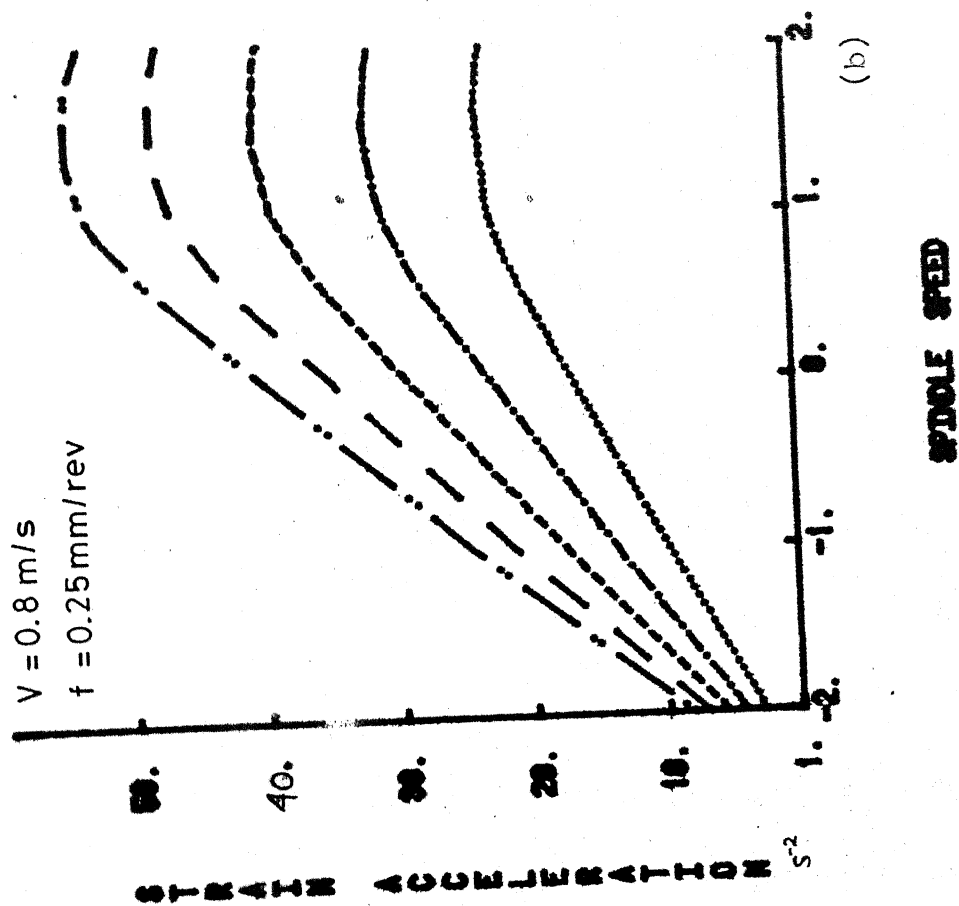
Fig. 4.20 Strain acceleration variation for Fig. 4.18.

At higher feed rate, the strain rate Fig. (4.17b) increases at low spindle speed anddecreases at high spindle speed. Since the absolute value of strain rate at lower spindle speed is higher, microhardness is also higher at lower spindle speed.

4.2.3 Taper turning:

Figs.(4.18a,b) show the variation of microhardness with spindle speed. The microhardness increases with increase in spindle speed.

This can be explained on the basis of the effect of strain acceleration. Strain acceleration produces two opposing effects on shear flow stress viz. the temperature lag effect and the effect on material properties (dislocation generation and interaction).

It is expected that at lower strain acceleration values, the effect on material properties may not be significant. Thus at lower strain acceleration values the effect of temperature lag may be dominant. At higher strain accelerations (Fig. 4.20) the effect inhibition of dislocation interaction and generation starts, and this dominates the effect of temperature lag.

The strain acceleration values during taper turning are quite low as compared to facing. Thus in taper turning the effect of temperature lag plays a significant role. In the above case the strain acceleration variation can be seen in figure (4.20). The increase in strain acceleration causes the deformation to occur at lower temperatures than it would
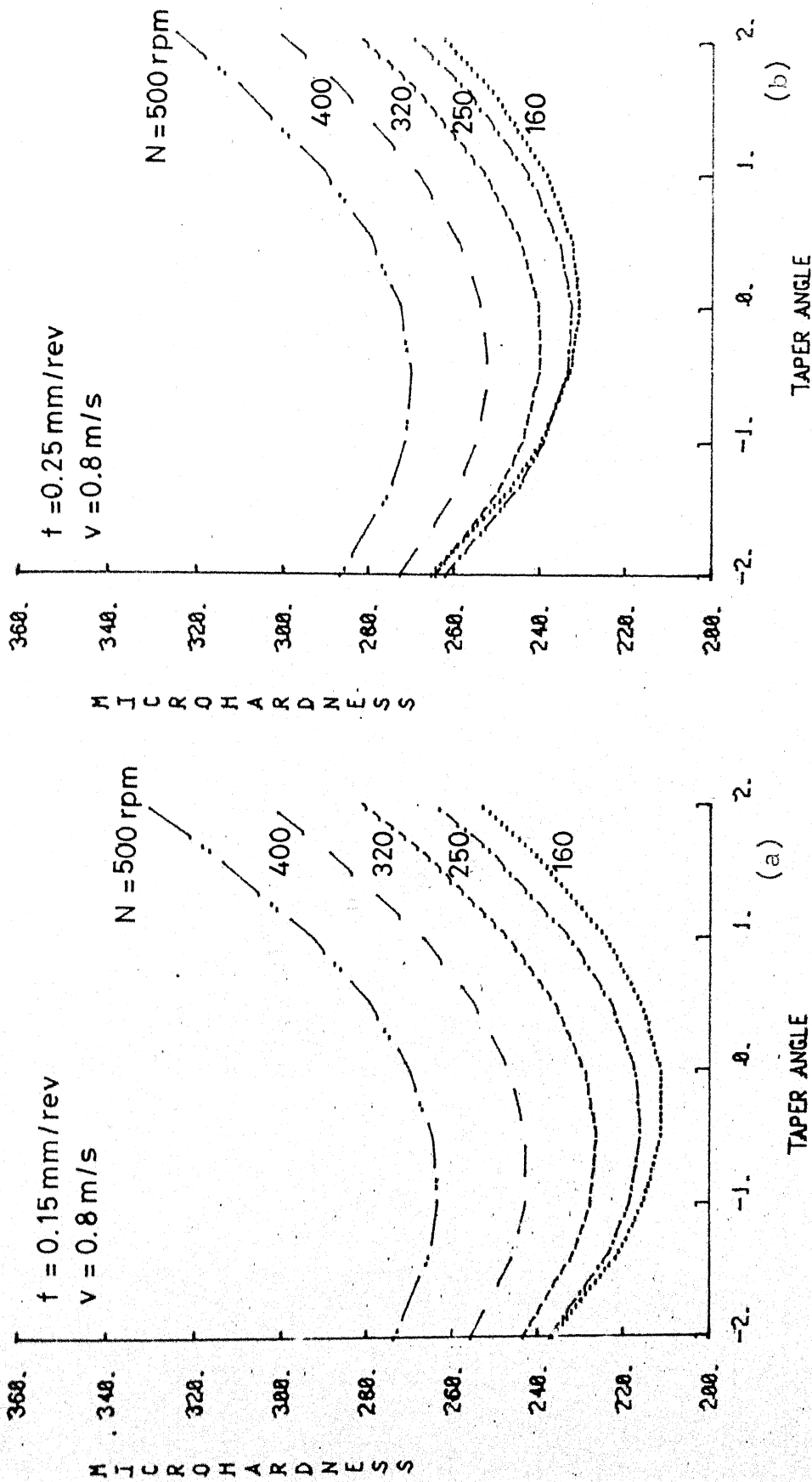
Fig.4.21 Effect of taper angle on microhardness during taper turning.

f = 0.25 mm/rev

f = 0.15 mm/rev

N (rpm)

.... 160
—··— 250
— — — 320
— — 400
—··— 500

TAPER ANGLE

(a)

(b)

STRAIN RATE S^{-1}

8000.
7000.
6000.
5000.
4000.
3000.
2000.
1000.
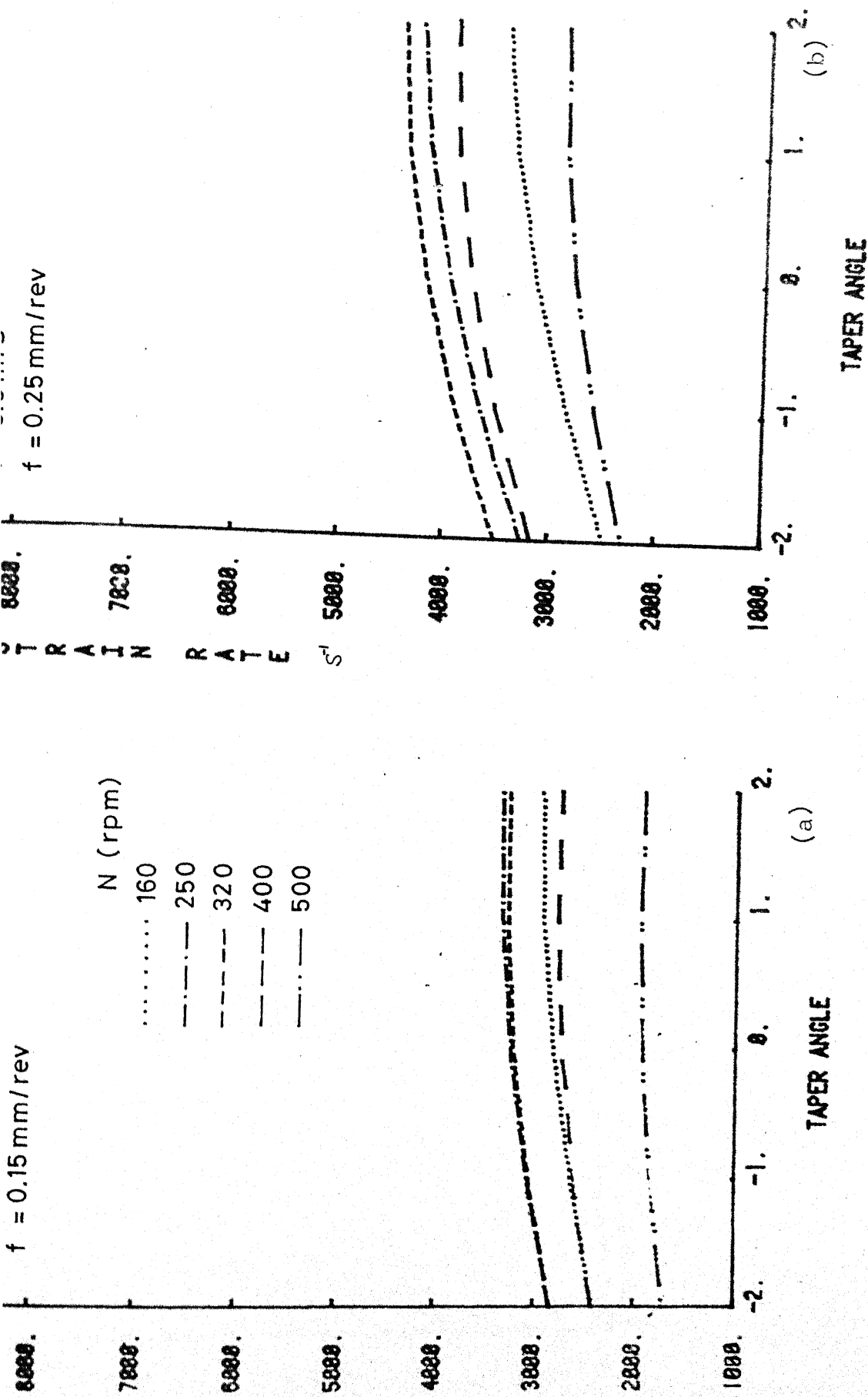
Fig. 4.22 Strain rate variation for Fig. 4.21.
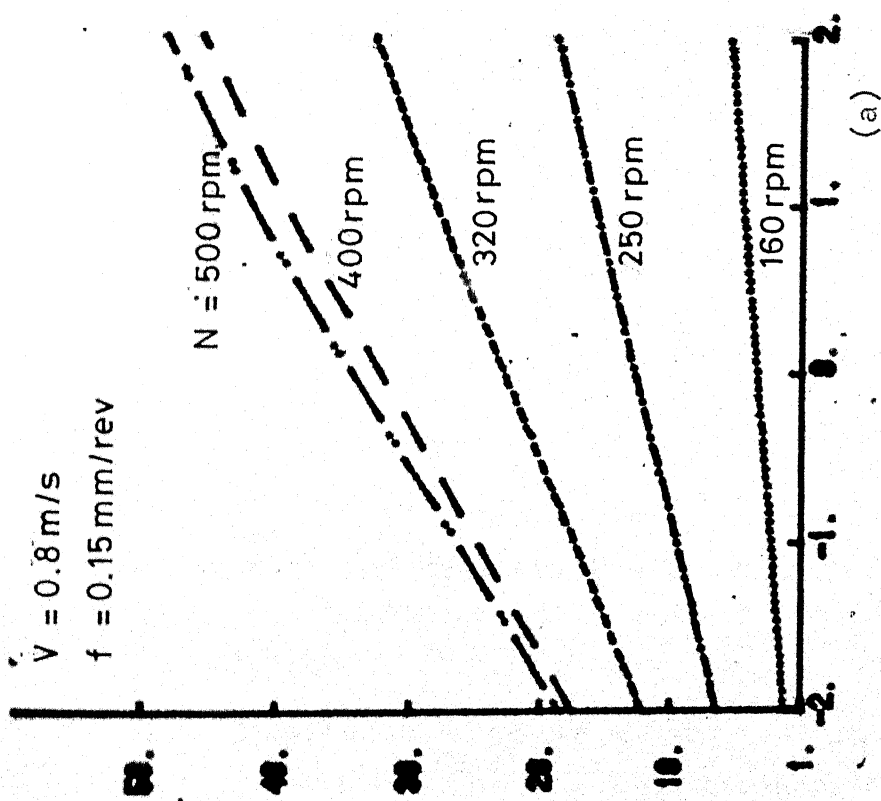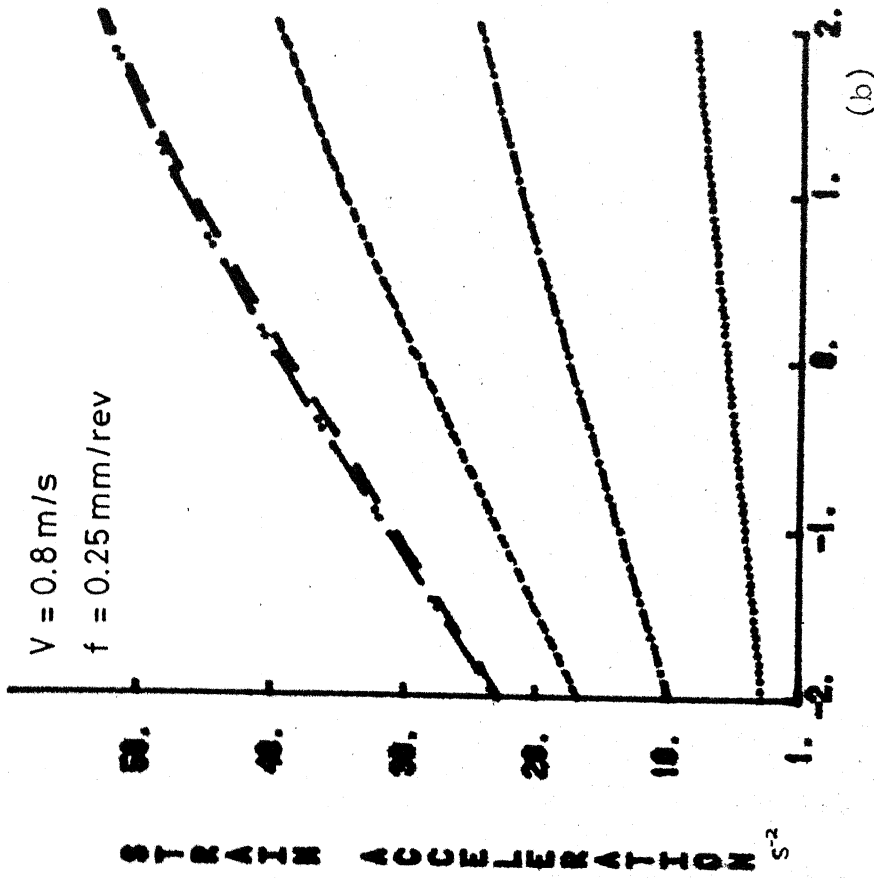
Fig. 4.23 Strain acceleration variation for Fig. 4.21.

normally occur. This leads to more strain hardening where strain acceleration is higher. This explains the increase in microhardness with increase in spindle speed.

Fig.(4.21) shows the variation of microhardness with taper angle. Microhardness increases with increase in taper angle except a slight dip at the begining.

Figs. (4.22a,b) and Figs. (4.23a,b) show that strain rate and strain acceleration both increase with increase with taper angle, so the microhardness increases with increase in taper angle.

Figs. (4.24a,b) show the variation of microhardness with feed rate. The microhardness decreases with increase in feed rate.

Figs. (4.25a,b) and Figs.(4.26a,b) show that while strain rate decreases slightely, the increase in strain acceleration is negligible. Thus the effect of thermal softening and the reduced strain hardening lead to a reduction of microhardness.

Fig. (4.27a,b) shows the variation of microhardness with cutting speed. The variation is not significant but a slight increase in microhardness is observed. This is due to the increase in strain rate with increase in cutting speed.

4.3 Overview:

4.3.1 Comparison of Shear angle:

The values of shear angle under similar machining
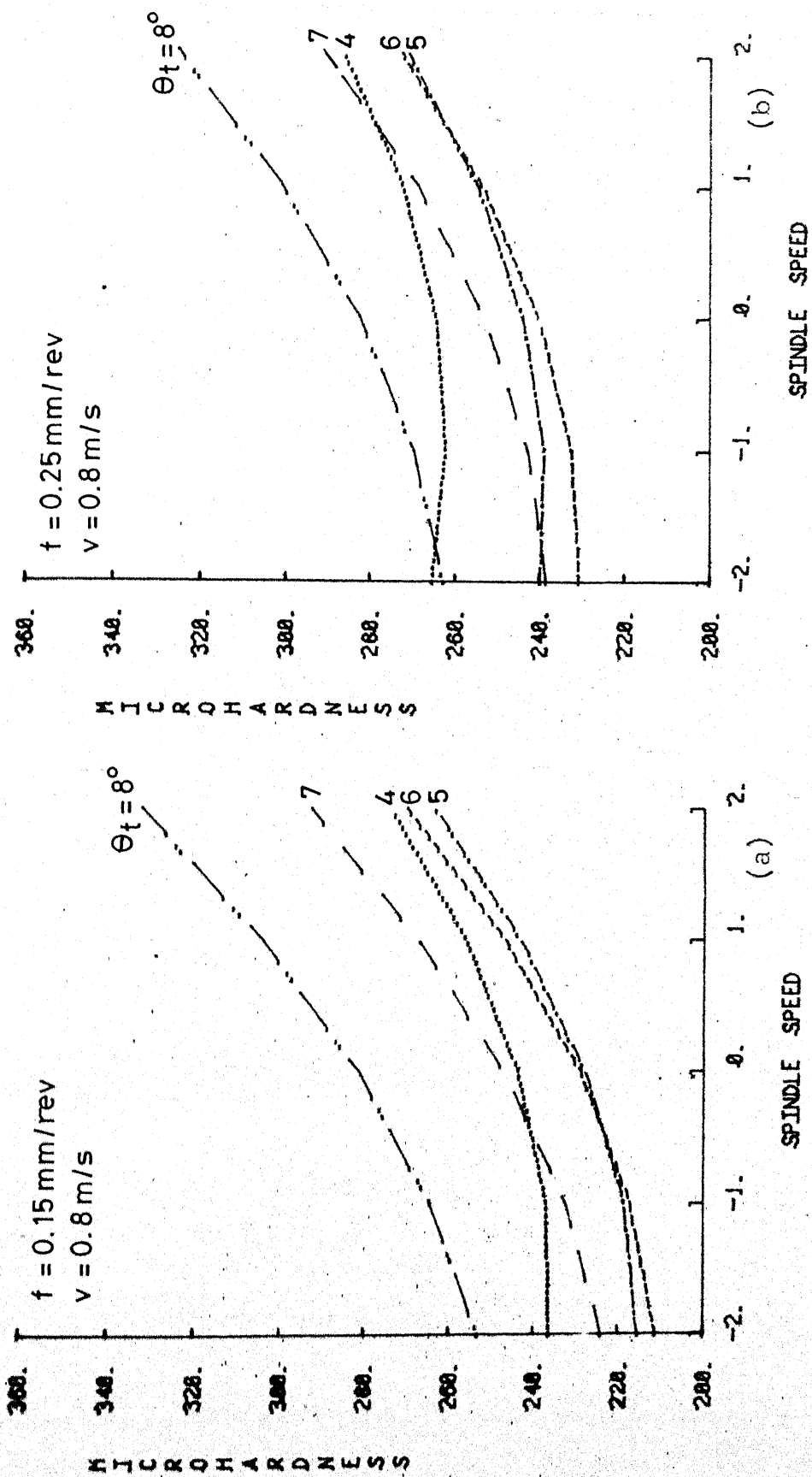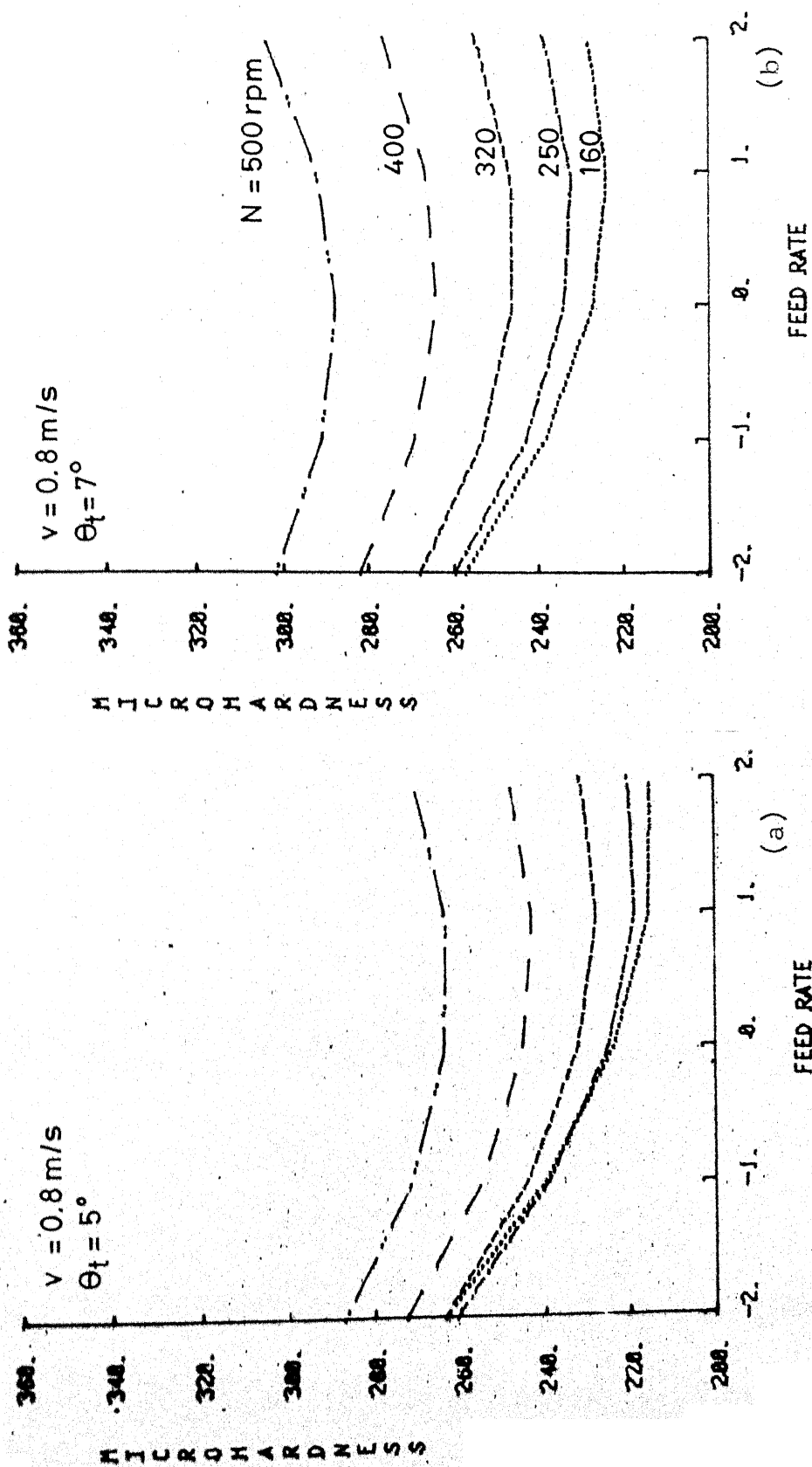
Fig. 4.24 Effect of feed rate on microhardness during taper turning.
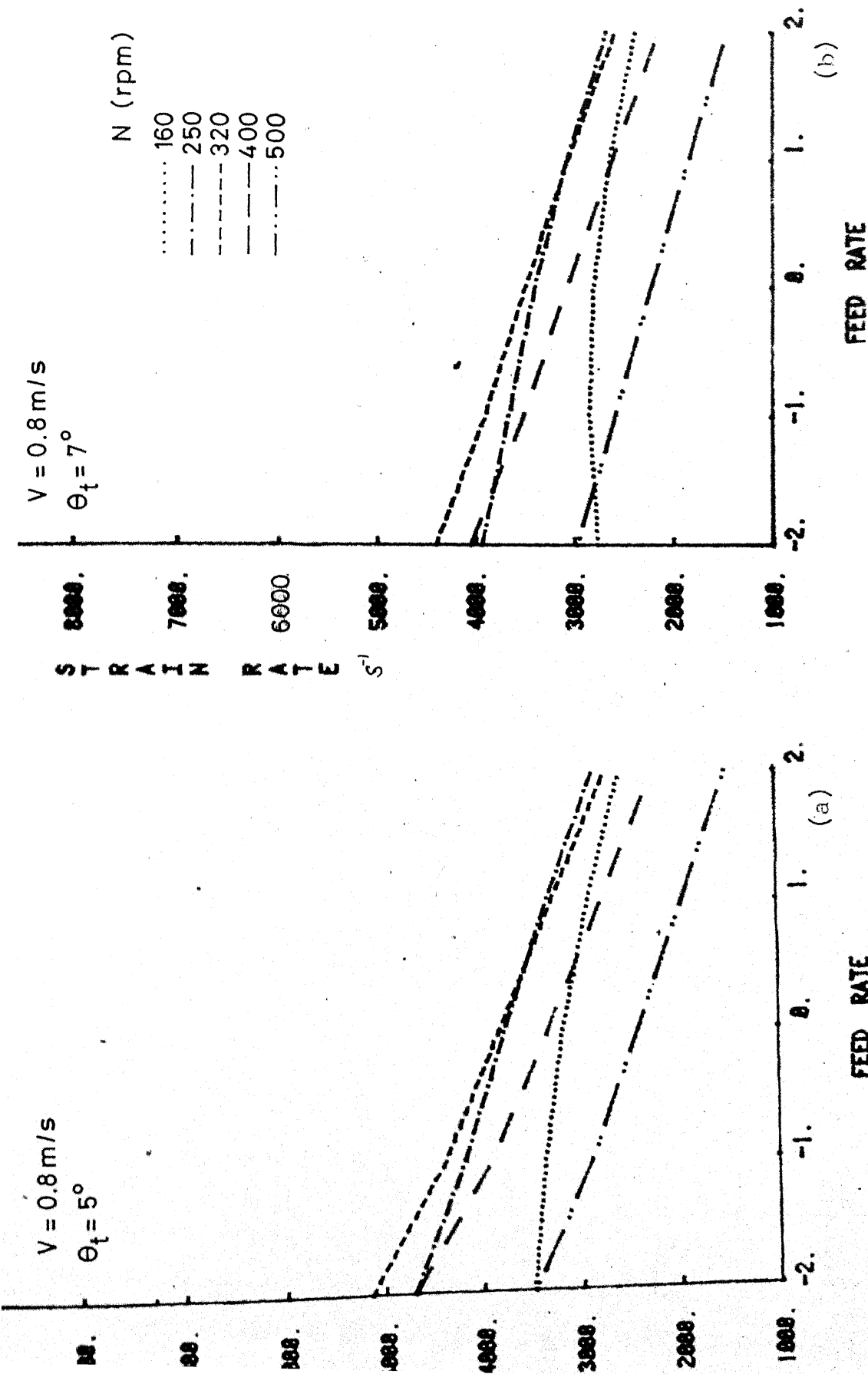
Fig. 4.25   Strain rate variation for Fig. 4.24.
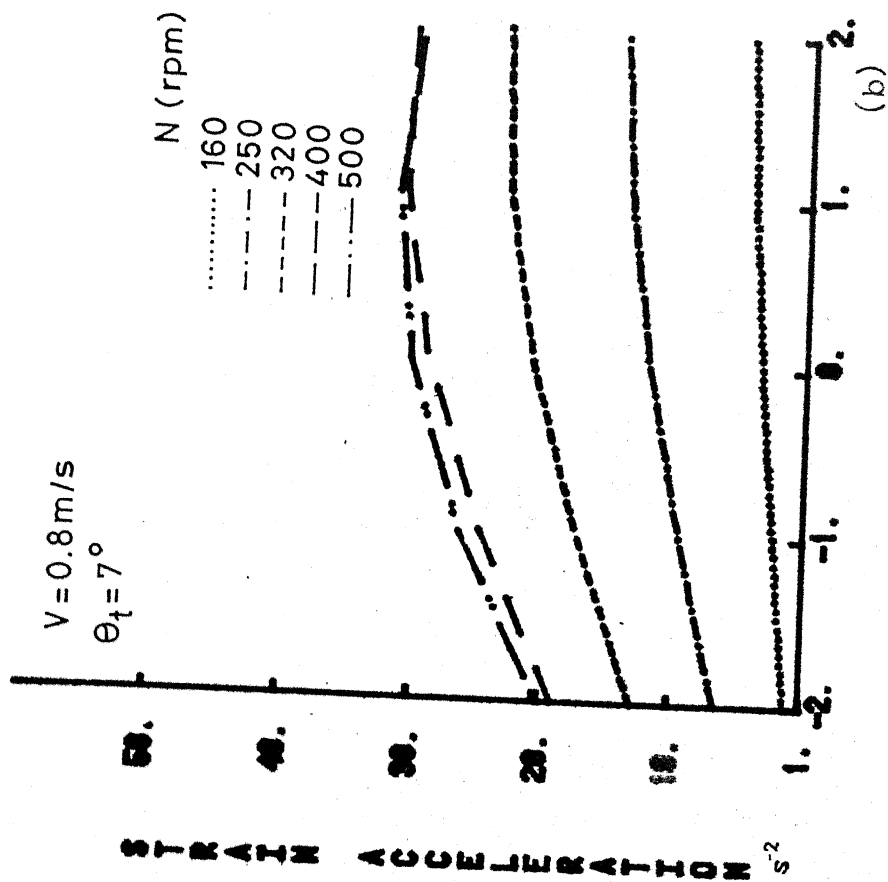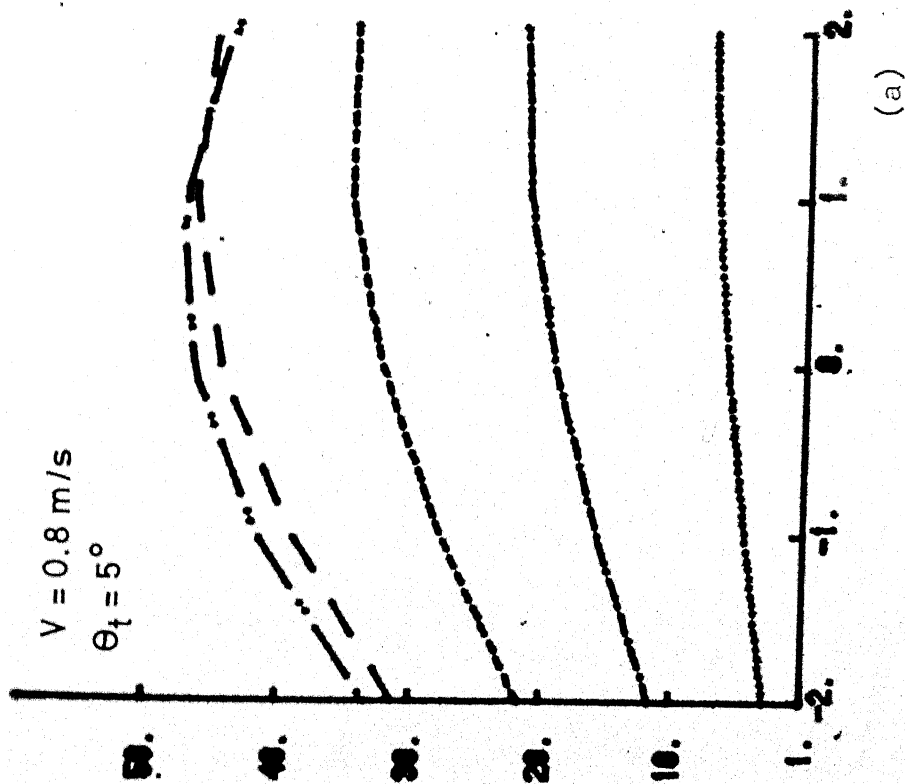
Fig. 4.26 Strain acceleration variation for Fig. 4.25.
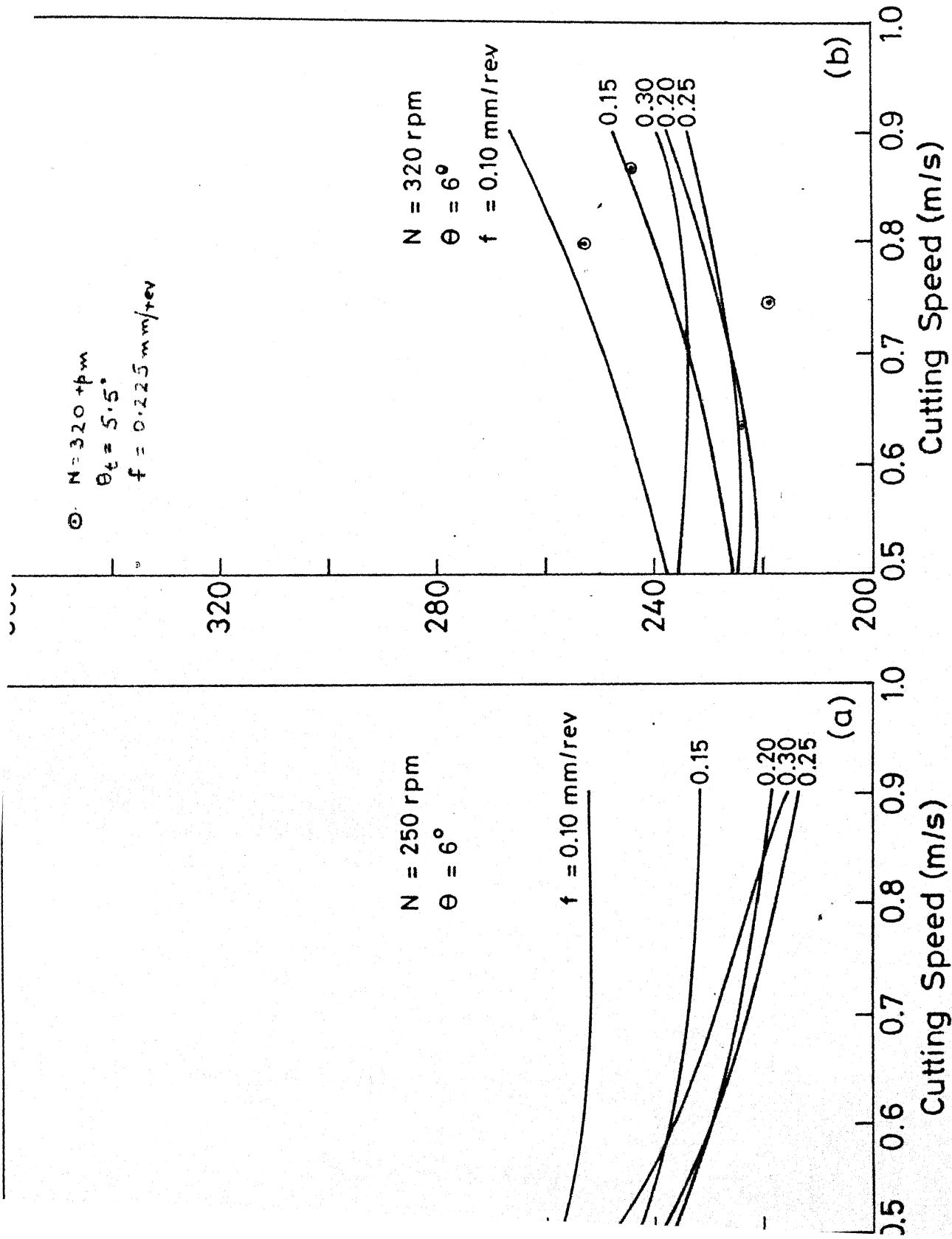
Fig 4.27 Effect of cutting speed on microhardness during taper turning.

Shear Angle (deg)

Feed (mm/rev)

(a)

N = 250 rpm
V = 0.6 m/s
$\theta_t = 6°$

(b)

N = 250 rpm
V = 0.8 m/s
$\theta_t = 6°$

△   Longitudinal turning
○   Facing
□   Taper turning

Longitudinal turning
Facing
Taper turning

330

290

250

210

170

Feed (mm/rev)

N = 320 rpm
V = 0.6 m/s
$\theta_t = 6°$

(b)

0.10   0.15   0.20   0.25   0.30   0.35

330

290

250

210

170

Feed (mm/rev)

N = 250 rpm
V = 0.6 m/s
$\theta_t = 6°$

(a)

0.10   0.15   0.20   0.25   0.30   0.35
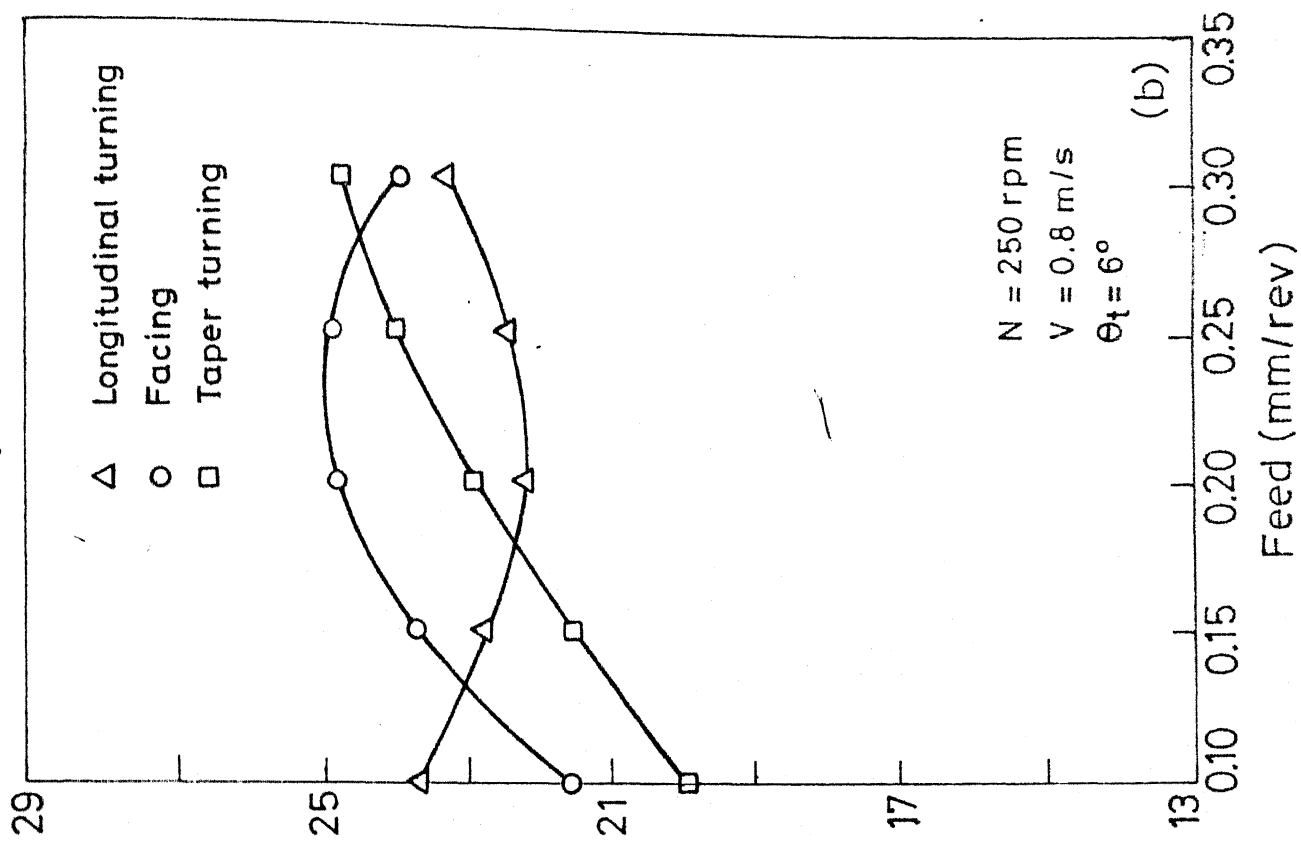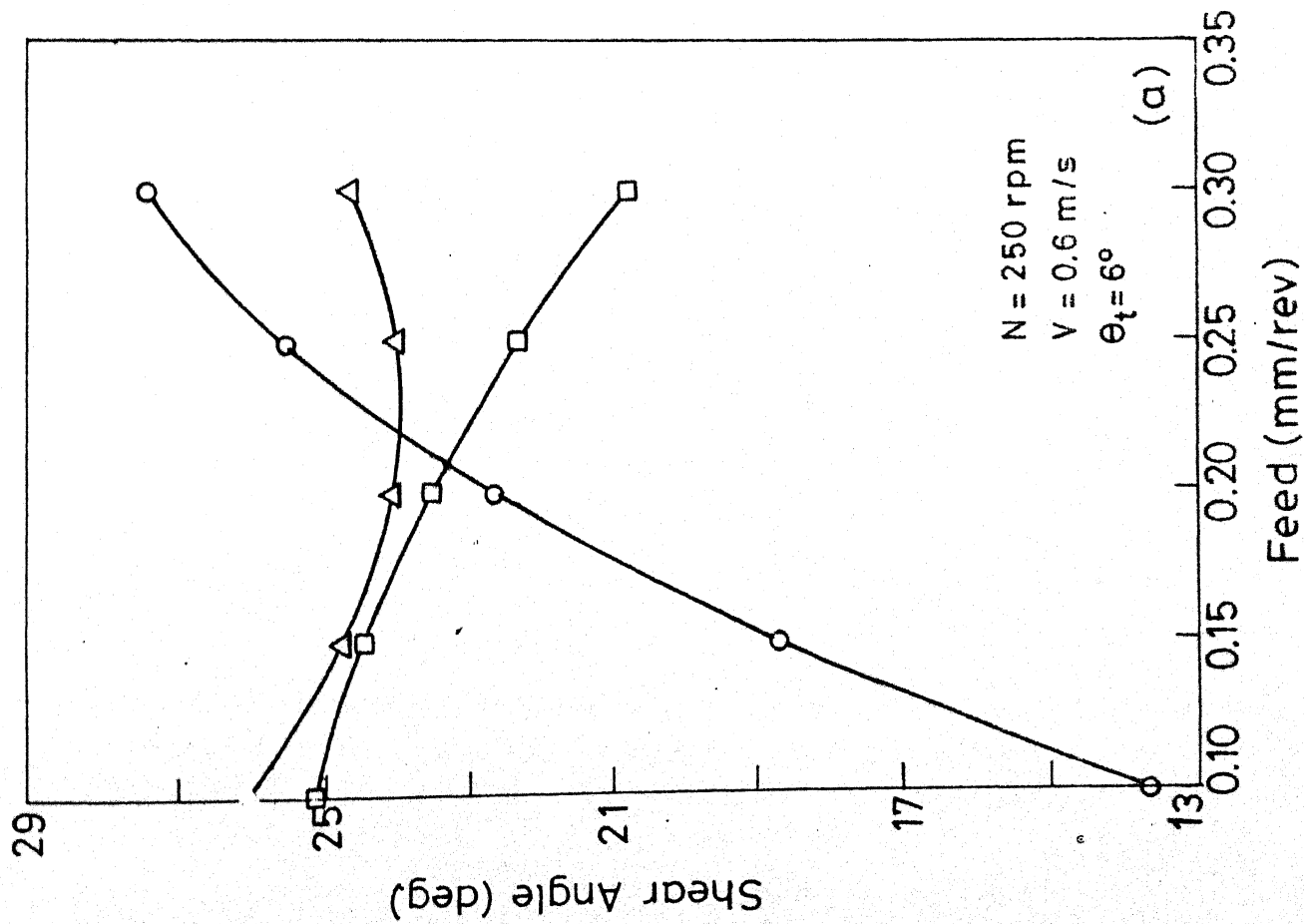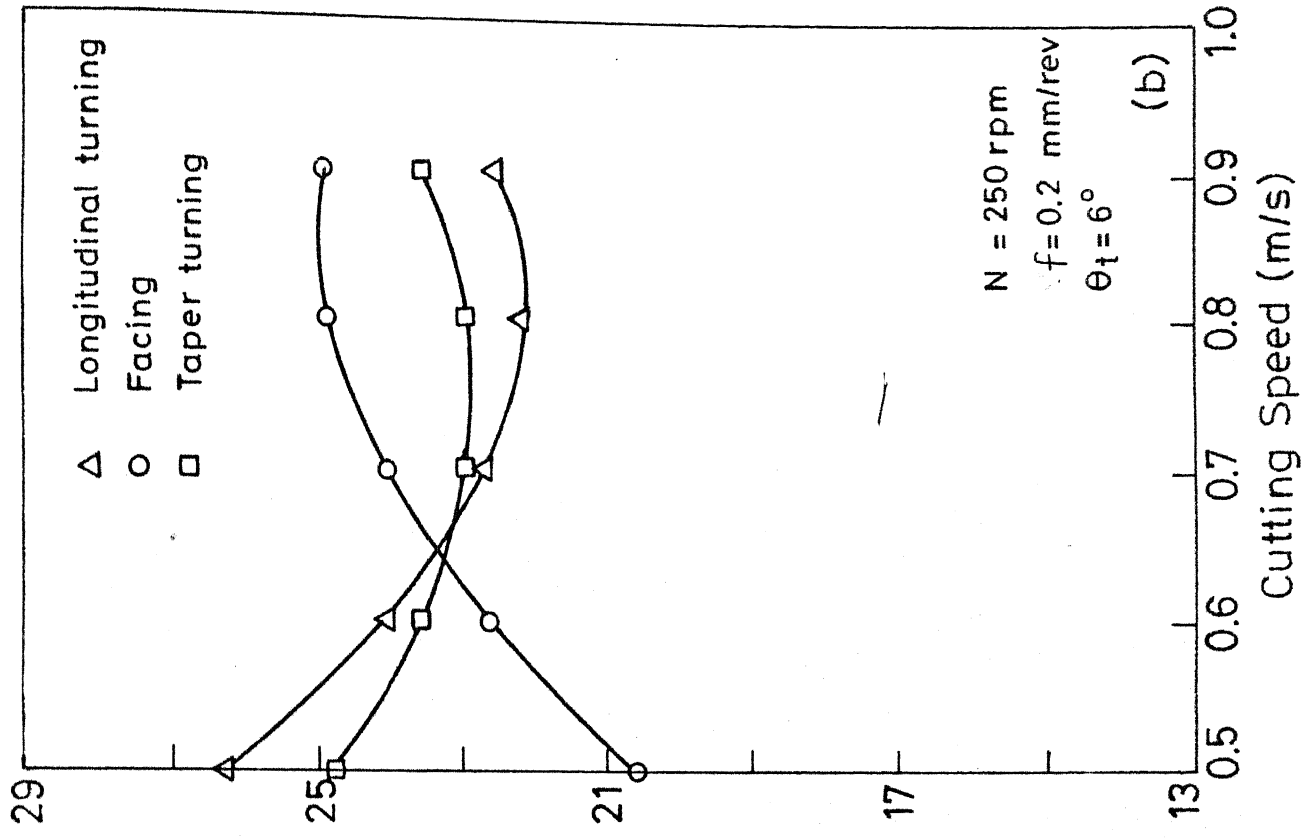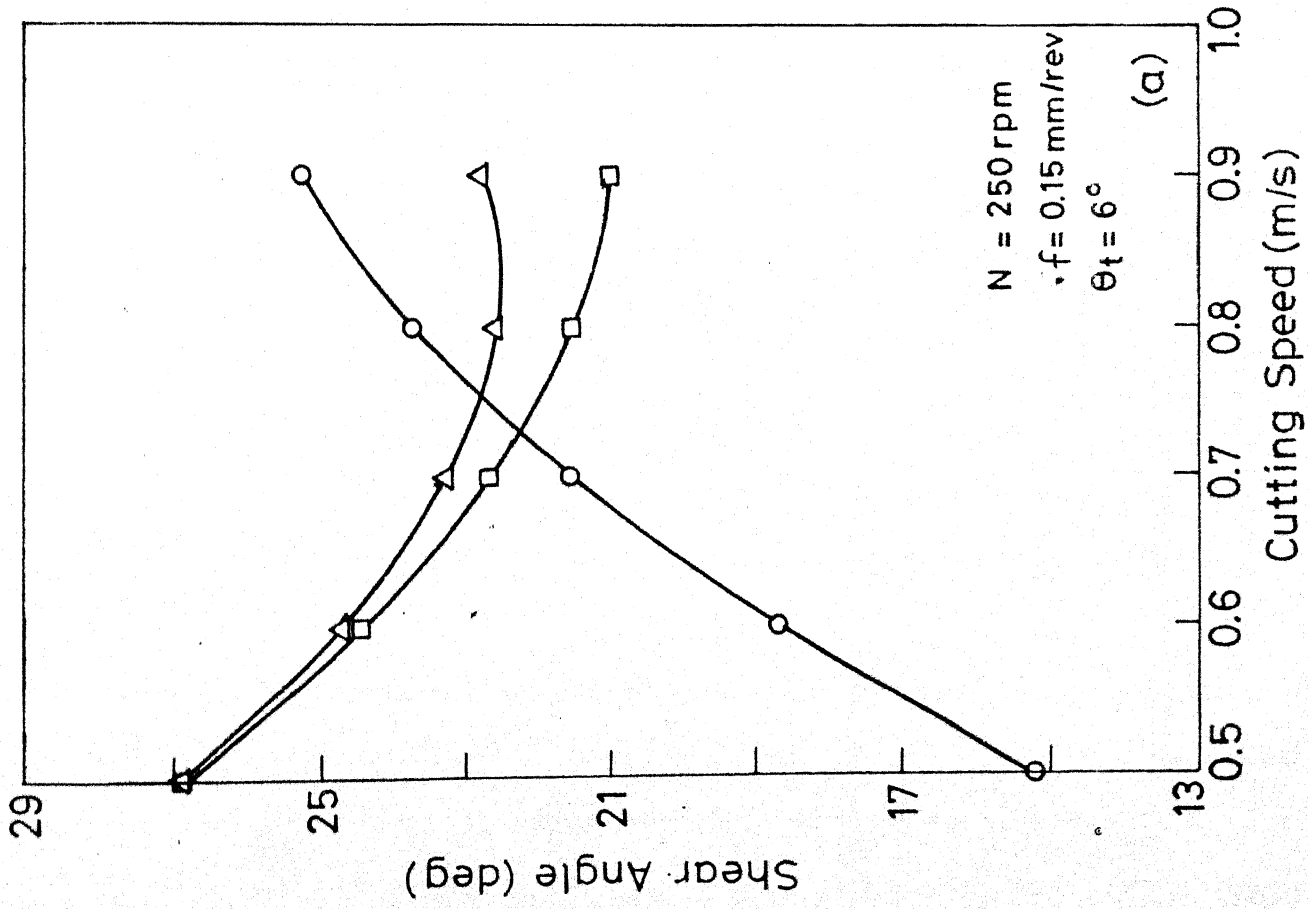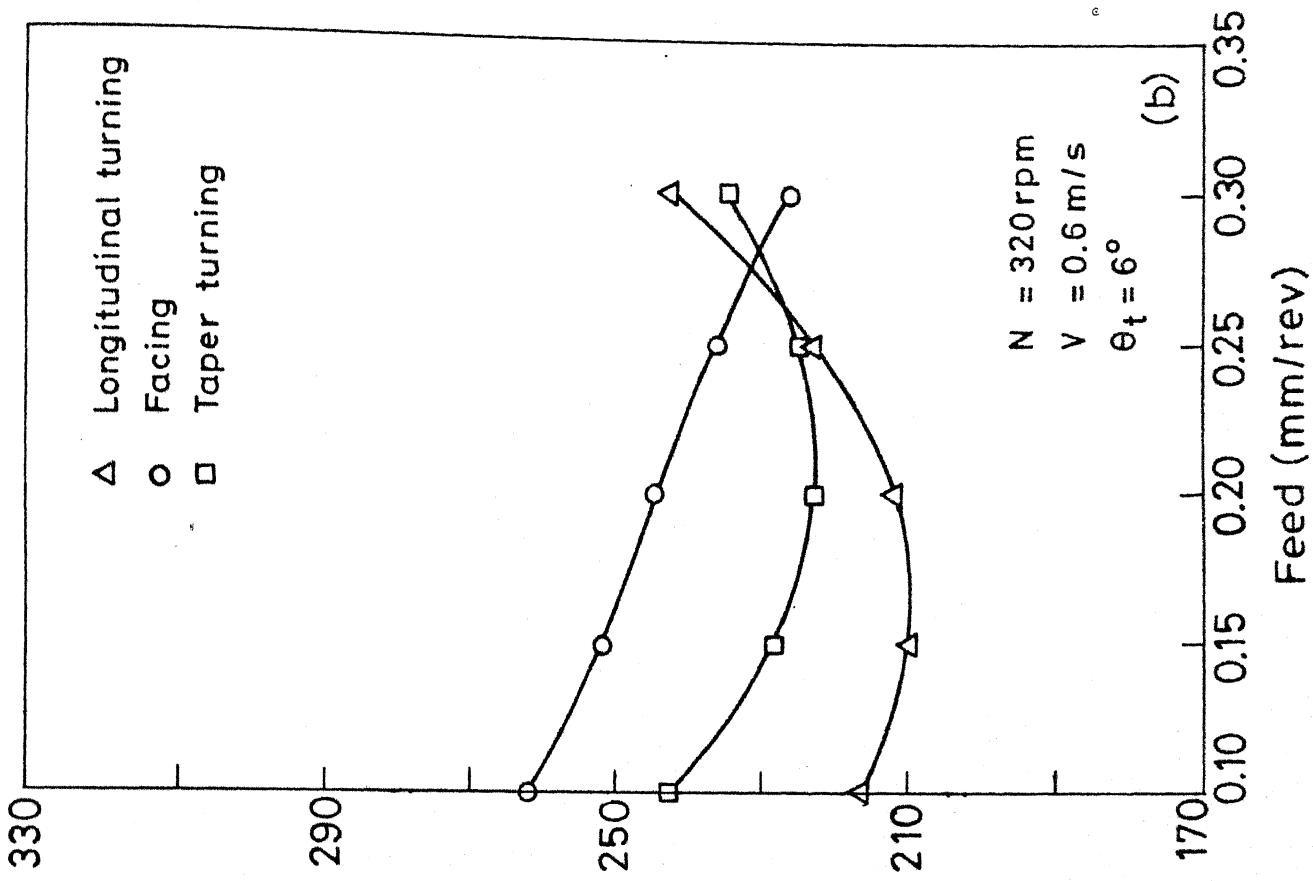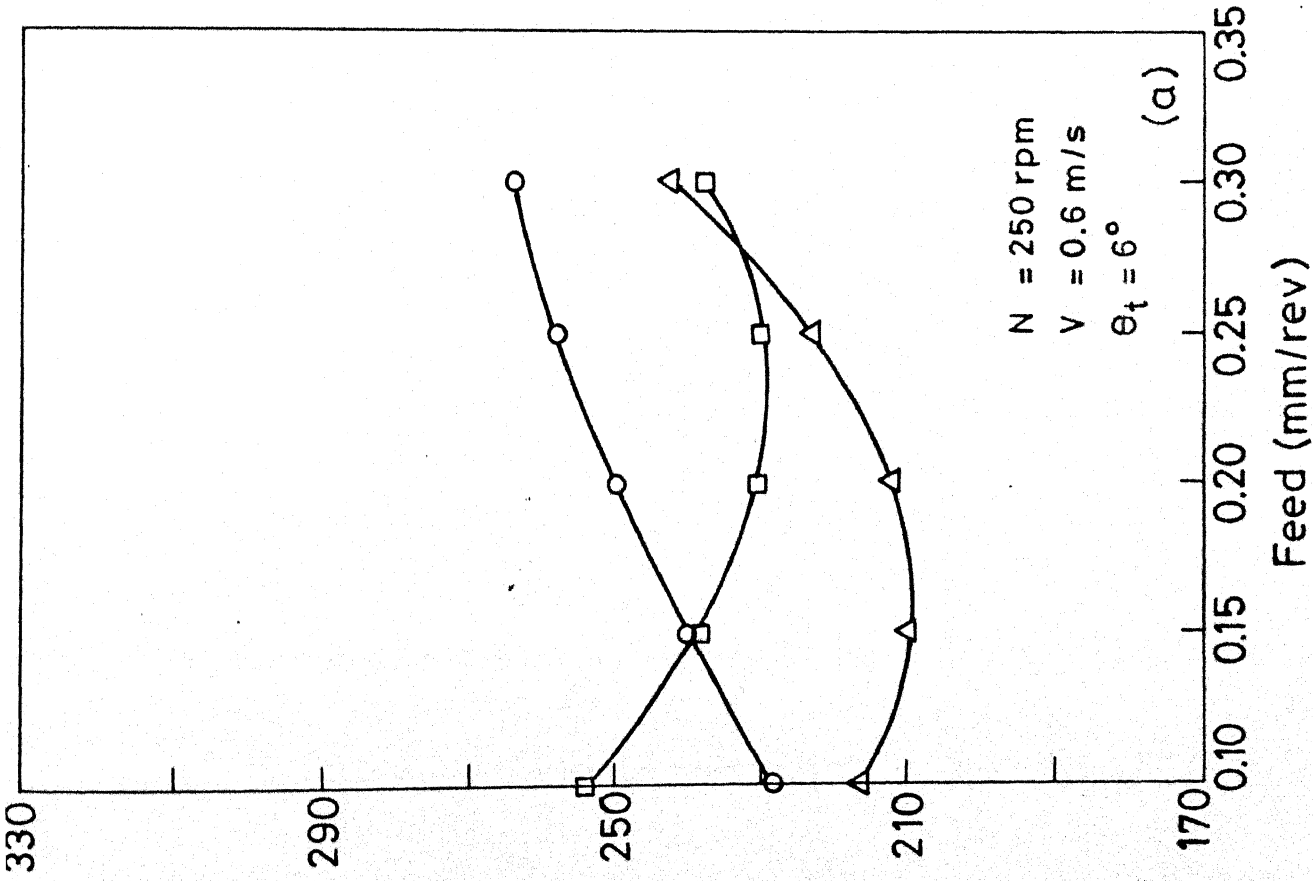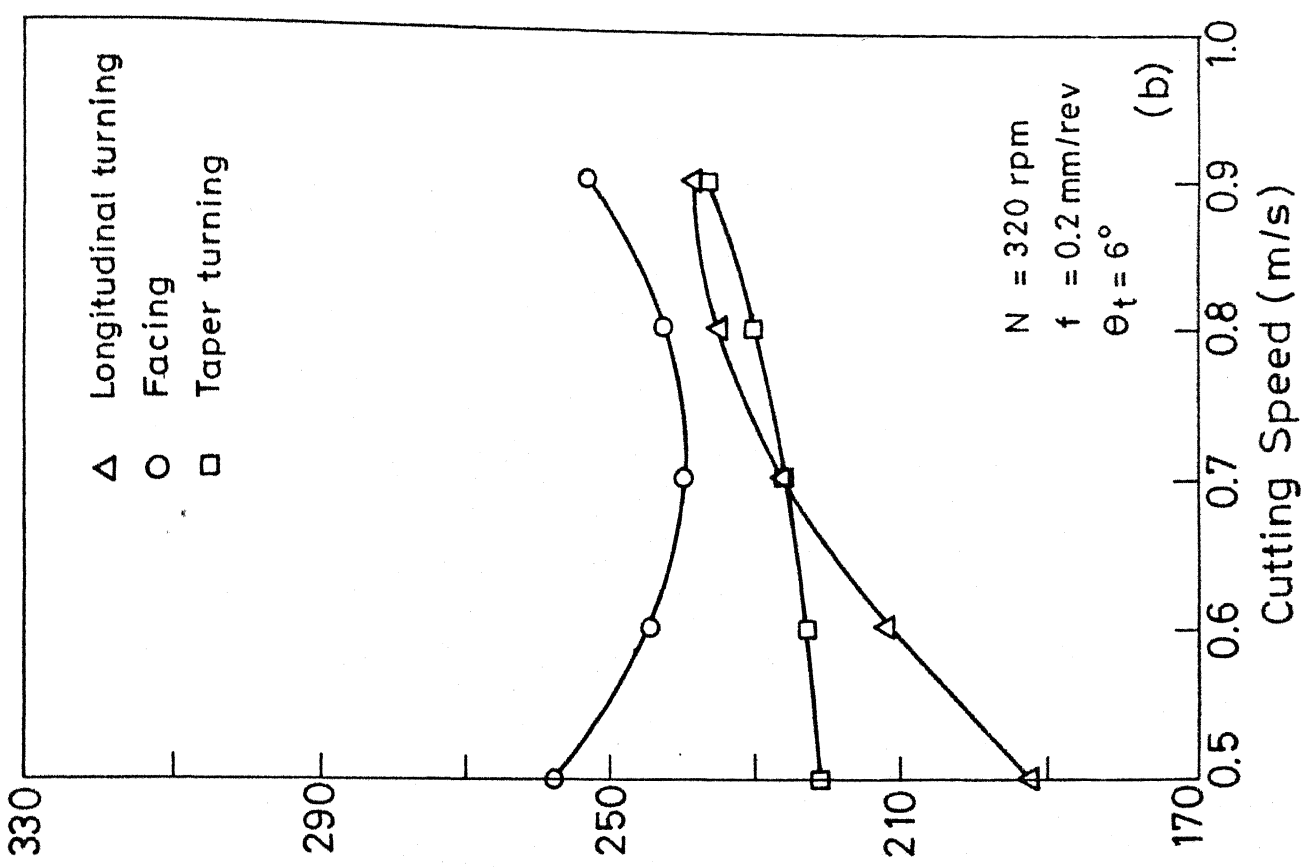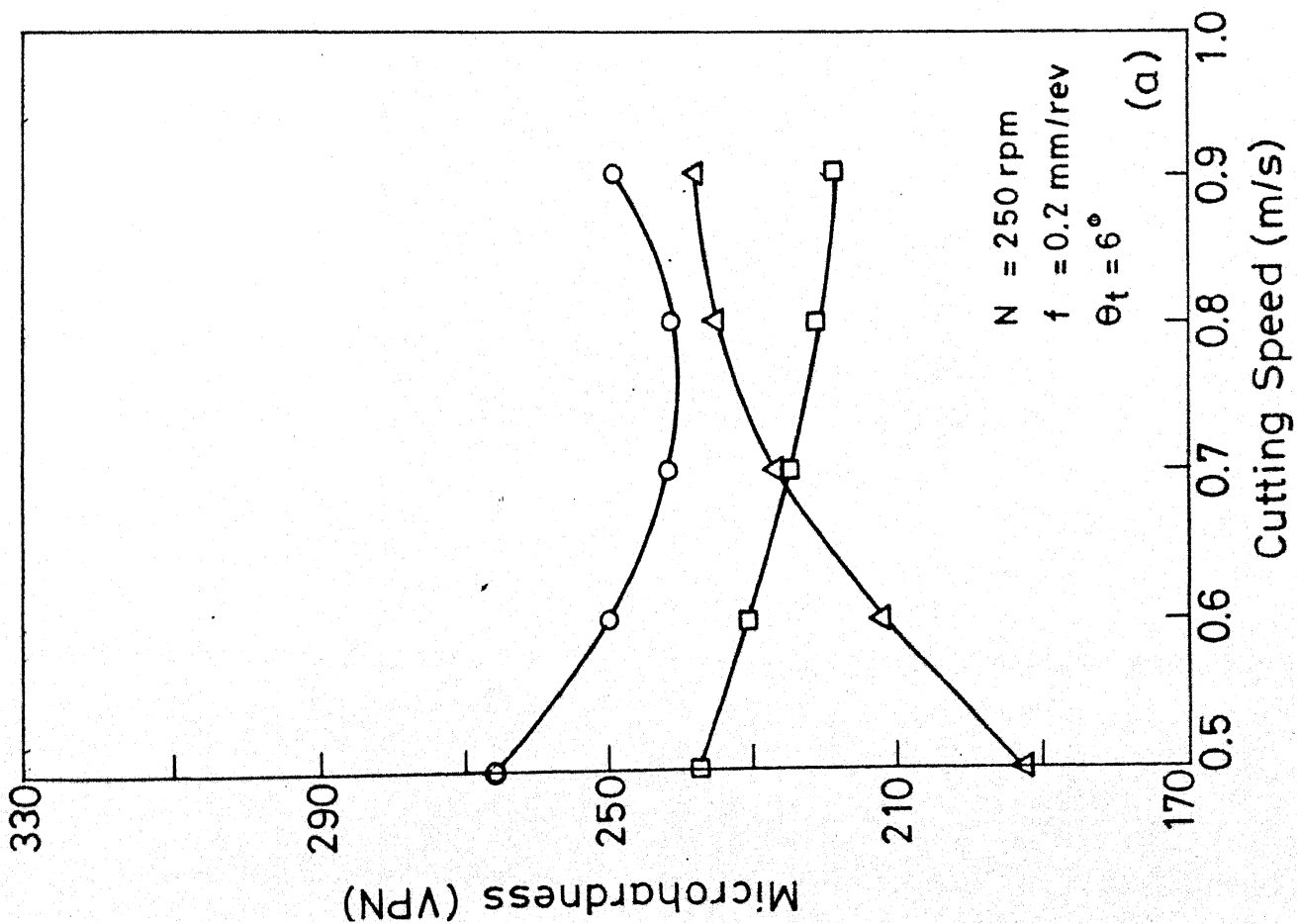
Fig 4.29(ii) Comparison of effect of cutting speed on microhardness.

a) $V = 0.7$ m/s ; $f = 0.7$ mm/rev

$\mu H = 256$ VPN
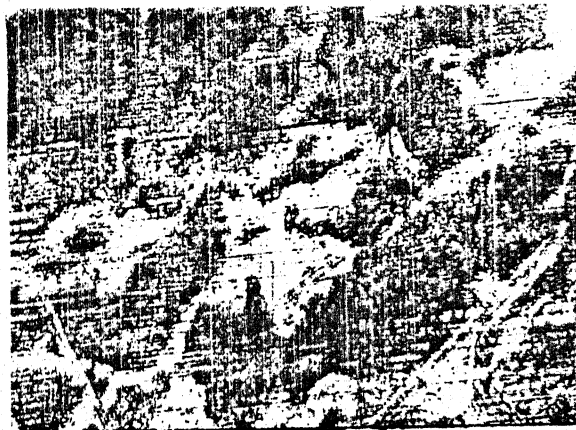
b) $V = 0.5$ m/s ; $f = 0.2$ mm/rev.

$\mu H = 226$ VPN.

FIG 4.30.i) LONGITUDINAL TURNING
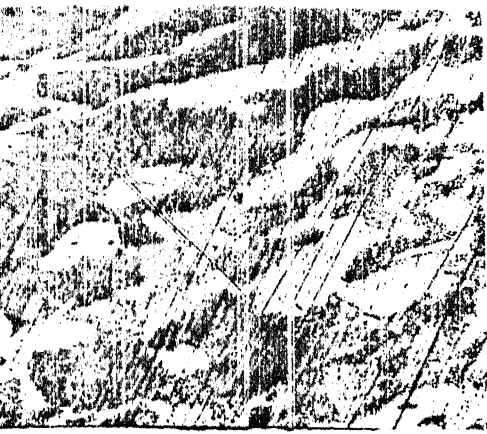
$$V = 0.7 \, m/s \quad ; \quad f = 0.2 \, mm/rev$$
$$\theta_t = 6° \quad ; \quad N = 160 \, rpm.$$
$$\mu H = 221.3 \, VPN.$$
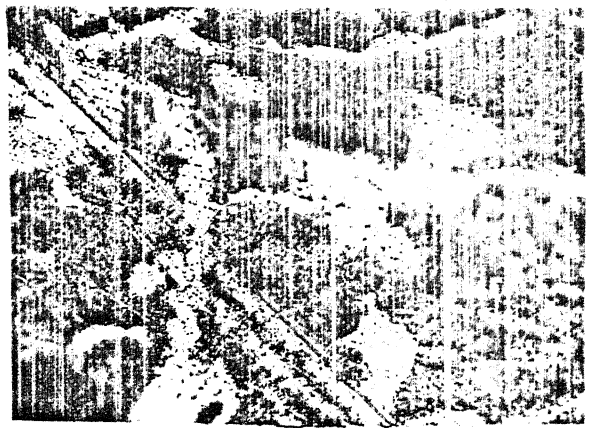
b) $\quad V = 0.7 \, m/s \quad ; \quad f = 0.2 \, mm/rev.$
$$\theta_t = 6° \quad ; \quad N = 320 \, rpm$$
$$\mu H = 226.8 \, VPN$$

FIG. 4.30 iii) TAPER TURNING.

c) $\quad V = 0.7 \, m/s \quad ; \quad f = 0.2 \, mm/rev$
$$\theta_t = 6° \quad N = 500 \, rpm$$
$$\mu H = 242.5 \, VPN.$$
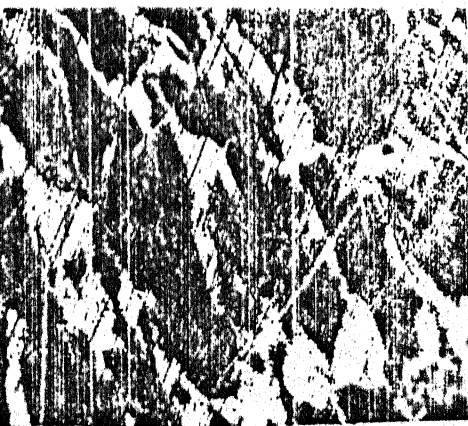
$V = 0.8 \, m/s \quad 3 \, f = 0.25 \, mm/rev$
$$\theta_t = 7° \quad ; \quad N = 250 \, rpm.$$
$$\mu H = 226.2 \, rpm.$$

e) $\quad V = 0.8 \, m/s \quad ; \quad f = 0.25 \, mm/rev$
$$\theta_t = 7° \quad ; \quad N = 400 \, rpm.$$
$$\mu H = 271.8 \, VPN.$$

a) $V = 0.7 \, m/s$; $f = 0.2 \, mm/rev$
   $N = 500 \, rpm.$; $\mu H = 274.5 \, VPN$
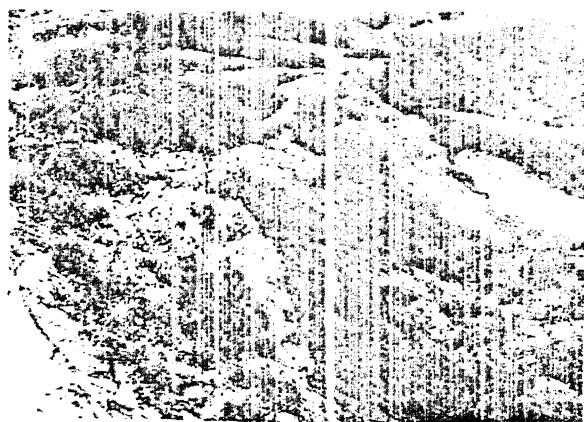
b) $V = 0.7 \, m/s$; $f = 0.2 \, mm$
   $N = 320 \, rpm$; $\mu H = 24$
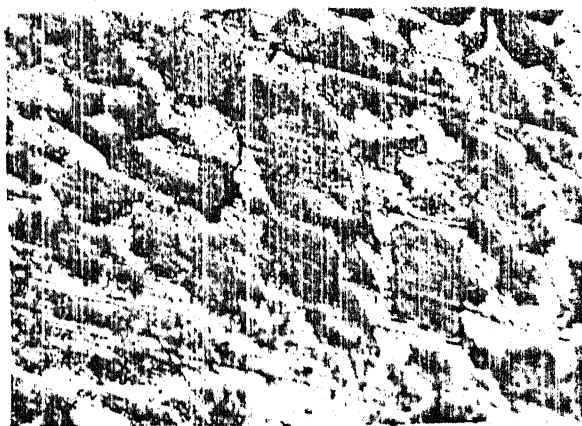
Fig. 4·30.ii) FACING

c) $V = 0.7 \, m/s$
   $N = 160 \, rpm$
   $f = 0.2 \, mm/rev$
   $\mu H = 257.6 \, VPN$
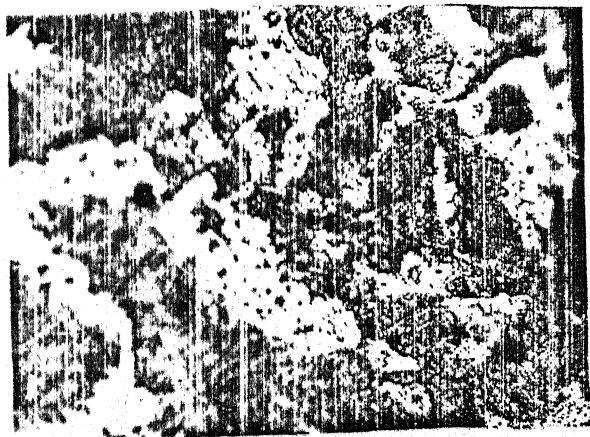
d) $V = 0.8 \, m/s$; $f = 0.26 \, mm/rev.$
   $N = 400 \, rpm.$; $\mu H = 256 \, VPN.$
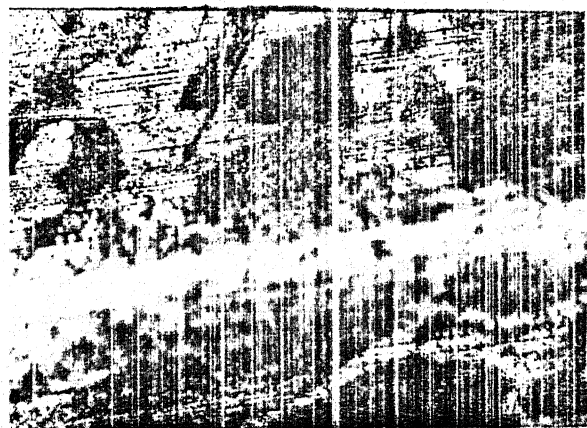
e) $V = 0.7 \, m/s$; $f = 0.2 \, mm$
   $N = 320 \, rpm.$ $\mu H = 244.$

are compared in Figs. (4.28a,b). The effect of feed and
cutting speed an shear angle is more pronounced during
facing and taper turning than in longitudinal turning. Also
values of shear angle in longitudinal turning generally lie
in between facing and taper turning. This however, depends
on the values of parameters (v, f, Θ_t) taken.

4.3.2 Comparison of microhardness:

Fig. (4.29a,b) shows the values of microhardness for
facing, taper turning and longitudinal turning, under similar
machining conditions (cutting speed, feed etc.).

It is evident that the values of microhardness in
facing are generally higher than those of longitudinal turning
and taper turning. This is because the strain rates in facing,
under similar machining conditions, are significantly higher.
Michrohardness values in taper turning are generally in between
facing and longitudinal turning.

4.3.3 Microstructure:

The photographs of the microstructure of the cross-
section of the chip at 500 X magnification were taken. A study
of the microstructure shows that at high spindle speeds in facin
the grains were more enlongated and appeared heavily strained.
In taper turning, this trend was observed to a lesser extent
and the microhardness values were also found to lie in between
facing and longitudinal turning. In longitudinal turning the
grain size was large and showed lesser sings of heavy deformatio

CHAPTER - 5

CONCLUSIONS

On the basis of experimental and analytical results, the following conclusions may be drawn.

I. Shear angle:

1. Shear angle increases with increase inspindle speed in facing and taper turning. At high feeds however, a reduction in shear angle value is observed in facing.

2. Shear angle for low feed decreases with cutting speed for taper turning and longitudinal turning, while it increases for facing. At higher feed, however, it decreases for facing too.

3. The shear angle variation with feed is similar to the variation with cutting speed.

4. The effect of taper angle en shear angle in taper turning is not significant.

5. The values of shear angle for taper turning are lowest. The variation for facing is maximum.

II. Microhardness:

1. Microhardness increases with spindle speed in taper turning and facing at low feeds. In facing however, at high feed this decreases.

2. Microhardness increases with increase in cutting speed at low feed in every case. At high feeds, there is a decrease in microhardness in longitudinal turning and

and taper turning .

3. The microhardness follows the same trained as cutting speed with feed rate, to a large extent. With taper angle, the microhardness increases.

4. Microhardness values for facing are generally the highest. For taper turning, these lie between those of facing and longitudinal turning. Changes in microhardness are more drastic in facing.

Scope for future work:

1. The scope, for work in the field of density variation during accelerated cutting and it's effect en material properties, is immense.

2. The stress field on the tool face, as also the diffusion rate variation, need to be studied.

3. More detailed microhardness studies are required to establish microhardness as a dependant parameter, reflecting the conditions in the machining zone.

4. Microhardness redings on the underside of the chip would perhaps show less scatter. This aspect could be explored.

REFERENCES

1. Lorenz. G. — ' The economic importance of machinability tests and some rapid test methods' —Met. Aust, 1 (15)1969 p176.

2. Heginbotham W, Pandey P.C. — ' Taper turning tests produce reliable tool wear equation'— Proc. of 7th IMTDR conference; Sept. 1966, Pergamon London 1967 p 515.

3. Pandey P.C., Jain V.K — ' Strain Aceleration — A new concept in metal cutting and its effects on accelerated machinability tests'. Int. J. of Engg. Prod. 3 (1) 1979 p 15.

4. Bandopadhyaya D.K — ' Investigations into shear angle during accelerated cutting'. M. Tech. (Thesis), Allahabad University, Allahabad 1982.

5. Venkatesh V.C., Chandrashekran C. 'Experimental methods in metal cutting('— Prentice Hall, India 1982.

6. Gupta B.K., ' Investigations into shear flow stress during accelerated cutting'. M. Tech. (Thesis) I.I.T. Kanpur 1985.

7. Cochran W.G., Cox G.M. — ' Experimental Design'. Asia Publishing house, 1977.

8. Clack V.W; Brewer R.C. ' New technique for shear zone thickness determination in orthogonal metal cutting'. Proc. Inst.of Mech. Engrs. London. V181, pt 1, 1966-67 p 667.

9. Mills B; Aktar S. — ' Proc. of Int. Symposium on Influence of Metallurgy on machinability'. A.S.M. Ed. V.A. Tipnis, V7, 1975 p 73.

10. Campbell. J.D., Fergusson W.G.— ' Temperature and strain rate dependance of shear strength of M.S.'Phil. Mag., V21, n169, 1970 p 63.

11. Manjoine M.J — ' Influence of rate of strain and temperature on yield stress of M.S.' Trans. A.S.M.E. V66; 1944 p 211.

12. Oshmori, Oshimaya et al. — ' Effect of deformation rate on strength and blue brittleness Temperature of M.S.'

9th Japan Congress on testing of Materials 1966 p 58.

13.   Zorev N.N. ' Mechanics of metal cutting'. Pergamon,
       London 1966.

14.   Seegar. A. ' Dislocations and Mechanical Properties of
       crystals'-John Wiley and Sons Inc. 1957, p 243.

15.   Dieter G.E. ' Mechanical Metallurgy'- Mcgraw Hill
       International Book Co. 1981.

16.   Li. J.C.M. - ' Dislocation Dynamics' Ed. Rosenfield et al.
       Mcgraw Hill. NY, 1968, p 87.

17.   Shetty M.N, Majumdar, A- ' Analysis of thermally activated
       deformation in HSLA steel. Int. Conf. on HSLA. steels' Univ.
       of Wollongong, Australia 1984.

18.   Rollason. E.C ' Metallurgy for Engineers'. ELBS and
       Edward Arnold Publishers, 1982.

19.   Boothroyd. G. - 'Fundamentals of metal machining and
       machine tools' Mcgraw Hill, 1975.

APPENDIX - 1

TABLE 1: LEVELS FOR DIFFERENT FACTORS
1(a) LONGITUDINAL TURNING

FACTORS	LEVELS				
	-2	-1	0	1	2
Feed, X_1 (mm/rev)	0.10	0.15	0.20	0.25	0.30
Cutting Speed, X_2 (m/s)	0.5	0.6	0.7	0.8	0.9

1(b) FACING

FACTORS	LEVELS				
	-2	-1	0	1	2
Spindle Speed, X_1 (r.p.m.)	160	(240*)250	320	400	(480*)500
Feed, X_2 (mm/rev)	0.10	0.15	0.20	(0.25*)0.26	0.30
Cutting Speed X_3 (m/s)	0.5	0.6	0.7	0.8	0.9

1(c) TAPER TURNING

FACTORS	LEVELS				
	-2	-1	0	1	2
Spindle Speed, X_1 (r.p.m)	160	(240*250)	320	400	(480*)500
Taper Angle X_2 (degrees)	4	5	6	7	8
Feed, X_3 (mm/rev)	0.10	0.15	0.20	0.25	0.30
Cutting speed, X_4 (m/s)	0.5	0.6	0.7	0.8	0.9

* Numbers netting brackets indicate calculated values of factors not available on machine tool.

TABLE 2 : PLAN OF EXPERIMENTATION AND RESPONSES

2(a) LONGITUDINAL TURNING

| | | PLAN | | | RESPONSES | | |
| | | | | | SHEAR ANGLE(φ) | MICROHARDNESS (μH) | |
S.No.	Expt. order no.	Feed Rate (mm/rev)	Cutting Speed (m/s)	φ (degrees)	σ $_s$*	μH (VPN)	σ m*
1	11	0.15	0.60	24.24	0.26	224.3	13.8
2	12	0.25	0.60	23.03	1.18	227.0	10.5
3	2	0.15	0.80	22.30	0.60	254.5	18.2
4	3	0.25	0.80	21.60	1.90	216.7	9.1
5	4	0.10	0.70	24.50	0.88	243.8	17.8
6	5	0.30	0.70	24.12	1.33	239.6	16.2
7	13	0.20	0.50	26.70	1.28	184.2	18.0
8	1	0.20	0.90	22.70	0.23	242.5	10.3
9	6	0.20	0.70	24.50	0.75	236.6	9.3
10	7	0.20	0.70	22.79	1.09	201.6	6.6
11	8	0.20	0.70	22.12	0.85	233.5	17.9
12	9	0.20	0.70	22.83	1.00	208.7	11.8
13	10	0.20	0.70	22.45	1.73	243.4	14.1

Additional Experimental data

S.No.	Feed Rate (mm/rev)	Cutting Speed (m/s)	φ (degrees)	σ $_s$*	μH (VPN)	σ m*
1	0.35	1.00	26.60	1.85	218.1	8.8
2	0.275	0.65	22.50	0.55	235.1	13.3
3	0.225	0.65	23.70	0.57	233.8	19.3
4	0.175	0.65	23.70	1.21	239.0	13.2
5	0.125	0.65	23.17	0.47	254.7	5.7

*σ_s = Standard deviation in shear angle value

σ_m = Standard deviation in microhardness value.

TABLE 2(b): FACING

| | | PLAN | | | RESPONSE | | | |
| | | | | | SHEAR ANGLE | | MICROHARDNESS | |
S.No.	Expt order no.	Spindle Speed (r.p.m.)	Feed (mm/rev)	Cutting Speed (m/s)	∅ (degrees)	σ_s	μH (VPN)	σ_m
1	19	250	0.15	0.6	18.17	0.56	222.0	11.7
2	4	400	0.15	0.6	24.90	1.66	271.8	18.0
3	18	250	0.26	0.6	25.30	0.90	259.8	8.0
4	5	400	0.26	0.6	26.50	0.92	228.2	12.2
5	17	250	0.15	0.8	23.99	0.41	219.0	15.4
6	3	400	0.15	0.8	24.12	1.42	270.8	16.3
7	16	250	0.26	0.8	25.40	0.82	254.6	10.0
8	2	400	0.26	0.8	21.80	0.77	254.5	10.0
9	20	160	0.20	0.7	23.50	1.85	267.1	10.1
10	1	500	0.20	0.7	20.78	0.47	271.7	9.9
11	7	320	0.10	0.7	20.50	0.02	255.3	14.4
12	8	320	0.30	0.7	23.19	0.78	219.5	15.3
13	15	320	0.20	0.5	23.09	1.00	265.6	11.6
14	6	320	0.20	0.9	21.90	0.18	248.8	11.7
15	9	320	0.20	0.7	22.41	0.02	246.7	11.3
16	10	320	0.20	0.7	28.80	1.97	242.0	9.3
17	11	320	0.20	0.7	25.84	1.50	219.7	7.8
18	12	320	0.20	0.7	21.90	0.81	244.8	16.6
19	13	320	0.20	0.7	21.22	0.47	241.3	12.7
20	14	320	0.20	0.7	25.15	0.24	244.7	14.7

Additional experimental data

S.No.		Spindle Speed (r.p.m.)	Feed (mm/rev)	Cutting Speed (m/s)	∅ (degrees)	σ_s	μH (VPN)	σ_m
1		200	0.23	0.75	23.20	0.75	215.6	4.0
2		200	0.23	0.85	21.10	0.47	263.3	18.1
3		200	0.23	0.90	21.30	0.62	252.0	10.7
4		200	0.23	0.95	21.80	0.03	241.8	13.2
5		142	0.23	0.65	25.05	0.61	255.2	11.1

TABLE 2(c), TAPER TURNING

S.No.	Expt order no.	PLAN				RESPONSE			
		Spindle Speed (rpm)	Taper Angle (deg.)	Feed (mm/rev)	Cutting Speed (m/s)	SHEAR ANGLE (Φ)		MICROHARDNESS (μH)	
						ϕ	σ_s	μH (VPN)	σ_m
1.	8	250	5	0.15	0.6	23.80	1.22	246.0	8.08
2	29	400	5	0.15	0.6	23.56	0.89	242.0	10.7
3	6	250	7	0.15	0.6	24.30	1.50	259.0	6.6
4	27	400	7	0.15	0.6	24.25	1.25	225.0	5.6
5	9	250	5	0.25	0.6	22.60	0.34	242.4	18.5
6	30	400	5	0.25	0.6	23.68	1.65	224.0	6.0
7	7	250	7	0.25	0.6	22.89	1.72	246.2	19.9
8	28	400	7	0.25	0.6	21.20	1.50	261.8	5.2
9	5	250	5	0.15	0.8	23.40	0.45	227.8	8.5
10	26	400	5	0.15	0.8	19.20	0.80	225.0	14.7
11	3	250	7	0.15	0.8	19.35	1.21	247.0	12.8
12	22	400	7	0.15	0.8	19.40	1.75	269.2	16.0
13	4	250	5	0.25	0.8	22.80	0.81	236.0	18.8
14	25	400	5	0.25	0.8	24.86	1.04	236.8	5.1
15	2	250	7	0.25	0.8	23.12	0.57	226.3	13.3
16	23	400	7	0.25	0.8	23.50	0.30	271.8	15.5
17	1	160	6	0.20	0.7	22.40	1.32	221.3	5.3
18	31	500	6	0.20	0.7	21.80	0.02	242.5	9.7
19	21	320	4	0.20	0.7	21.49	0.47	243.4	10.0
20	10	320	8	0.20	0.7	23.49	0.47	263.8	8.3
21	11	320	6	0.10	0.7	21.80	1.50	251.7	13.8
22	12	320	6	0.30	0.7	23.58	0.84	220.1	14.4
23	24	320	6	0.20	0.5	24.05	1.82	206.2	9.1
24	14	320	6	0.20	0.9	25.02	1.14	240.8	12.1
25	13	320	6	0.20	0.7	22.04	0.33	254.7	5.2
26	15	320	6	0.20	0.7	22.04	1.13	221.3	15.1
27	16	320	6	0.20	0.7	23.40	0.89	208.7	6.4

Contd..

CONTD.... TABLE 2 (c)

28	17	320	6	0.20	0.7	24.90	0.46	217.2	8.6
29	18	320	6	0.20	0.7	23.86	1.98	210.6	18.0
30	19	320	6	0.20	0.7	23.77	0.61	242.8	15.8
31.	20	320	6	0.20	0.7	21.22	0.75	226.8	13.2

Additional experimental data

S.No.								
1	320	0.225	5.5	0.85	24.48	0.28	278.5	3.4
2	320	0.225	5.5	0.85	23.16	1.00	246.6	16.4
3	320	0.225	5.5	0.80	22.10	0.25	254.0	15.1
4	320	0.225	5.5	0.75	22.36	0.70	218.0	12.9
5	320	0.225	5.5	0.65	22.90	0.20	225.8	9.7

TABLE - 3

Values of constant of Response Surface Model for shear angle and microhardness

Source	Longitudinal turning		Facing		Taper Turning	
	Shear Angle	Microhardness	Shear Angle	Microhardness	Shear angle	Micro-hardness
B_0	22.68	225.99	24.42	239.17	23.03	226.01
B_1	-0.22	-3.62	-0.06	4.95	-0.16	4.13
B_2	-0.94	11.37	0.85	-3.63	-0.08	5.72
B_3	—	—	-0.12	-1.03	+0.45	-3.78
B_4					-0.36	3.88
B_{11}	0.33	4.31	-0.42	7.10	-0.29	2.89
B_{22}	0.42	-2.77	-0.52	-0.90	-0.19	8.32
B_{33}		—	-0.32	-4.04	-0.14	3.89
B_{44}	—				0.32	0.77
B_{12}	0.13	-10.12	-1.16	-16.66	0.00	2.61
B_{13}	—	—	-1.21	3.13	0.39	2.01
B_{14}	—	—			-0.05	8.42
B_{23}	—	—	-1.42	4.19	-0.03	2.45
B_{24}	—	—	—	—	-0.24	1.30
B_{34}	—	—	—	—	1.15	-1.79

APPENDIX - 2

Calculation of average microhardness values:

The average value $(\bar{x}_1)$ was found for these 12 to 16 values of each run and then the standard deviation was calculated the control limites of $\bar{x}_1 \pm 3 \frac{\sigma_1}{\sqrt{n}}$ were used the points line outside the limits of $\bar{x}_1 \pm 3\sigma_1/\sqrt{n}$ were dropped out and a new mean $(\bar{x})$ and a new standard deviation was computed.

$$\text{Upper control limit} = \bar{x}_1 + \frac{3\sigma_1}{\sqrt{n}}$$

$$\text{Lower control limit} = \bar{x}_1 - \frac{3\sigma_1}{\sqrt{n}}$$

where σ = standard deviation

          n = sample size

          $\bar{x}$ = average microhardness (VPN)

e.g.

In an experiment following microhardness were measured

207, 210, 210, 190, 187, 214, 193, 200, 207, 210.

For above observation $= \bar{x}_1 = 202.8$

                         $\sigma_1 = 9.13$

Now, $\text{UCL} = 202.8 + \dfrac{3 \times 9.13}{\sqrt{10}} = 211.4$

         $\text{LCL} = 202.8 - \dfrac{3 \times 9.13}{\sqrt{10}} = 194.2$

so the values 187, 190, 193, 214 were dropped.

the new average, $\bar{x} = 207.34$ and new $\sigma = 3.54$

The average values of microhardness in VPN and σ are given in tables (2a,b,c).

ME-1987-M-KUM-Inv